

https://dspace.org/

A study of large-scale focusing Schlieren systems

Goulding, John Stuart

2008-05-19T06:57:23Z
http://hdl.handle.net/10539/4841

Downloaded from a DSpace repository. https://dspace.org/

A STUDY OF LARGE-SCALE FOCUSING SCHLIEREN SYSTEMS

John Stuart Goulding

A Research Report submitted to the Faculty of Engineering and the Built Environment, University of the Witwatersrand, Johannesburg, in partial fulfilment of the requirements for the degree of Master of Science in Engineering.

Johannesburg, 2006

Declaration

I declare that this research report is my own, unaided work. It is being submitted for the Degree of Master of Science in Engineering in the University of the Witwatersrand, Johannesburg. It has not been submitted before for any degree or examination in any other University.

_____

J.S.Goulding

_____ day of _____ 2006.

Abstract

The interrelationship between variables involved in focusing schlieren systems is fairly well understood, however how changing the variables affects the resultant images is not. In addition, modified grids and arrangements, such as two dimensional, colour and retroreflective systems have never been directly compared to a standard system. The existing theory is developed from first principles to its current state. An apparatus was specifically designed to test grid and arrangement issues while keeping the system geometry, optical components and the test object identical. Source grid line spacing and clear line width to dark line width ratio were varied to investigate the limits of diffraction and banding and to find an optimum grid for this apparatus. Two dimensional, colour, retroreflective and a novel projected arrangement were then compared to this optimum case. In conclusion, the diffraction limit is accurately modelled by the mathematical equations. The banding limit is slightly less well modelled as additional factors seem to affect the final image. Inherent problems with the two dimensional and colour systems indicate that while they can be useful, they are not worth developing further though chromatism in the system meant that colour systems were not fully investigated. The retroreflective and projected systems have the most potential for large scale use and should be developed further.

Acknowledgements

Firstly I'd like to thank my supervisor, Professor Skews, for all his help and guidance. Thanks are also due to Mr. Voorvelt of the Physics Department. He has contributed in many small ways to this project, not least of which includes advice and loan of equipment. Thanks are due to the mechanical engineering laboratory staff, as always, for their constant competence in the manufacture of apparatus. I also owe thanks to Professor G. Settles of Pennsylvania State University (PSU) for permission to reproduce some of the pictures in his book and for the help given in finding some of the references. Finally I would like to thank all my fellow students, in particular, Kamil Midor, Francis Kwei, and Antun Andries for their help and suggestions.

Contents

Declaration i
Abstract ii
Acknowledgements ii
Contents iv
List of figures vi
List of Tables viii
Nomenclature ix
1 Introduction 1
1.1 Review of Schlieren Techniques 3
1.2 Optics 9
1.3 Focusing Schlieren 11
1.4 Historical Development 19
2 Objectives 25
2.1 Scope of research 26
3 System Analysis 28
3.1 Derivation of Mathematics 28
3.2 Discussion of Mathematics 38
4 Apparatus 40
4.1 System Requirements 40
4.2 Detailed System Description 47
4.3 System Geometry 69
4.4 Data Processing 71
4.5 System Imperfections and Sources of Error 72
5 Experimentation 77
5.1 Exploration of Focusing Schlieren Systems 77
5.2 Development of alternative Focusing Schlieren Systems 81
5.3 Other Issues 88
6 Presentation and Discussion of Results 89
6.1 Variation of Source Grid Line Spacing 89
6.2 Variation of Source Grid Light Transmission Ratio 108
6.3 Demonstration of a 2D System 114
6.4 Demonstration of a Retroreflective System 119

6.5 Demonstration of a Projected Grid System 122
7 Conclusions 124
7.1 Variations of Source Grid Line Spacing 124
7.2 Variation of Source Grid Light Transmission Ratio 125
7.3 Demonstration of a 2D System 126
7.4 Development of Colour Systems 126
7.5 Demonstration of a Retroreflective System 127
7.6 Demonstration of a Projected Retroreflective System 127
8 Recommendations 128
8.1 Recommendations for the current work 128
8.2 Recommendations for further work 129
9 References 130
10 Bibliography 134
Appendices 136

List of figures

Figure 1.1 Conventional z-type schlieren system 4
Figure 1.2 Interaction of a source image and a knife-edge 6
Figure 1.3 A multiple source schlieren system arrangement 11
Figure 1.4 A focusing schlieren system arrangement 13
Figure 1.5 Large scale retroreflective focusing schlieren system 17
Figure 1.6 Burton's focusing schlieren arrangement (Burton, 1949) 19

Figure 3.1a Large scale schlieren system showing variables 28
Figure 3.1b Focusing schlieren grid variables 29
Figure 3.2 Effects of moving the test section position (l/L) 37

Figure 4.1 Focusing schlieren system configuration 43
Figure 4.2 Retroreflective system configuration 45
Figure 4.3 Projected retroreflective system configuration 46
Figure 4.4 Optical rail a) Profile, b) Drawing, c) Photograph 48
Figure 4.5 Slide mount a) Fit on rail, b) Drawing, c) Photograph 49
Figure 4.6 Precision mount a) Assembly drawing, b) Photograph 50
Figure 4.7 Tilting mount a) Section view, b) Drawing, c) Photograph 52
Figure 4.8 Light Source a) Drawing, b) Photograph with shroud, c) Power supply, d) Circuit diagram 54
Figure 4.9 Fresnel lens support a) Drawing, b) Photograph 55
Figure 4.10 Source grid support a) Drawing, b) Photograph 56
Figure 4.11 Cutoff grid support a) Drawing, b) Photograph 57
Figure 4.12 General support a) Drawing, b) photograph with lens 58
Figure 4.13 Screen support a) Drawing, b) Photograph 59
Figure 4.14 Baffle between the light source and the Fresnel lens 60
Figure 4.15 Fresnel lens 61
Figure 4.16 Projection lens, primary on the left, secondary on the right 62
Figure 4.17 Panasonic Lumix camera 63
Figure 4.18 A variety of source and cutoff grids 65
Figure 4.19 Standard Test Section a) Drawing, b) Photograph 66
Figure 4.20 Retroreflective fabric 68

Figure 4.21 Enhanced portion of a typical image showing chromatism 74
Figure 4.22 Complete apparatus for first configuration 76

Figure 5.1 Different methods of varying cutoff in a 2D system 82
Figure 5.2 a) Centered, b) middled and c) off center conditions for 100% cutoff grid 83

Figure 6.1 Results of variations in source grid width 90
Figure 6.2 0.15 mm grid enhanced image of disk 93
Figure 6.3 0.90 mm grid a) enhanced disk halo, b) inverted 97
Figure 6.4 3.75 mm grid banding 100
Figure 6.5 a) candle plume at $\phi = 1.25$ and b) heat extractor at $\phi = 2.8$ 107
Figure 6.6 Results of variations in source grid light transmission ratio 108
Figure 6.7 Results and comparison of a 2D system 114
Figure 6.8 Results of a retroreflective system 119
Figure 6.9 Results of a projected retroreflective system 122

List of Tables

Table 4.1 System Geometry and Characteristics 70
Table 5.1 Varied line spacing grid specifications and expected performance 78
Table 5.2 Varied light transmission grid specifications and expected performance 80

Nomenclature

n	:	Refractive index.
k	:	Gladstone-Dale coefficient (for air 0.00023 m^3/kg).
ρ	:	Density.
P	:	Pressure.
R	:	Gas Constant (for air 287.1 kJ/kgK).
T	:	Temperature.
ε	:	Angle of deflection of light due to a density field.
ε_{min}	:	minimum detectable deflection with a given system, i.e. optimum sensitivity.
a	:	width of light passing both source and cutoff grids.
Δa	:	amount source grid image shifts relative to cutoff grid due to schliere.
k	:	resolving power of a lens (in line pairs per mm).
f	:	lens focal length.
A	:	lens aperture.
L	:	distance to source grid (from lens).
L'	:	distance to cutoff grid (from lens).
l	:	distance to test section (from lens).
l'	:	distance to image screen (from lens).
F	:	gap between cutoff grid and image screen.
S	:	source grid size.
I	:	image size.
e	:	width of source grid bands.
b	:	width of cutoff grid bands.
C	:	percentage cutoff.
n	:	cutoff grid spacing (in line pairs per mm).
m	:	magnification ratio of the test object.
m'	:	magnification ratio of the source grid.
E	:	Illuminance.
DU	:	depth of field.
w	:	resolution of test section.
λ	:	wavelength.
ϕ	:	number of overlapping images at any given point in image plane.

1 INTRODUCTION

Schlieren imaging has long been used as a method of flow visualization. The ability to 'see' air density variation enables the researcher to photograph phenomena in compressible flows, heat flows and chemical mixing processes. In practice, most schlieren systems are used for viewing high speed flows in shock tubes or supersonic wind tunnels.

Robert Hooke, in *Micrographia* (1665), first published a schlieren method, however it was August Toepler (1864) who first did much work on schlieren and succeeded in making it generally known. At the time, it was primarily used for optical component testing and for observing heat flows, such as the heat plume rising from a candle.

It is only in the last 60 years or so, owing to the widespread use of supersonic wind tunnels and shock tubes, that schlieren has come into general use. Now schlieren techniques have developed into many speciality methods, each suited to different applications.

Of particular relevance to the current research is the method of focusing (also known as large scale) schlieren in which two patterns are focused on one another to highlight bending light rays. A complete description of the operation is given in Section 1.3. The main benefit of focusing schlieren systems is to extend three limitations of conventional schlieren methods (Burton, 1949). These are:

- The field of view is limited to the diameter of the optics,
- Any striations in the entire system are visible in the image, not just those in the test section,
- And the light source needs to approximate a point source.

There is naturally a price to pay for these benefits, most notably alignment, sensitivity and manufacturing issues. The net result of these differences though, is that there exists another method of schlieren imaging which has significantly different and useful properties which make it a better flow visualization tool under certain circumstances.

A final year project done at the University of the Witwatersrand (Goulding, 2002), demonstrated that such a system could be constructed with a one meter test section relatively quickly and cheaply. The duration of the project was not sufficient to allow much refinement of the system however, and

several major flaws remained. This seems to be a trend in the published work as well and despite some excellent work in developing the field, most notably Fish and Parnham (1951) and more recently Weinstein (1993), who together develop all the fundamentals of focusing schlieren, there are still no comprehensive resources covering focusing schlieren.

In fact, about half the work done on focusing schlieren systems is done to extend the capabilities of the method to suit whatever the researcher is actually working on. This application driven approach has extended the boundaries of focusing schlieren, however it leaves many gaps.

For example, several focusing systems have been built for specific wind tunnels (Behun, 1956, Boedecker, 1959). The apparatus is specified but there is no comparison with a conventional schlieren system. One article (Rotem *et al*, 1969) describes the use of colour but they do not discuss the effects, limitations or uses to any great extent. Several authors (Settles, 1995, Peale and Summers, 1996) have proposed that the large size capability of focusing schlieren can be used to make systems for gas leak detection on industrial sites. No-one has actually built such a system however.

There is also a need to formalise the current literature in terms of the terminology. Names from Sharp Focusing Schlieren, Multiple Source Schlieren, Moire-schlieren, Negative Positive Schlieren and even Zebra Schlieren, to name a few, are all used to describe the same thing. On the other hand, there are two distinct methods of achieving the focusing effect, which few authors have acknowledged.

During the final year project, it also became apparent that a projected, and thus one ended, schlieren system might be possible, using the focusing schlieren technique with a retroreflective screen. This system has the potential to solve many of the problems that exist with current gas leak detection ideas. This needs to be investigated further.

1.1 Review of Schlieren Techniques

Schlieren has been defined as 'a local inhomogeneity, in a transparent medium, which causes an irregular light deflection' (Merzkirch, 1974) and as 'small gradient disturbances in inhomogeneous density fields' (Settles, 2001). Ultimately schlieren imaging is the process of making small ray deflections of light (or schliere) visible, usually on a screen or camera. There are as many methods of doing this as there are applications for which it is used. Normally schlieren is applied to visualising density variations in air due to high speed flows or heat.

1.1.1 Density and Light

There are two fundamental principles of schlieren in all its forms. The first is that light bends towards regions of higher air density. This is because the higher the air density, the higher the optical density (and refractive index) of the air and the lower the local speed of light. These differences are tiny, usually not changing the refractive index of air by more than the fourth decimal place, however it is enough to be detected.

The relationship between air density and air refractive index is given by (Holder and North, 1963):

$$n = k\rho + 1 \qquad \ldots 1$$

where n is the refractive index, ρ is the air density and k is the Gladstone-Dale coefficient (about 0.00023 m^3/kg for air). The deflection of a light ray can be found by integrating the deflection along the ray path, where the deflection at a point on the ray path is a function of the perpendicular refractive index gradient. This can be expressed mathematically as follows:

$$\varepsilon_x = \frac{1}{n_0}\int \frac{\delta n}{\delta x}\delta z \qquad \ldots 2$$

where ε_x is the deflection in the x direction, given that the undisturbed ray travels in the z direction. n is the local refractive index and n_0 is the refractive index of the surroundings. The same equation obviously holds for deflections in the y direction as well, provided x is exchanged for y.

The second operating principle of schlieren systems is that of background distortion. All schlieren systems rely on some sort of high contrast background (usually a light source with a narrow slit) which is distorted in a test section to form an image with lighter and darker patches corresponding to the deflected rays.

This principle is most obvious when observing the heat plume from a campfire or the jet exhaust of an aircraft as it passes the horizon, it is not the plume itself that is visible, it is the distortion in the background which enables the schliere to be seen. In a conventional system, an image of the light source is formed at the knife edge. A distorted image of the light source forms in a slightly different position due to a deflected ray, causing more or less light to get through to the image plane. From the image plane end, this is seen as a shift in the position of the background, namely the light source.

1.1.2 Conventional Schlieren

The development of conventional schlieren systems is not within the scope of this research, however a brief discussion of the basics is necessary for comparison with focusing schlieren systems. A modern Z-Type schlieren system is shown in Fig 1.1. It is by no means the only method but it is the most common and optically similar to most conventional methods.

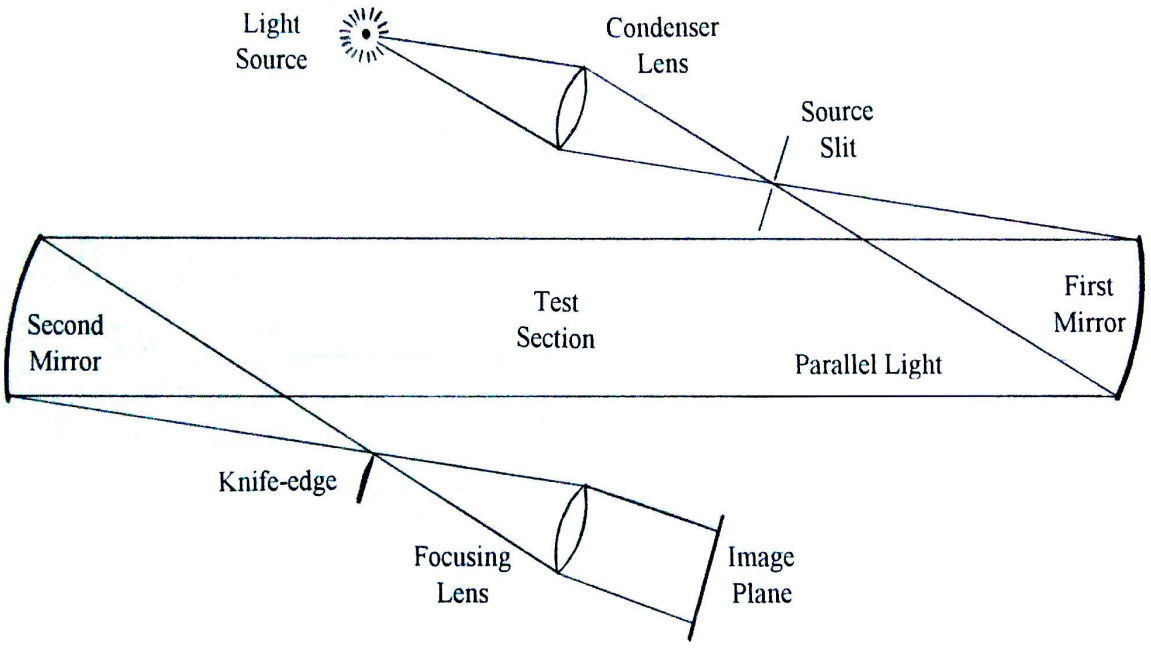


Figure 1.1 Conventional z-type schlieren system

In this system, a light source is focused by a condenser lens onto a source slit, usually about 1 mm wide and several millimeters long. This makes the system more sensitive in the 1 mm direction. The knife-edge is placed parallel to the source slit. The condenser lens should be chosen to project as much light as possible onto the first mirror.

The source slit is placed at the focal length of the first mirror to get a parallel beam of light from the mirror. After the test section, a second, usually identical, mirror is placed to focus the light down to an image of the source slit at its focal point. A knife edge is placed at the source slit image so that it blocks part of the image. The Z shape of the optical axis prevents the light source and imaging components from blocking the test section. By keeping the off-axis angles small and equal, most optical aberrations are kept to a minimum.

Finally another lens is used to focus the test section on the image plane. This lens is necessary to make a sharp image on the image plane. While a point light source would have infinite depth of field, a finite light source requires this lens to focus the test section sharply. The depth of field is very large though, so the exact position of the lens is not that critical.

The z-type arrangement developed from a system using lenses instead of the mirrors. The use of mirrors increases the diameter of the test section for a given cost, since mirrors are cheaper than similar sized lenses. Also on the plus side, mirrors prevent chromatic aberrations due to their reflective, rather than refractive, nature.

Unfortunately they suffer some drawbacks as well. They are prone to coma and astigmatism. This can be minimised by making the angles between the incident and reflected light rays as small as possible and by making the two mirrors identical. Also, they tend to be very far apart to prevent interference between the test section and the non-parallel sections of light. This allows air currents to become a problem, since they cause small density fluctuations which can be picked up in sensitive systems. Space for the system can also be a problem, though plane mirrors can be used to fold the optical axis. The size of the test section is limited to the diameter of the mirrors.

As a final note, the source slit and the knife-edge form conjugate optical planes. This means that they are focused on one another. It also means that different pairs of slit and knife-edge can be used for different effects. For example, a circular source with a circular knife-edge results in a system which is sensitive in both horizontal and vertical directions. Much work has been done on different

configurations, including the use of colour knife-edges, graded knife-edges (which fade gradually from black to transparent) and different knife-edge shapes. Settles' (2001) work contains a number of examples.

1.1.3 Range and Sensitivity

Two of the most important aspects of a schlieren system are its range and sensitivity. The sensitivity of a schlieren system is the smallest deflection of a ray (ε) that causes a noticeable change in the light intensity on the image plane. Generally this is accepted to be a 10 % change in the incident light (Settles, 2001). Thus if a 2 arcsecond ray deflection causes a 10 % change in contrast, the sensitivity of the system is 2 arcseconds.

Most schlieren systems have a finite light source which is focused onto the knife-edge. This means that none, some, or all of the light can be blocked, depending on the exact position of the knife-edge. The fraction of the source image that is blocked is called the percentage cutoff, thus if the knife-edge is set at 50 % cutoff, half the light is cut off. A typical knife-edge and source slit image are shown in Figure 1.2:

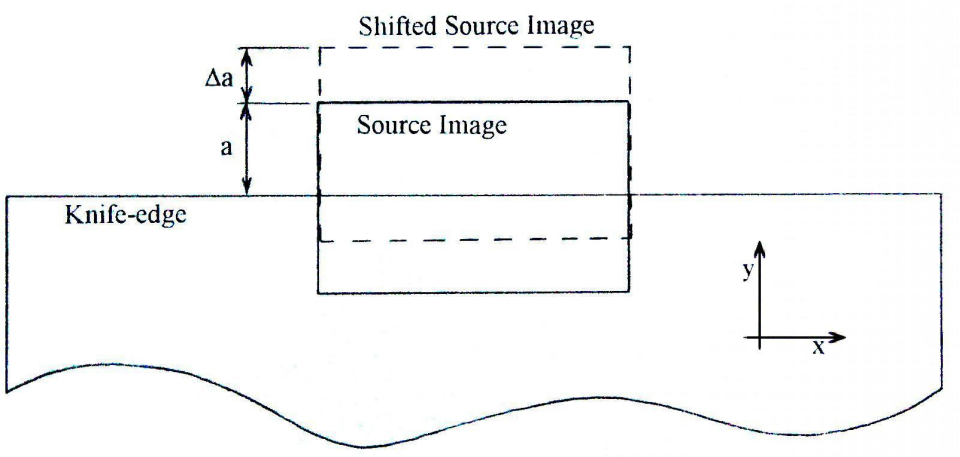


Figure 1.2 Interaction of a source image and a knife-edge

The height of the unblocked portion is denoted *a*. If a ray in the test section is deflected in the +*y* direction ('up') by a distance denoted *Δa*, it will allow more light to pass, causing part of the image to get brighter. Conversely if the ray is deflected down, less light gets through, causing part of the image to get darker. These brightness changes occur in the image plane in a position corresponding to the position of the ray deflection in the test plane.

Only changes in position perpendicular to the knife-edge make a difference. Thus assuming a horizontal knife-edge, the system will be sensitive to deflections with vertical components only. The horizontal component will be lost, since it makes no difference which part of the knife-edge cuts the light off.

As the gap, a, through which light can pass gets smaller, the ray deflections necessary to miss the knife-edge reduce. Also, the total quantity of light decreases, making a given deflection of light appear brighter. Thus the sensitivity can be improved by increasing the amount of light cut off by the knife-edge. Unfortunately, diffraction effects at the knife-edge limit how sensitive the system can become. The best achievable sensitivity is denoted $\varepsilon_{\min}$.

At 100 % cutoff, ignoring diffraction effects, the image is black and only light that is bent up will make any difference. Thus the system is only sensitive to density gradients in one direction.

When the cutoff is reduced, the image gets brighter (called brightfield) and the sensitivity gets worse. Also now, light deflected up can only increase the brightness slightly. Light bent down, on the other hand, can make part of the image quite a lot darker. Similarly, when the cutoff is increased, the image (now darkfield) is more sensitive, however it is affected more by light bent up than by light bent down.

This effect brings the discussion to the second aspect, the range of a schlieren system. Range is the maximum deflection which still results in a change in the incident light. Say a gradient in the test section causes a ray bundle to be deflected up. As the gradient gets stronger, the bundle is deflected more until it clears the knife-edge entirely. Once the ray bundle clears the knife-edge, deflecting it further no longer affects the image brightness. This is the range of the system. A similar argument holds for ray bundles deflected downwards.

Range and sensitivity are closely related, since the better the sensitivity, the smaller the range. Making the source slit smaller will both improve sensitivity and reduce range, as will increasing the cutoff. Thus, when making any schlieren system, the approximate ray deflections should be known, so that the system can be made to show them clearly. Typically, the range is about 20 times the sensitivity for conventional systems, though this depends on the components and geometry used.

Sensitivity and range are both angles measured in arcseconds. This extremely small measure is required to express the small deflections which arise from most schlieren objects. To give some examples, the heat from a human hand is visible at about 2 arcsec. A small reading lamp is about 10 arcsec while a candle typically appears to be about 20 arcsec. Shock waves can be anything from a few tens to a few hundred arcseconds, depending on the flow medium, density, Mach numbers and so on.

When the sensitivity is too poor, the resulting image has only vague areas which are slightly lighter or darker. The finer details of the phenomenon being observed are often lost. If the range is insufficient however, the image is a mess of black and white patches which make the image difficult to interpret. Ideally, all flow features should be easily seen and sharply focused, without being overpowering.

The sensitivity of schlieren systems can be improved further after the photograph has been taken. A few methods exist for developing film to enhance features, particularly pictures that are too dark or too light. The real improvement however, comes once the pictures are stored digitally. There are many software packages which allow for the manipulation of pictures and the results can be very impressive, particularly for poor pictures.

1.2 Optics

The following section is a brief summary of thin lens theory and some of the optical aberrations which were encountered. Most of it is paraphrased from Smith (1966).

When a light ray is transmitted from a region of one refractive index to another, the angle it makes at the plane of intersection is related by Snell's Law. This relationship is given in equation 3:

$$n_1 \sin(\theta_1) = n_2 \sin(\theta_2) \quad \text{... 3}$$

where n_1 and n_2 are the refractive indices of the two regions and θ_1 and θ_2 are the angles the ray makes with the plane of intersection. Using this relationship and assuming that the front and back surfaces of a lens are close together and planar, the thin lens approximation, given in equation 4, can be demonstrated.

$$\frac{1}{f} = \frac{1}{d_i} + \frac{1}{d_o} \quad \text{... 4}$$

where f is lens focal length, d_i is the distance from the lens to the image and d_o is the distance from the lens to the object. This is a simple equation for relating the position of an image for a lens based on the lens focal length and its position relative to the object. The object plane and the image plane form conjugate optical planes. That is, anything in either plane is focused to a corresponding position in its conjugate plane. This idea of conjugate planes is particularly useful in multi-element lenses and lens systems.

The equation is reasonably useful to get an idea of placement and geometry however it loses accuracy with thick or multi-element lenses. For accurate optical component design the paraxial theory (Smith, 1966) is much better and is now generally done on computer. This uses Snell's Law at each lens/air or lens/lens interface to calculate image positions. For this work however, the thin lens approximation is adequate. All final positioning was done by hand to ensure correct placement.

One of the results of current lens manufacturing techniques is that most lenses have some sort of aberration. The most common two are chromatic aberration and spherical aberration. Other

aberrations, coma, astigmatism and distortion, are less common though no less significant when they do occur.

Chromatic aberration occurs because the refractive index of most substances is a function of the wavelength of light. This means that blue light and red light have different ray deflections, by Snell's Law. The net result is that the blue light has a focal point which is closer to the lens than the focal point for red light because it deflects more. Achromatic lenses solve this by having two or more elements of different focal lengths and different refractive indices. The lenses are designed so that the chromatic aberration of the first element is cancelled by the equal and opposite aberration of the second.

Spherical aberration is caused by the fact that most lens surfaces are ground to a spherical surface, hence the name. A spherical surface does not bring all the light to one clear focal point. Instead, the rays striking the rim of the lens typically focus closer than those near the center. Aspheric lenses are ground to a slightly different shape which makes parallel light rays pass through the same focal point.

1.3 Focusing Schlieren

It has already been stated that focusing schlieren provides a number of differences from conventional schlieren. This section looks at how focusing schlieren works and where these properties come from. In addition, the literature is quite confusing with regard to names and methods. A multitude of different names have appeared in the texts for what is called focusing schlieren in this report. An attempt is made to formalise the current terminology.

Since the beginning of focusing schlieren, there have been two main methods of achieving the focusing effect. What is interesting is that very little attempt is made to separate them in the literature even though they are quite different. The two methods are described below. They are distinguished here by naming them multiple source schlieren and focusing schlieren, though they are both focusing techniques.

1.3.1 The Multiple Source Schlieren System

The first of the two systems is very similar to conventional schlieren with the exception of the light source and knife-edge. The light source is replaced by a set of light sources making up a pattern or positive grid. Generally speaking this is a set of grid lines, though it can also be as few as two point sources. Each source must have a corresponding knife-edge or negative grid. This can also be thought of as a conventional system with multiple sources, hence the name used here of multiple source schlieren. The basic system layout for a simplified system with two light sources is shown in Figure 1.3:

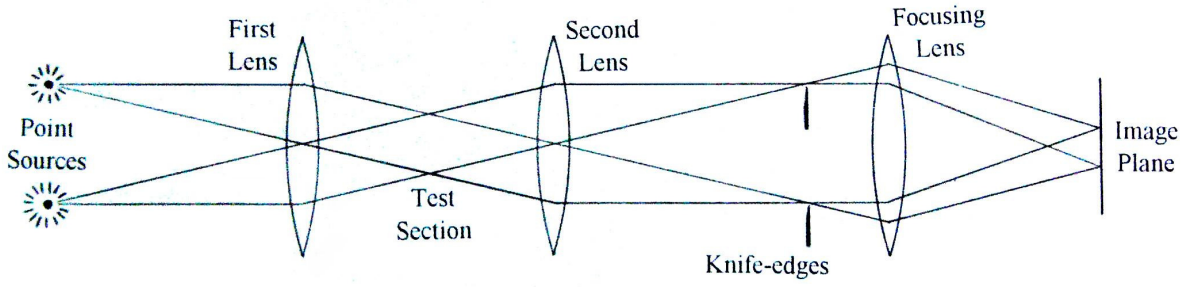


Figure 1.3 A multiple source schlieren system arrangement

Each light source can be regarded as a separate schlieren system, however an object placed at the refracting plane will be focused on the image plane by the focusing lens. Thus, while each system has infinite depth of field, the images from each source are only superimposed at the image plane. This gives the system its focusing effect, since there is a unique image plane for each refracting plane for which the two images superimpose exactly.

By adding more sources, such as a grid, the effect can be improved. Also, the full range of knife-edges possible for conventional systems, such as one and two dimensional, graded knife-edges and colour systems, can all be implemented with some thought.

Because of this arrangement's similarity to conventional schlieren, many of its characteristics are similar too. Like conventional schlieren, the test section size is limited by the size of the optics, although with this system the size of the test section is often smaller than the optics due to vignetting. Depending on the size of the light source, the test section is usually about two thirds of the diameter of the lenses (Fish and Parnham, 1951). The sensitivity equations for a conventional system will hold for a multiple source system, though there are added equations for depth of field.

The differences are in the focusing effect and in the range of the system. Normally, once the range is exceeded, a conventional system can no longer distinguish angles of deflection. However, with a multiple source schlieren system, if the sources are close together, such as with a grid type source, it is possible for the light source of one system to interact with the knife-edge and gap of an adjacent system.

This can be a problem if conventional schlieren pictures are desired but can also be used to create isophotes or lines of constant deflection. With enough lines the pictures begin to look like interferometry pictures and this can be quite useful for quantitative studies, since each light/dark interface corresponds to a known deflection. Practically such a system might require unrealistically high resolution lenses and very accurately aligned grids.

The advantages and disadvantages of a multiple source schlieren system are summarised below:

- Focuses on a 2D plane within the test section, thus reduced noise from out of test section disturbances.
- Similar to conventional schlieren from a design and mathematical point of view.

- Sensitivity is theoretically as good as a conventional system.
- Smaller test section than conventional schlieren due to vignetting.
- Lenses (or mirrors) must be good quality, particularly with regards to off axis aberrations.
- Setting up conjugate knife-edges to their sources can be difficult, particularly to get constant cutoff at each knife edge. Grids can be used to simplify alignment matters but then construction and accurate positioning of suitable grids becomes a problem.

1.3.2 The Focusing Schlieren System

The second focusing system is a more commonly used method to achieve the focusing effect than the first and works on a slightly different principle to conventional schlieren. A schematic of the arrangement is shown in Figure 1.4:

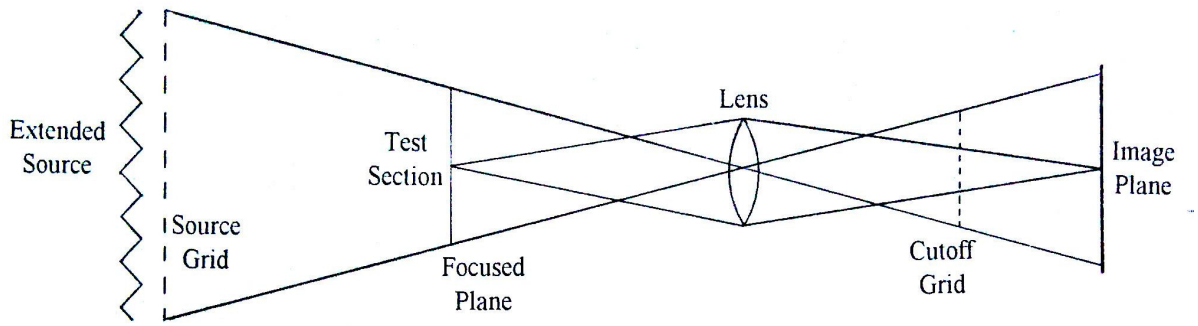


Figure 1.4 A focusing schlieren system arrangement

An extended light source is used to backlight a source grid. The source grid generally consists of closely spaced black and transparent stripes evenly spaced. The light passes through the test section to the lens, which focuses the source grid onto a cutoff grid. Ideally the cutoff grid is a perfect negative of the source grid image. Each bright band of the source grid is like a source slit and each corresponding black band in the cutoff grid is the corresponding knife-edge. By adjusting the position of the cutoff grid minutely, varying cutoff between 0 % and 100 % is possible.

The lens also focuses the focused plane in the test section onto the image plane. For an undeflected ray in the focused plane, since it comes from a bright band in the source grid, the ray is blocked by the cutoff grid, assuming 100 % cutoff. A deflected ray will pass through the cutoff grid, assuming

the deflection is not sufficient for the ray to be blocked by the next dark band in the cutoff grid (i.e. the range of the system has not been exceeded), thus creating a bright region on the image plane.

For 0 % cutoff, the dark bands in the cutoff grid overlap the shadows formed by the source grid image. In this case, undeflected rays pass through, while deflected rays are cut off causing dark regions on the image plane. For cutoff values between the 0 % and 100 %, ray deflections will cause the image plane to get brighter for deflections in one direction and darker for deflections in the opposite direction.

A deflection in the focused plane only affects a small region on the image plane because the lens focuses the deflection on the image plane in a position corresponding to that deflection. Conversely, ray deflections which occur far from the focused plane will still cause light to pass the cutoff grid however it will not be focused when it reaches the image plane. Thus it will cause a small brightness change over a large area, rather than a large brightness change over a small region. This is how the focusing schlieren system focuses on a single plane, simply through the focusing properties of the lens itself.

The above description makes a number of assumptions, including: the cutoff grid is a perfect negative and perfectly positioned, the lens is infinitely sharp and free of aberration, the source grid consists of sufficiently small gridlines and diffraction effects are ignored. Some of the more practical aspects of each of the components are discussed below.

There are many different ways of achieving an extended source and this can have a large effect on the rest of the system. Early systems employed a diffuser screen lit from behind by a powerful lamp. Unfortunately this results in uneven illumination of the diffuser screen, being brighter in the middle and darker at the edges. The modern approach however, is to use a backlit Fresnel lens in place of the extended source. This ensures that the maximum amount of light possible goes through the lens and provides more or less even illumination over the entire area.

Unlike conventional schlieren systems the lamp does not have to be as small and as bright as possible, in fact neon tubes in a light box would work quite well. This is because the source grid is the actual 'source' used by the system. It is the width of the source gridlines which define all the characteristics of the system, not the size of the lamp filament.

The source grid can also have many variations. In fact, it does not have to be a grid at all. A grid of evenly spaced vertical lines is the most common form of source grid used and it is easy to describe the operating principle using a grid, hence the generalisation. A vertical grid will only detect horizontal deflections (i.e. horizontal density gradients). Similarly a horizontal grid will only detect vertical deflections.

There are several advantages to using grids. These are that the construction and alignment is greatly simplified, the percentage cutoff can be varied easily and constantly over the whole area and the meaning of the images is clear. The only disadvantage is that the system can only detect density gradients in one direction.

Systems detecting gradients in two directions are certainly possible as is the use of colour, they are just harder to implement. For example, the source grid could consist of a black panel with a pattern of small circular holes allowing light through approximately 50% of the area. The cutoff grid would then consist of a pattern of black circles on an otherwise transparent film. In principle this would work perfectly, however alignment would be more difficult and the percentage cutoff could not be changed without changing the cutoff grid.

The lens in the system has to focus the source grid onto the cutoff grid with very little or no distortion. It also has to focus the test section onto the image plane. The lens has to be selected carefully from the requirements of the system. It affects the system in many ways, from sensitivity to image size to the overall length of the system and thus it will be discussed more in the design section.

Once again, the advantages and disadvantages of the system are summarised below, as compared to a conventional schlieren system:

- Focuses on a 2D plane within the test section, thus reduced noise from out of test section disturbances.
- The size of the test section is independent of the optics, thus very large fields of view are possible at relatively low cost.
- The light source does not have to be a very bright point-like source.
- Less space is required either side of the test section than for a conventional system.

- Source and cutoff manufacture is a problem, due to the very high accuracy required over a large area.
- Alignment of the cutoff is difficult, particularly with respect to achieving constant cutoff over the whole area.
- The sensitivity is typically not as good as a conventional system. This is related to the lens quality and the difficulty of alignment.
- There are potential problems with 'banding' and diffraction (described in the design section).

Initially, this description sounds very similar to the multiple source schlieren system however there are a few important differences. First, in the multiple source system, each source slit is expanded to pass through the entire test section, thus a ray deflection near the edge of the test section will affect every light source/cutoff pair. In a focusing system, each source passes through a different part of the test section. Thus a ray deflection near the edge will only affect those rays near that edge.

The second main difference is that in a multiple source system, each source illuminates the entire image plane and all the images overlap. With a focusing schlieren system, each source illuminates only a part of the image plane. Because the spacing of the sources is so close, the image formed by each overlaps most of its area with the adjacent system. This overlay of all the images forms the full picture. Stated another way, if one of the source slits is blocked in the multiple source system, the entire image gets dimmer by a small amount. Blocking one source in the focusing system causes a specific region within the image to get darker.

The final major difference is that in a multiple source schlieren system each individual system has a very large depth of field and it is the overlapping of the images which causes the focusing effect. In a focusing system, each individual system focuses its part of the image before they are overlapped. Another result of this is that the focusing schlieren system typically has a narrower depth of field than a multiple source schlieren system.

In summary, if the multiple source schlieren system is considered to be a set of conventional systems all sharing a common optical axis and image but each offset by different amounts from the optical axis, the focusing schlieren system can be considered as multiple adjacent systems all with slightly different optical axes and with partially overlapping images.

Ultimately, it is the properties of the focusing schlieren system which are of interest to this report, specifically the large scale, low cost capabilities. The multiple source schlieren system, while a focusing method, is not capable of large fields of view and is thus not taken any further. In particular it is the capabilities of the retroreflective system which has the most potential for large scale application. This special case of a focusing schlieren system is discussed below.

1.3.3 The Retroreflective Focusing Schlieren System

Retroreflective material is any material which reflects light back at its source. It can be paint or a fabric and is primarily used for road signs and high visibility clothing to make them more visible at night. Typically small glass spheres are used since they reflect a large quantity of light back at the source through total internal reflection. They scatter a large portion of the incident light, however they do reflect a much greater amount back at the source than in any other direction. More information on the properties of some retroreflective screens for use in schlieren and shadowgraphs can be obtained from Winburn *et al* (1996), though any retroreflective material will work.

By using bright lights in front of the source grid, near to or co-axially to the lens, the light is reflected back, simulating a large crude spherical mirror of variable focal length. The focal length is half the distance between the light source and the screen. A large scale system using a retroreflective screen is shown in Figure 1.5:

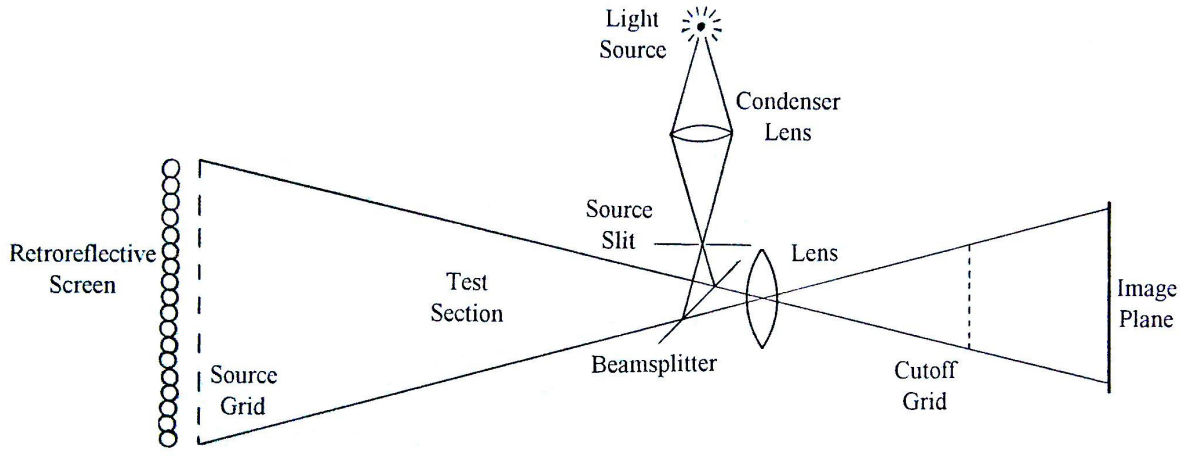


Figure 1.5 Large scale retroreflective focusing schlieren system

Except for the retroreflective screen which replaces the light source, the system is identical to a focusing schlieren system. The image and light source have to have nearly the same optical axis, so either a beam splitter is required or the light source must be placed very close to the lens.

The primary advantage to using a retroreflective screen is the fact that it can be virtually any size for very low relative cost. At the time of writing, a one meter diameter concave mirror costs roughly 250 times the cost of the fabric or paint required to make a one meter test section retroreflective system. To simplify construction, the source grid is usually painted or bonded onto the screen rather than being a freestanding component.

1.4 Historical Development

The origins of focusing schlieren are a little ambiguous. Settles (2001) credits Schardin (1942) for the first published work, however Schardin, who called it schlieren method no. 4, credits H. Maecker for the invention. Mortensen (1949) on the other hand credits Mr F. Larris with the invention at the suggestion of Dr J. Hartmann (1940) who in turn published notes on the method. Both of these publications refer to a focusing system as opposed to a multiple source method.

Whatever the origins, three authors (Burton, 1949; Mortensen, 1949 and Kantrowitz and Trimpi, 1950) each published a work dealing specifically with focusing schlieren methods at about the same time.

Burton used what is called the focusing schlieren technique in this report, though he originally referred to it simply as a 'modified schlieren apparatus' and in his later work (1951) as the 'multiple source schlieren system'. Burton's system layout is shown in Figure 1.6:

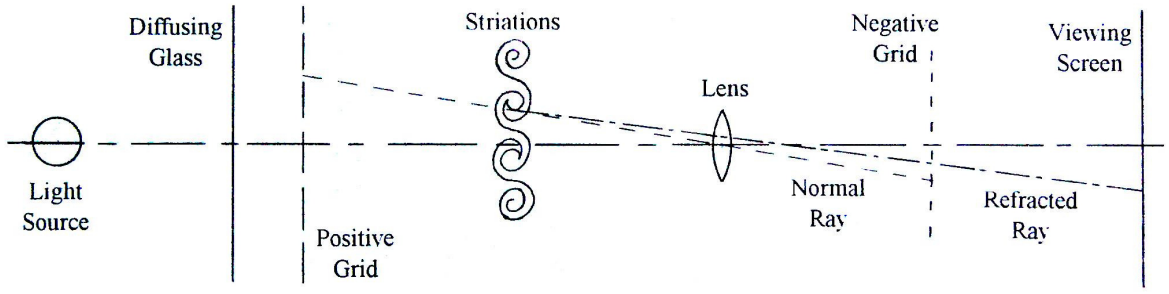


Figure 1.6 Burton's focusing schlieren arrangement (Burton, 1949)

As can be seen Burton used a backlit diffuser screen to achieve an extended light source. His source grid was a sheet with very many pinholes to act as individual sources, thus giving a system capable of detecting deflections in two dimensions. The cutoff grid was constructed by placing a photographic plate in place of the cutoff grid and exposing it. Once the negative was developed, it was used for the cutoff grid.

Most authors have subsequently used this technique to produce the cutoff grid. It has the advantage of creating a very accurate cutoff and has the additional benefit of coping with any distortions in the

lens. There are three main disadvantages to this method. Firstly the film negatives can warp with time. Additionally, the focus has to be perfectly sharp when making the cutoff. Finally, the contrast ratio between the bright and dark parts of the resulting cutoff has to be sufficiently high to allow light through the clear parts while blocking light at the dark parts.

Burton seems to be the first and one of a few authors who note the large scale possibilities of this schlieren method. He also mentions the other main advantages of focusing and the ability to use an extended light source. While Burton obviously had a good understanding of the system and its possibilities, he did not obtain particularly clear results from his system.

He later published a second paper (Burton, 1951) which discusses a few of the problems of focusing schlieren and some methods to prevent them. The first of these is the grating diffraction effect at the grids, as a result of using very fine grids. For this he proposes a formula as an aid to designers to prevent this from occurring. The formula, converted to the units used throughout this work, is given in equation 5:

$$Fn^2 \leq 800 \qquad \text{... 5}$$

where F is the distance between the image plane and the cutoff grid and n is the number of gridlines per mm in the cutoff grid. He also proposed a formula to prevent a phenomenon now called banding where the cutoff grid casts a shadow on the image plane if the gap between them is too small:

$$F \geq 40\frac{f\#}{n} \qquad \text{... 6}$$

where $f\#$ is the f-number of the lens. Both of these criteria have now been superseded by more accurate and less conservative guidelines. Finally, Burton also discussed a few of the practical issues of grid manufacture and gives a mechanical design for the lens, cutoff and camera part of the system.

Mortensen (1949) also describes in detail a focusing schlieren system, much the same as Burton's. The main difference is the use of a large condenser lens for the light source, instead of a diffuser. This significantly improves the brightness and uniformity of the images. He states the main advantages of the system as larger test sections, brighter images and a shorter overall system length compared to conventional schlieren methods. Mortensen primarily deals with conceptual discussions

of how the system works, rather than the practicalities and does not present any images obtained with the system.

Kantrowitz and Trimpi (1950) discuss in detail a multiple source schlieren system. The system used consisted of four achromatic lenses and an extended source grid of 0.1 mm lines spaced 0.9 mm apart. The system had a test section of about 40 mm diameter due to vignetting. They demonstrate three different examples of how this system focuses on a specific plane without noticeable interference from other disturbances as compared to a conventional system, such as from distorted glass windows and boundary layers. In addition, they demonstrate that by blocking specific source grid slits, they could prevent unwanted reflections from components in the test section. The net effect of this is to reduce the overall light level slightly and remove the reflection, without otherwise affecting the final image. They appear to have obtained their best pictures with sensitivity at its lowest, as this means the cutoff grid can be most crudely aligned. They also appear to have had some trouble with grid construction and alignment.

Each of these three authors worked on, and wrote about, practical systems which were constructed and tested, however very little emphasis had been placed on the conceptual and design aspects. This changed when Fish and Parnham (1951) published a paper focusing mainly on the mathematics, the design and the operating principles of three focusing schlieren systems. The three systems include both focusing (after Burton) and multiple source (after Kantrowitz and Trimpi) schlieren systems. In addition, they investigate the possibility of an enlarged source grid to simplify the construction of the grid. This concept was soon dropped however, as the difficulties outweighed the benefits of such an arrangement. The analysis is a comprehensive account of the relationship between geometric variables, such as the size of the source grid and the lens focal length, to the characteristics of the system, such as sensitivity and range.

While the analysis is largely mathematical, they do compare the practical aspects, such as construction and alignment of cutoff grids and sources of error. It is somewhat longer than a typical paper, thus affording a more detailed description than most papers. Until Weinstein's work (1993), this was the definitive work on focusing schlieren systems.

In 1959, Boedecker completed a Master’s thesis involving two main sections. The first was a comparison of three different focusing schlieren arrangements on a mathematical level. The first of these is a moiré schlieren system in which the source and the cutoff grid are both placed upstream of

the lens, either side of the test section. The next two are very similar to the focusing and the multiple source schlieren arrangements described above. The second section is the design and building of a particular system for a transonic wind tunnel. By a comparison of the results of the first section, a focusing schlieren arrangement was selected and a system was built, tested and described.

Between 1960 and 1990, little work was done on focusing schlieren methods themselves. Generally speaking researchers focused more on their applications than the method used for obtaining results. There are studies of chemical explosions (Groves, 1960), flat flames (Dixon-Lewis and Isles, 1962) and fire spread studies (Butler, 1974). Holder and North (1963) mention both the focusing and multiple source schlieren methods under the names 'Methods for Large fields' and 'The Sharp-focus Method' respectively however this is simply a summary of their operation.

Some authors did expand the method to allow them to visualise their application better. Buzzard (1968) extended the method for high speed photography, Rotem *et al*. (1969) used a coloured cutoff grid with a multiple source system, though with only a very few sources, Bowker (1970) constructed a system large enough for a 5 foot transonic wind tunnel and Waddell (1982) introduced a retroreflective screen into the system.

This slow and rather haphazard progression changed when Weinstein (1991 and 1993) published a set of equations which describe focusing schlieren systems very simply and concisely. The paper served not only as a summary of the best methods to date but also allowed the reader to design a system based on their own requirements, such as test section size, available resources, sensitivity and focused depth of field. This paper forms the basis of the analysis and nomenclature which follows in section 3 and so will be described more fully in that section.

Since this paper, there have been many articles using Weinstein's method to construct a system but only a few have been on advancing the theory. Collicott and Salyer (1994a and 1994b) and Salyer and Collicott (1996) have investigated the noise reduction capabilities of focusing schlieren systems, using Fourier optics. Noise in this sense is density variations outside the test section. Hanenkamp *et al.* (2000) also provide a Fourier description of a multiple source schlieren system and demonstrate how additional sources can be added to a conventional system to give a focusing effect.

There have been several other articles on improvements to the basic method. The first of these is the development of an adaptive cutoff grid by Downie (1995). This consists of a thin film of

bacteriorhodopsin, an organic protein which changes from black to transparent when exposed to yellow light (570 nm). It can be made to change back again by exposure to blue light (410 nm). A laser at each wavelength passes through the source grid however one laser is used to force the source grid image to form on the bacteriorhodopsin film, thus causing a perfect cutoff grid to form. With a now perfectly aligned cutoff grid, the second laser is passed through the test section and through the grid. While the wavelength of the first laser was designed to change the BR film, the wavelength of the second is chosen to have as little effect as possible. This means that the light from the second laser is cut off by the cutoff grid.

The advantage of this system is that the cutoff grid is perfectly aligned, since the resolution of the BR film is several thousand line pairs per mm. Also, lens defects are compensated for and the time taken to change setup is reduced. There are, however, many disadvantages. The contrast ratio (ratio between the quantities of light passing through the transparent parts of cutoff grid relative to the dark parts) is time dependent, and about 8.5 to 1 after only 30 seconds. Also, the nature of the bacteriorhodopsin used is important as it can be varied considerably in terms of reaction rate and stability. Another issue is the cost and complexity of setting up and aligning a two laser system. Downies work was extended by Peale *et al.* (1997) to be used with a white light source with coloured filters.

Another interesting development is that of a holographic system by Doggett and Chokani (1993). This consisted of a focusing system in which a holographic plate was exposed to take the picture. By reconstructing the hologram, a fully three dimensional density image results, where moving the image plane corresponds to different planes in the flow field.

Probably the most significant diversion from the basic method is the exploitation of the large scale capabilities of the focusing schlieren system. While several relatively large scale systems have been constructed (Behun, 1956 and Bowker, 1970), the introduction of a retroreflective screen by Waddell (1982) is really the starting point of a large system.

More recently, Settles *et al.* (1995) has revealed a large scale retroreflective schlieren system with a 2.1 by 2.7 meter test section. Since then he has published a large number of papers dealing with a multitude of examples, from air ventilation flows (Settles, 1997) to aviation security (Settles, 1998) and more recently outdoor gunshot shockwaves (Settles *et al*, 2004). His book (2001) also contains a comprehensive summary of large scale techniques.

With a large scale system, it has been suggested that it would be convenient to use this method for detecting gas leaks on industrial sites. Finding leaks currently involves using very expensive chemical 'sniffers'. To solve this problem, Peale and Summers (1996) proposed a mobile retroreflective system. Later, Settles (1999) proposed a scanning method, in which a long thin light source is traversed across a test section and a corresponding knife edge is moved at the same time to form a schlieren image on the film plane. While no system was built, similar work by Weinstein (1994 and 1997) has demonstrated that such an approach can be used for outdoor schlieren photography. Technically this is not a focusing schlieren system but it deserves mention due to its large scale capabilities.

Another large scale method not investigated but deserving a reference is the Background Oriented Schlieren, or BOS, method (Richard *et al.*, 2000). In this, a photograph of a textured background is taken before and during a test. By comparing the two pictures, the distortion of the background can be used to provide deflection information. This in turn can be converted into equivalent schlieren or shadowgraph pictures. Since 2000, much work has been done in this field.

2 OBJECTIVES

For the purposes of this research, the multiple source schlieren system is not really useful, owing to the limited test section size and its expense. While it undoubtedly has a niche, namely reducing noise through focusing of conventional systems, it does not have the capability of a focusing schlieren arrangement for large scale and low cost construction.

The experimental part of this research can be loosely grouped into two parts. The first involves experimenting with different source and cutoff combinations for a focusing schlieren system, testing system limits and optimising the design. The second part is the development of novel and almost novel arrangements, to demonstrate some of the unexplored possibilities of focusing schlieren systems. Hopefully it will also fill in some of the gaps in the published literature. In addition to the experimental research, some more mundane objectives have to be realised first. These include the construction of a suitable apparatus and the relevant literature research.

The individual objectives for the first section are described below:

- Make and test different source grid line spacing to determine the optimum grid spacing, as well as examining the limits of banding and resolution.
- Make and test differing amounts of light passing the source grid for a given line spacing to see if improvements can be realised.

The objectives of the second part of the research project are to:

- Make and test a 2D arrangement involving various patterns of dots and holes.
- Make and test colour systems.
- Make and test a 1D retroreflective system.
- Make and test a 1D projected retroreflective system.

Each of these tests will be described completely in Section 5.

The purpose of the first part of the research is to compare a wide variety of source and cutoff pairs to find out what is possible and what works well. This should also find and examine the limits of the

system. In addition it provides a basis of knowledge for the comparison of the additional systems in the second part of the research.

The second part of the research focuses specifically on comparing several different configurations. It starts with the use of two dimensions, which has been largely forgotten since Burton (1949), and discusses colour systems. A retroreflective method is compared to the basic arrangement to determine what penalties are paid to achieve a very large test section area. Finally, a new method, using a projected source grid on a retroreflective screen is demonstrated and evaluated. This new configuration in particular holds potential as an easy to set up and use system. Wherever possible, anything learnt which may aid the future researcher will be noted.

2.1 Scope of research

While it is very tempting to list every aspect of focusing schlieren which can be improved and then work on it, this is a process that never ceases. It is therefore necessary to establish some limits of the research. Thus the following limits will be imposed:

The work will be focused on the focusing schlieren method and will be aimed generally at methods that can be applied to large scale systems. While there are other methods of producing large scale schlieren images, such as background oriented schlieren (BOS) methods and large mirror systems, these will not be examined.

The work will further be restricted to the construction of one set of apparatus for conducting experiments. It would be desirable to include the design and building of a portable, large scale, projected schlieren system but this will have to be excluded. The principles of the system will still be investigated however.

No new digital post processing will be done. This is a huge field of knowledge in its own right. While digital post processing methods will be used to improve the quality and sensitivity of the images, it will not be developed further. Existing methods will be used.

A few authors have made extensive use of Fourier optics to describe the operation (Hanenkamp *et al*, 2000) and noise characteristics (Collicott and Salyer, 1994, Salyer and Collicott, 1996) of focusing

schlieren systems. The analysis and use of Fourier optics will not be covered by this research. In general, simple ray tracing methods are used for designing systems and the more empirical approach of comparing results is used for evaluation. The focus is not on the mathematics itself but rather on real life appearance of the images.

In essence, the work will be focused on trying out different configurations of focusing schlieren systems and comparing the results. The emphasis will be placed on finding the limits of use and the benefits of each method. The scope will be limited to trying different layouts, different patterns and trying a projected system.

3 SYSTEM ANALYSIS

This section looks at overall system design from a conceptual and mathematical point of view. Actual component level design is covered in the section on apparatus (Section 4). This section starts with a derivation of the mathematics, is continued with a list of possible further assumptions and discusses a general design process. The section on apparatus will discuss the specific design of the system used for this work.

3.1 Derivation of Mathematics

The analysis below is true for focusing schlieren systems, not for multiple source schlieren systems. Detailed mathematics relating to multiple source schlieren systems can be obtained from Fish and Parnham (1951) or Boedecker (1959). While Weinstein (1993) has a complete mathematical description, it is very brief. It is elaborated on here with some help from Settles' (2001) work. To simplify the derivation, a focusing system comprising two grids is considered throughout. This is a mathematical convenience since it then becomes essentially a two dimensional system. Figure 3.1a and Figure 3.1b contain all the dimensional variables used for dealing with focusing schlieren systems.

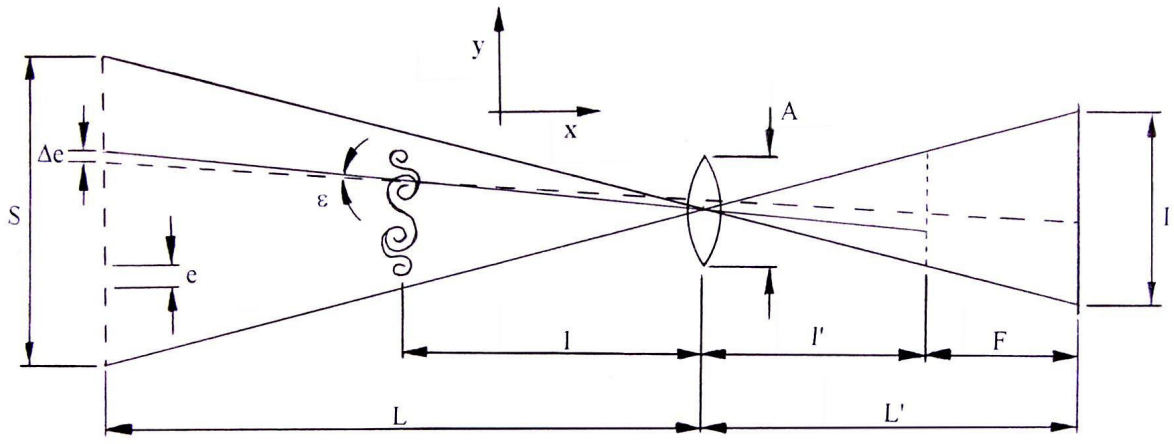


Figure 3.1a Large scale schlieren system showing variables

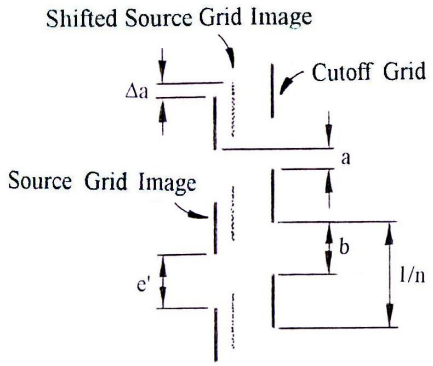


Figure 3.1b Focusing schlieren grid variables

3.1.1 System Basics

To begin the analysis it is necessary to apply the thin lens approximation (eqn. 4), apply geometric relations and define the magnification, thus:

$$\frac{1}{f} = \frac{1}{L} + \frac{1}{L'} = \frac{1}{l} + \frac{1}{l'} \quad \text{... 7}$$

$$m = \frac{l}{l'} \quad \text{... 8}$$

$$m' = \frac{L}{L'} \quad \text{... 9}$$

$$e' = \frac{e}{m'} \quad \text{...10}$$

$$F = l' - L' \quad \text{...11}$$

where f is the focal length of the lens, m' is the magnification ratio of the grids, m is the magnification ratio of the test section and image plane and all other variables are defined in Figure 3.1.

The interaction between the source grid image and the cutoff grid causes the schlieren effect, thus, the design of the grids used has wide ranging effects on the system characteristics. A grid has five variables, of which any two uniquely define the grid. These are the width of the clear and the opaque lines (in mm), the grating parameter or grid spacing (the distance from a point on one line to the corresponding point on an adjacent line in mm), the line density (in line pairs per mm) and the percentage area which is blocked by opaque lines.

3.1.2 Sensitivity

In a focusing schlieren system, the spacing of the source grid is a major factor determining the practical sensitivity of the system. The ability of the lens to project an image of the source grid is limited by the lens resolving power, *k*. As the lines in the source grid image become thinner, so they become less distinct until they disappear completely. For a lens with aperture *A* and a resolution of *k* lines per mm, the minimum width of *a*, the height of one distinct stripe of the source grid image projecting past the cutoff grid is:

$$a = \frac{2}{k} \qquad ..12$$

since it takes 2 line pairs to define the bright band *a*. From the definition of sensitivity (Section 1.1.3) it can be shown that best sensitivity occurs when:

$$\frac{\Delta E}{E} = \frac{\Delta a}{a} = 0.1 \qquad ..13$$

where ΔE and *E* are the change in illuminance and base illuminance of the image plane, respectively and Δa is the change in source grid image position due to a ray bundle passing through a density gradient. The source grid image shifts because the source grid itself appears to shift from the lens's perspective by a distance Δe. From similar triangles we have:

$$\frac{\Delta e}{L} = \frac{\Delta a}{L'} \qquad ..14$$

where Δe is the apparent change in position of the source grid due to the density gradient as seen by the lens. The apparent movement Δe is caused by a deflection in the test section between the test section and the lens. Thus:

$$\Delta e \approx \varepsilon\left(L - l\right) \qquad ..15$$

since tanε tends to ε as the angle of deflection tends to zero and the angles dealt with here are exceptionally small. Replacing Δe in eqn. 14 with the value in eqn. 15 and rearranging for Δa gives:

$$\Delta a = \frac{\varepsilon(L-l)L'}{L} = \frac{\Delta E}{E}a \qquad ..16$$

which is equated to Δa from eqn. 13. This is stated by Fish and Parnham (1951), without proof. Rearranging for ε at minimum detectable contrast gives:

$$\varepsilon_{\min} = 0.1a\frac{L}{(L-l)L'} \qquad ..17$$

Assuming that the test section is located midway between the source grid and the lens (I.e. l = ½L) and knowing that there are 206265 arcseconds in a radian, this simplifies to:

$$\varepsilon_{\min} = 41253\frac{a}{L'} \qquad ..18$$

At this point, Settles (2001) states that L' is approximately the same as f (the lens focal length) for very large systems, thus:

$$\varepsilon_{\min} = 41252\frac{a}{f} \qquad ..19$$

However it is worth including all the terms for smaller systems. From the thin lens equation (eqn.4):

$$\varepsilon_{\min} = 41253a\left(\frac{1}{f}-\frac{1}{L}\right) \qquad ..20$$

This equation gives the sensitivity of a focusing schlieren system as a function of three basic variables which can be chosen by the designer. In order to make the system as sensitive as possible, it is necessary to keep the distance between the source grid and the lens, L, as small as possible, while

using a lens with as long a focal length, *f*, as possible. Typically *L* varies from approximately 4*f* for small systems to about 12*f* for large ones.

The dimension of the light passing through both grids, *a*, must be kept as small as possible without exceeding the resolving power of the lens or causing diffraction effects (discussed later). This is simply a case of adjusting the percentage cutoff caused by the cutoff grid. Using less than optimum cutoff will reduce sensitivity linearly with cutoff percentage while using too much cutoff will blur the schlieren object or cause diffraction blurring of the image or both, depending on which limits are exceeded.

To conclude this discussion on sensitivity, a note must be made concerning the source grid bright band width, *e*. While it has no effect on the best sensitivity, it has an effect whenever less than ideal cutoff is used. At 0 % cutoff, the value of *a* is equal to *e*', thus the sensitivity is indirectly a function of *e*. At any value of cutoff between 0 % and optimum cutoff, the sensitivity varies linearly between the best sensitivity and that obtained using $a = e'$. The full effect of varying the source grid spacing will be investigated further in the experimental section of the report.

3.1.3 Range

As with conventional schlieren, the range in the 'up' and 'down' directions will not be the same for cutoffs other than 50%. In the case of focusing schlieren systems, it can be seen from Figure 3.1b that the range of the system is exceeded if:

$$a + \Delta a > b \quad \text{or} \quad a + \Delta a > \frac{1}{n} - b \quad \text{or} \quad a + \Delta a < 0 \qquad ..21$$

The first two conditions are exclusive, only one or the other applies. If the bright bands (width: *b*) on the cutoff grid are narrower than the dark bands (width: *1*/*n* - *b*), the first condition applies. If the dark bands are narrower, the second applies. If they are equal widths, both conditions will be met at the same time. The third condition indirectly sets the range to ten times the sensitivity in the -*y* direction (down), due to the definition of sensitivity (since $\Delta a = 0.1\ a$).

Unlike a conventional schlieren system which, once the range is exceeded, merely fails to register any further change, the repeated nature of a grid system means that once the range is exceeded, the shadows start to get light again. This can result in a series of light and dark density gradient contours for very strong schlieren objects. While not a big problem, it does make images more difficult to interpret. The sensitivity of a system with 0 % cutoff is equal to the range of that system.

3.1.4 Depth of Field

In order to optimise the depth of field, it is first necessary to define it. Roughly speaking it is the depth (in the *x* direction) either side of the test plane which can be regarded as focused. Obviously, there is no sharp line at which things stop being in focus, however a rough definition exists based on the angle made between a point on the test plane and the extremities of the imaging lens (Weinstein, 1993):

$$DU = 4\frac{l}{A} \qquad ..22$$

where DU is the depth of field of the image plane and 4 is an arbitrary constant chosen from experience. While the equation is useful to get a rough idea of depth of field and gives a means for comparing designs on paper, it is not going to give an exact answer to which items in the test section will be in focus. From the equation, it is necessary to use a large aperture lens and to keep the test section close to the lens, in order to keep the depth of field as small as possible.

3.1.5 Image Resolution

The image resolution is not the resolving power of the lens; it is the resolution of the schlieren object. For example, if a candle is in the test section, the resolution of the gas field above the candle is the image resolution. Obviously if the resolution gets too low, the finer details of the schlieren object become lost or blurred in the general background.

The main cause of loss of resolution in focusing schlieren is diffraction at the cutoff grid. When light passes through a slit, it is diffracted, causing it to change into a fuzzy central band with a pattern of

fringes either side. As the slit gets narrower, this effect can cause a sharply focused object to become surprisingly blurry. Jenkins and White (1950) define the resolution limit of light passing through a slit as:

$$d = \frac{F\lambda}{b} \qquad ..23$$

where d is half the width of the central bright band in the image plane, F is the distance between the slit and the image plane, λ is the wavelength of light and b is the slit width. Weinstein (1993) concludes that since $F = (l'-L')$ and moving the resolution from the image plane to the test section (by dividing by the magnification, m), equation 24 results:

$$w = \frac{2(l'-L')\lambda}{mb} \qquad ..24$$

where w is the resolution of schlieren features in the test plane. Generally even one line per mm is enough to be able to distinguish most flow features. If the magnification or the cutoff grid lines are too small, or if the gap F is too large, resolution can become a problem. Generally speaking, if F is large, then m and b are as well, so resolution is quite stable. The main problem occurs when trying to design systems to have a small image size, such as for a 35 mm camera. Image resolution is most easily varied by changing the size of the source grid slits (and hence b) however, this soon becomes a compromise between resolution and sensitivity. Technically, the source grid will also cause diffraction but this is not a problem, as the grid itself is seen as the light source of the system. Scattered light at the source will not affect the operation of the system.

3.1.6 Image Banding

As already stated, each source slit illuminates a different portion of the image. By combining overlapping images, a complete image of the entire test section results. Banding occurs when too few source slits illuminate a particular portion of the image. Typically, this occurs when the source grid is too coarse (e is large) or the gap between the cutoff grid and the image, F, is too small. Weinstein (1993) gives an equation for the number of overlapping images falling on a point on the image plane:

$$\phi = An\frac{(l' - L')}{2l'} \qquad ..25$$

where ϕ is the number of overlapping images, A is the lens aperture and n is the number of gridlines per mm in the cutoff grid. Weinstein suggests that using $\phi > 5$ is a minimum, while $\phi > 8$ gives good results. This phenomenon is called image banding because if ϕ is too small with a grid system, it results in a series of light and dark bands forming on the image plane. This will be investigated further in the experimental part of the report.

3.1.7 Further Assumptions

For the most part the optimisation of each variable has already been discussed. However there are a few assumptions which can be, or often are, made for focusing schlieren systems. These are discussed below:

The first assumption which should be made is that the cutoff grid is a negative of the source grid image. Despite sounding intuitively correct and being strongly recommended, it is not actually required. Provided the source grid image and the cutoff grid have the same grating parameter, a schlieren image will result. The consequence of not using a negative is that the range of the system becomes more complicated and is generally reduced.

For example, if a system blocks 80 % of the light at the source grid and a further 80 % at the cutoff grid, the system will only be sensitive when the two light bands are interacting. Thus for a range of deflections, there will be no change in the image. Similarly in any system in which the sum of both grids blockage is more (or less) than 100 %, strange effects are manifest. This assumption results in the following equation which states that the bright band of the source grid image is the same width as the dark band of the cutoff grid (and with rearrangement, vica versa):

$$e' = \frac{1}{n} - b \qquad ..26$$

A similar assumption is that the range should be made to be equal in the up and down directions. If the optimum cutoff (the cutoff at which best sensitivity is achieved) is made to be 50 %, then the

system has symmetrical range, best possible sensitivity for a given configuration and an additional design requirement. That is:

$$b = 2a \qquad ..27$$

This assumption will lead to very fine grids which are difficult to set up well. In addition, the system will be right at the edge of the lens resolution and on the diffraction limit. The same sensitivity and a greater range (in one direction) can be achieved with a larger grid and a greater percentage cutoff. The requirement for a symmetrical range is an artificial one since the human eye perceives brightness on a logarithmic scale, rather than linearly. This assumption will not be used for the grids designed for this report.

The last assumption to do with the grid design is that the source grid has equally wide bright and dark bands. Together with the two assumptions above, this uniquely specifies the source and cutoff grid requirements, depending on lens resolution by equation 12. For the most part this is a simplification which makes the system easier to construct, align and use. There are benefits and penalties to using different widths however.

If the source grid has narrower bright bands and the cutoff grid has wider ones, the diffraction limit is more difficult to reach, since the gaps in the cutoff grid, causing the diffraction, (b) are bigger. The sensitivity and most other variables are unaffected, since they depend on the gap a or the grid spacing n, which are unchanged. The down side is that the range is not continuously variable. When the bright band from the source grid image overlaps part of the dark bands on the cutoff grid, the system behaves as normal. As soon as the bright bands from the source grid image are wholly within the bright bands in the cutoff grid, the image does not see any more change in deflection. There is little point in making the source grid bright bands wider than the dark bands as this will simply increase the chances of banding, as well as adversely affecting the range. This particular variable will be experimented with in the report.

Another reasonable assumption for design purposes is that the test section is located midway between the source grid and the lens (I.e. $l = ½L$). This has already been assumed for the sensitivity derivation (equations 17 and 18) for simplicity. By moving the test plane towards the source grid, the size of the test section is increased linearly until at the source grid it is the same size. The disadvantage is that the closer the test plane is to the source grid, the lower the sensitivity, the worse the resolution and the

more likely banding is to occur (since the gap F reduces). There is also a practical limit in that the test plane can never be brought within the focal length of the lens, as a virtual image results.

Below is a graph showing the relative effect of moving the test section position for a system in which the source grid is $4f$ from the lens. All variables are made unity at the midpoint of the source grid and lens ($l = \frac{1}{2}L$). Below $\frac{1}{4}f$, no image is formed. The relative test section position is the distance between the test section and the lens divided by the distance from the source grid to the lens. Sensitivity, resolution and banding should generally be as low as possible while the test section and image size should be as large as possible.

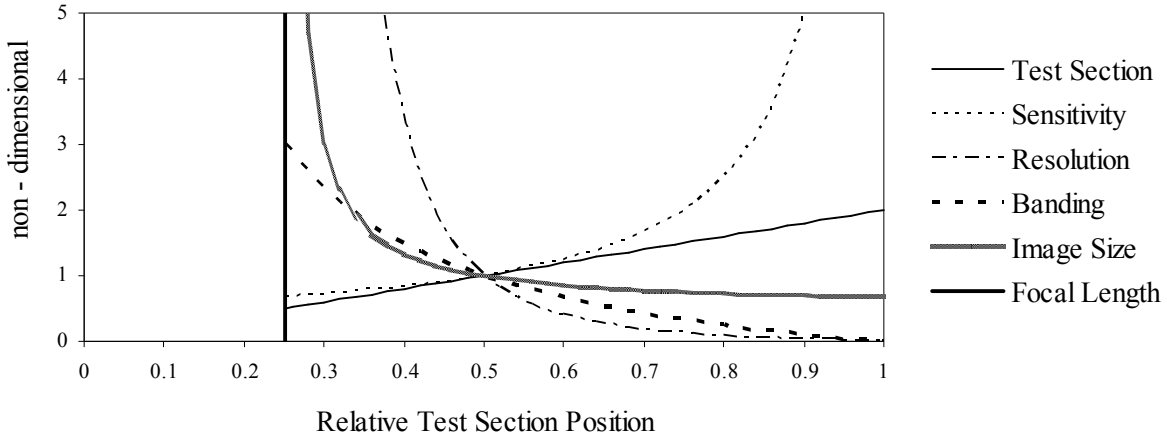


Figure 3.2 Effects of moving the test section position (l/L)

3.2 Discussion of Mathematics

Generally speaking, the designer of a focusing schlieren system wants to optimise the design in terms of sensitivity, depth of field, size of test section or compact overall size. In addition, there are three main sets of variables which need to be balanced against the design requirements. These are the lens variables (focal length, aperture, resolution), the source and cutoff grid variables (type, spacing, etc.) and the basic geometry (lengths, image size, test section size, etc).

Now that all the fundamental equations and assumptions have been presented, the actual design work can begin. The system has 34 variables and only 26 equations. There are a few assumptions which can be made to simplify the situation but ultimately, there is going to be a point at which some decisions are made. As far as possible, these should be based on the system requirements, such as sensitivity, resolution, available space and so on.

Generally, quite a lot is already known about the system. Usually the size of the test section, the size of the image plane and the available space are known. With these variables constrained, the requirements of the system are added. For example, if the system must be able to detect a deflection of 10 arcseconds, this should be taken as fixed.

Possibly the lens itself will be a constraint due to lack of availability of suitable lenses. This depends on the timeframe and budget of the project. The lens should have good resolving power and little aberration, particularly chromatic or spherical aberration. Typically lenses with a focal length from 200 to 400 mm are of the right order of magnitude to begin calculations. Focal lengths shorter than this result in poor sensitivity, while longer focal lengths result in overly long systems. For once the aperture of the lens is not that important, unless a narrow depth of field is required.

The resolving power of the lens defines the best sensitivity of the system and also begins to clarify the dimensions of the grids. Once a is known and the minimum width for b is found from the requirement to prevent banding, the dimensions of the grids should be more or less known.

Ultimately, the best solution is to use some spreadsheet software to try many different configurations in a very short time. Equations should be rearranged to become functions of those variables which are important overall or easily changed, such as the source grid line spacing or the lens focal length.

If enough variables can be constrained, carpet plots can be produced to give a better idea of the compromises made.

For this work, the system geometry and capabilities needs to be as adaptable as possible for experimentation, thus very little can be taken as fixed. Carpet plots are generally too specific to be of much use, requiring too much artificial restriction on the system. On the other hand, since the design is to be so adaptable, it does not have to be very precise.

A system of equations was drawn up in a spreadsheet, depending on seven input variables. These were the size of the source grid (S), the lens focal length (f), resolution (k) and aperture (A), the test section position (l/L), the grid magnification (m') and the source grid line spacing ($1/n'$). Strictly speaking, the source grid line spacing has no influence on geometry, only the system characteristics. The source grid was assumed, at first, to have equally wide bright and dark bands and to be a negative of the cutoff grid. This enabled the geometry and grid properties to be calculated, as well as allowing the deeper system characteristics (for example, sensitivity and optimum cutoff) and constraints (banding and resolution) to be checked. Later this restriction was lifted to allow for all sorts of grid design.

Unfortunately, the requirements of each system are unique so it is difficult to be more specific than the above process. The requirements and design of the system used in the experimental part of the report are discussed in more detail in the next section, the apparatus. Some of the components, particularly the lens and the source grid have a significant bearing on the overall system design. For this reason, the specific dimensions used for experimentation are reserved until after the apparatus has been discussed.

4 APPARATUS

Previous experimentation (Goulding, 2002) demonstrated that a working apparatus could be assembled in a few weeks, however much was learnt about the failings of such a system. For the most part, the item most lacking was a method of precision adjustment for each of the components, especially the cutoff grid. In addition, the light source was far too dim and the method of capturing images was poor.

There is a reasonable quantity of optical table equipment in the university's storerooms, however none of it is quite suitable, either being designed for use with lasers and interferometry systems or being too bulky to be convenient. A cursory look at the kind of prices for suitable equipment in the market soon showed that even small, basic components commanded impressive prices and would take several months to arrive. In addition, some of the more specialised components were not readily available.

It was decided that a system of components should be built from scratch. This allows better customisation, ensures everything fits together and works out somewhat cheaper. Cost is a little difficult to estimate, since the work done by the university laboratory staff is not charged to the job directly. In the estimation of the author, the cost probably worked out to about half what it would have cost to purchase all the components commercially. Design quality would be somewhat lower, since commercial optical component manufacturers spend more time and money developing their designs but the advantage of customisation means that each piece is better suited to its role than an off the shelf component.

Before any work can be done, the requirements of the system need to be identified more specifically. These are described below.

4.1 System Requirements

While this research relates to the large scale applications for focusing schlieren, the actual testing system does not have to be a large scale system. In the interests of reducing costs and saving time, a smaller system is better. The system has to fit on an optical table about 1.5 x 2 meters in size. The

longest axis possible is about 2.5 meters. This means the system has to be designed to operate with a lens around 200 mm focal length, longer focal lengths result in systems that are too long, shorter focal lengths tend to reduce sensitivity.

Overall, the system needs to be able to accommodate a wide variety of component positions. The lens, source grid and cutoff grid should all be quick and easy to replace and the position of all the components must be able to be adjusted over a wide range easily and very accurately. Thus each component's mount must be capable of the required adjustability. Three different configurations of apparatus must be used to achieve the objectives, thus all must be accommodated, with as little change of components as possible.

It would also be beneficial to make the system easy to move from one place to another and it would be convenient to limit the use of bolts to two or three sizes of cap screw, so that the entire system can be stripped and rebuilt using a few hexagonal keys. Also, on all points of adjustment, thumbscrews should be used so that no tools are required at all for adjustment. The apparatus should be as versatile as possible, so that future projects can be accommodated with little modification.

4.1.1 Design Decisions

To satisfy these requirements as easily as possible, the use of an optical rail is envisaged. This provides a stable base and a mounting point for all the components. The components can be divided into one of three groups, depending on function. The first of these are the components which make up the focusing schlieren system itself, such as the lens and the source grid, which have to be held in the right place and be easy to change. The second group are the component supports which hold the components in the right place. Finally, the third group are all the mounts. These connect the component supports to the optical rail and provide for precision adjustment as required.

The rail is divided into two parts. The first consists of all the components upstream of the test section, the light source, Fresnel lens and source grid, while the second part consists of all the downstream components, the lens, the cutoff grid and the image. With this technique, all the components are bolted to one of two large pieces. This makes the system much more resistant to being bumped and, if it is, it can be realigned simply by repositioning one piece. By making each

piece relatively light, it is easy to move the entire schlieren system to another place and have it working within minutes.

During the design phase, it became clear that the larger the image is, the easier it is to create a system which works. Whatever specific requirements there may be with regard to sensitivity, avoiding banding, available space and so on, they are pretty much all improved through the use of a large image. For this reason, the system is planned from the outset to produce an image of roughly 125 mm in height, rather than the usual 35 mm or 60 mm for ease of photography.

Practically there are additional problems with small images. One of the main problems with small images is that they invariably require the cutoff grid and the image plane to be close together. Thus if a screen is used it is difficult to see the image properly as it is both small and behind something. If a camera is used, the flip-up shutter invariably gets in the way of the cutoff grid. If the image is smaller, the cutoff grid is similarly smaller, requiring even higher precision both in manufacture and positioning, over and above some already quite stringent requirements. Cameras without shutters can be used but then the light source needs to be a flashed source, the environment needs to be completely darkened and so on.

By using a large image, the gap between the cutoff grid and the image increases substantially. This means the image is very easy to see on a screen and photography of the screen itself becomes possible. By using perspective correcting software, it is possible to get accurate pictures of the resulting image as seen from in front of the image. The use of a large format camera is also possible, subject to using a flashed light source and a darkened environment. Placing a camera behind a frosted glass pane was also tried without much success. The center of the pane is much brighter than the edges and the picture looses the sharper details of the image.

The use of digital cameras is the preferred solution as they have good low light capabilities and close focusing capabilities. In addition, the pictures are instantly in a useful format for post-processing. Auto-focus cameras traditionally have problems in low light conditions, so a manual focus override is preferred.

4.1.2 Co-ordinates

Each component has to be adjusted, relative to some reference frame. It is thus convenient to define a co-ordinate system so that the capabilities of the component supports can be described. The co-ordinates of the system are defined as follows:

- *x* - axis: Parallel to the optical axis, origin at the source grid and positive towards the lens.
- *y* - axis: Vertical, origin at the bottom surface of the optical rail and positive upwards.
- *z* - axis: Horizontal distance from the optical axis, origin at the optical axis and positive to the left of the optical axis as seen from the light source end.

Note that the definition of the *x* - axis means that folds in the optical axis (from mirrors or a beam splitter) result in folds in the *x* - axis. It is not useful to define it in absolute terms, as all components are adjusted relative to the optical axis.

4.1.3 Configurations

As stated earlier, there will be three different configurations. The first is useful for testing all the variables of a focusing schlieren system and thus fulfilling all the objectives relating to different source and cutoff grids. It is a standard focusing schlieren system except for the large image and is shown in Figure 4.1:

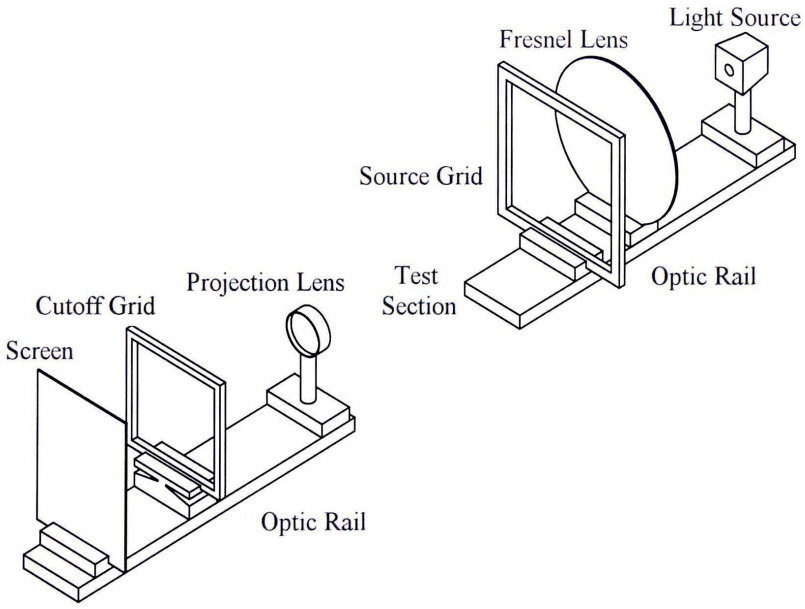


Figure 4.1 Focusing schlieren system configuration

In addition to the layout, all the pieces which are needed to support the system are shown. Each support has to be able to be adjusted so that the associated component is in the correct place. Rough positioning along the *x* - axis is possible for every component since each support is mounted on the optical rail. This is not sufficiently accurate adjustment for some components however.

Naturally, not all the components have to be adjustable, one can remain fixed. This was chosen as the Fresnel lens because it is the component which protrudes furthest below the optical axis. Since each dimension of adjustability takes a certain height, the largest component is fixed so that the optical axis is as close to the table as possible. This makes the entire assembly more stable and means less material is wasted making sure all the components are of the correct height.

By fixing the Fresnel lens, the rest of the components must be adjustable to fit with it. Thus the following rough or fine adjustment capability is necessary:

Light source support:	fine *x*, rough *y*.
Source grid support:	rough *x*.
Projection lens support:	rough *x*, rough *y*.
Cutoff grid support:	fine *x*, fine *z* and fine *yz*.
Image support:	fine *x*.

Fine adjustment in *x* and *z* can be achieved using precision mounts, described in section 4.2.3. For the cutoff grid *yz* adjustment, a tilting mount is required, as described in 4.2.4. Finally, adjustments in *y* are all achieved within the component support, as seen in sections 4.2.8 and 4.2.10.

The second configuration is for the retroreflective system. In this system, the backlit Fresnel lens light source is replaced by a front lit retroreflective screen. Most of the same mounts and supports can be used, only the retroreflective screen and a beam splitter or mirror is added. The Fresnel lens can be replaced with a suitable condenser lens but was retained for simplicity as it has a low enough *f*-number to fulfil this function very well. The source grid becomes a freestanding component in front of the retroreflective screen. To enable comparisons between the three configurations, the functional geometry should remain the same. The configuration is shown in Figure 4.2:

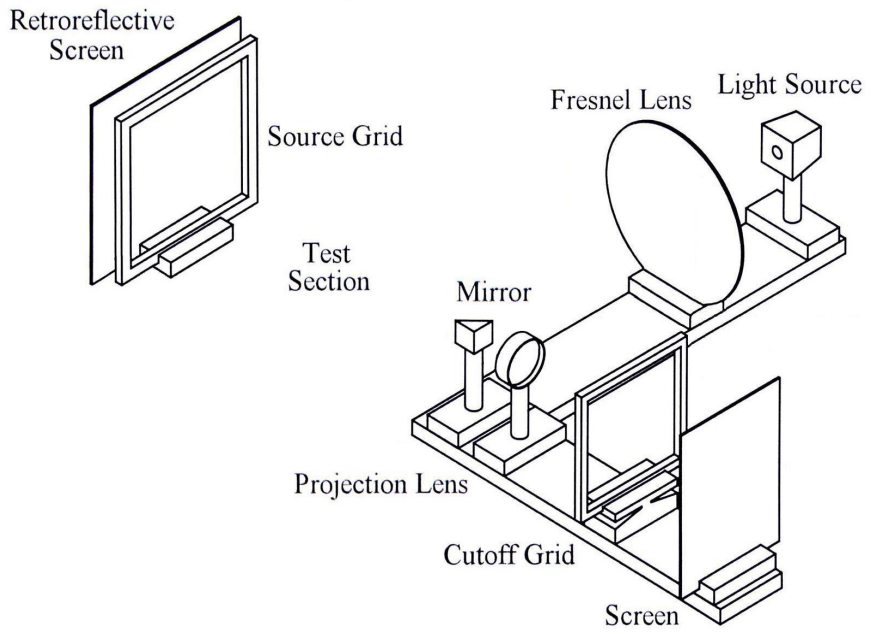


Figure 4.2 Retroreflective system configuration

The beam splitter for this arrangement was a thin sheet of glass. As only light is reflected, the fact that it forms a double image of the light source at the retroreflective screen is not important as it is an extended source anyway. In addition, the placement of the glass sheet is not important, provided the angle between the light source, the glass and the image plane is correct. Similarly, the exact placement of the retroreflective screen is not important, provided it is located behind the source grid. To make things simpler, it was mounted just behind the source grid in the same mount. The distance between the projection lens and the source grid support is important and difficult to adjust. Ideally, the optical rail should be long enough to reach the source grid, however in this case, the source grid was mounted against a wall and the distance adjusted by moving the projection lens on the optical rail. As the two new components do not need fine adjustment, they were given no special consideration.

The final arrangement is for the projected system. In this system, an image of the source grid is projected onto the retroreflective screen. This returns the source grid to right next to the Fresnel lens and adds a secondary projection lens to form an image of the source grid on the retroreflective screen. This introduces another level of complexity, as to keep the geometry the same, the image formed of the source grid on the retroreflective screen has to be kept the same as the previous systems. This in term means that the geometry of the source grid projection system has to be very accurate. As all the elements from the light source to the projection lens are linked geometrically, the only effective means of adjustment is to move the optical rail small amounts.

Using a projected image also means that a sheet of glass is no longer suitable as a beam splitter due to the double image formed. To solve this, a small mirror was used. While this blocked a portion of the primary projection lens, the aperture was smaller, so enough light was transmitted to form a good image at the image plane. Finally, for this arrangement, more baffles were used than in the previous systems. The configuration is shown below in Figure 4.3:

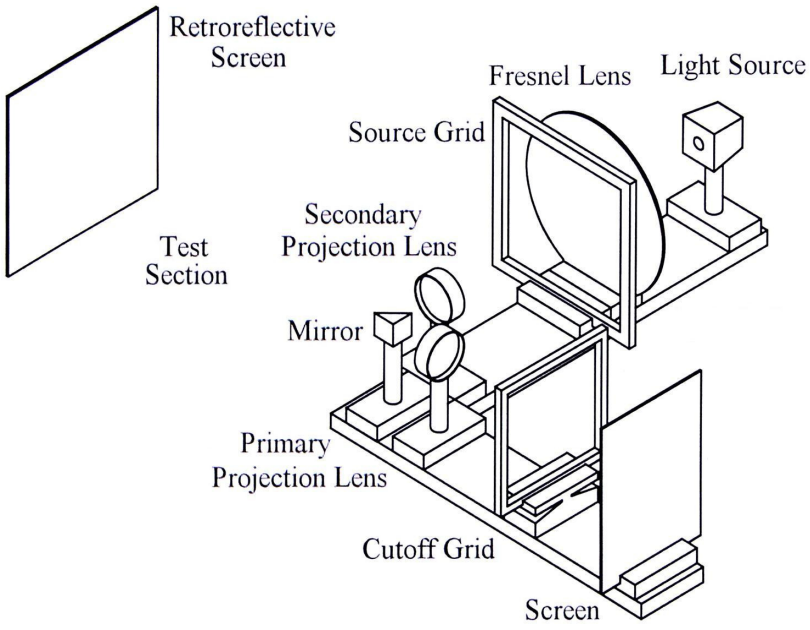


Figure 4.3 Projected retroreflective system configuration

4.2 Detailed System Description

In retrospect, designing the entire rail and mounting system took a long time and was not entirely necessary. However, it did work out cheaper and much was learnt about component design. The entire apparatus was made out of aluminium, both to save weight and to improve corrosion resistance. Aluminium costs about three times more than steel by mass and has about one third the density. This means that for a given volume, the cost is very similar. In addition, the cost of the materials involved is almost insignificant when compared to the cost of manufacturing. This makes the entire system more portable and faster to machine.

Each component, from the optical rail to the camera used to capture images will now be described. The drawing files of all manufactured components are contained in Appendix A in Solid Edge format.

4.2.1 Optical Rail

The optical rail is the main structural component of the apparatus. Originally it was going to be two sections, 0.5 and 1.5 meters long and made from extruded aluminium, however, scanning several catalogues of profiles revealed nothing appropriate for the role, either being an unusable shape or not being stiff enough. Finally, the rail was made from a machined solid section. The profile machined into the aluminium is shown in Figure 4.4a. This profile ensures that the mounts can get a strong grip on the rail, while being flat enough and wide enough to be stable. Using a wide flat profile also limits the height of the optical axis off the table and the cost of the material. The cutout made in the top middle of the profile ensures that components mounted above have a clearance for protruding screws. The 45° cuts ensure that the mounts can be located positively and makes sure that any manufacturing fillets do not prevent components fitting correctly. In retrospect, they are not really necessary, and would be left out were the project done again due to their difficulty of manufacture.

Because the travel of the milling machine used was limited to 600 mm, the rail had to be made up in three sections, two of which were joined for the longer rail section, resulting in the two sections being 0.6 and 1.2 meters in length. This in turn means a method of joining the sections together had to be devised, while maintaining a precision running surface for components. To join these sections, two slots were machined into the lower surface of the rails and holes drilled through the section through the slots. Next, two gauge plate lower guides were drilled and threaded corresponding to the holes in

the rails. Finally a 1 mm thick strip of gauge plate was placed on the upper surface of the rail, both to increase rigidity and to prevent the cap screws from damaging the aluminium surface. Because the tolerances are very high, there was a slight interference fit, so joining the parts was a little difficult but the parts are very rigidly and accurately connected.

Once the shapes had been made, the upper surfaces of the rails were sprayed matt black, to absorb light. The running surfaces were not sprayed but were given a light coat of thin oil. Finally black rubber strips were glued to the bottom surface to prevent the rail from moving easily if bumped. The upper gauge plate was also sprayed black and the longer rail section assembled.

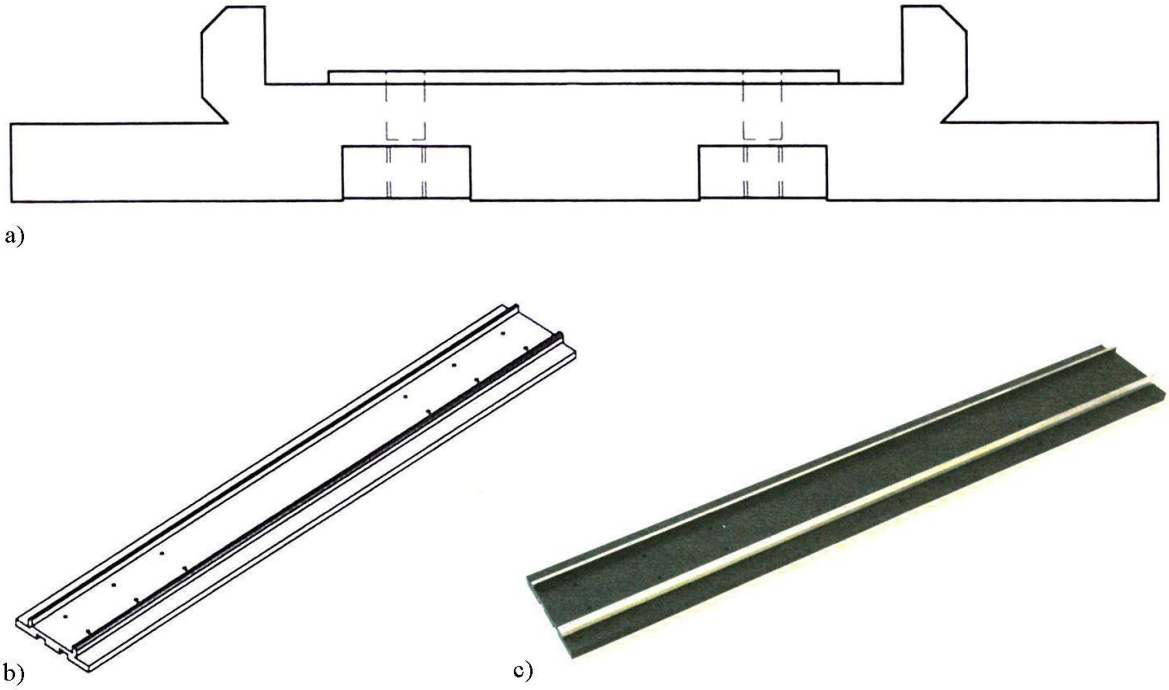


Figure 4.4 Optical rail a) Profile, b) Drawing, c) Photograph

4.2.2 Rail Slide Mounts

To mount the other components onto the rail, a rail slide mount had to be designed. The mount clamps onto the running surfaces of the optical rail and can be slid up and down to the required position. The slide mount has to be flat and grip the rail solidly. It also has to be able to be loosened, moved and tightened with a thumbscrew. Finally, it has to have a few screw mounting points, so that other components can be mounted on it.

The slide mount assembly consists of three parts, the base, the locking plate and the thumbscrew. The thumbscrew is used to move the locking plate within the base to clamp onto the rail. Figure 4.5a shows how the slide mount fits onto the rail. Eight slide mounts were manufactured to mount all the components. Once again, all surfaces except surfaces moving against other parts were sprayed matt black. An assembly drawing and a photograph are shown in Figure 4.5b and 4.5c respectively.

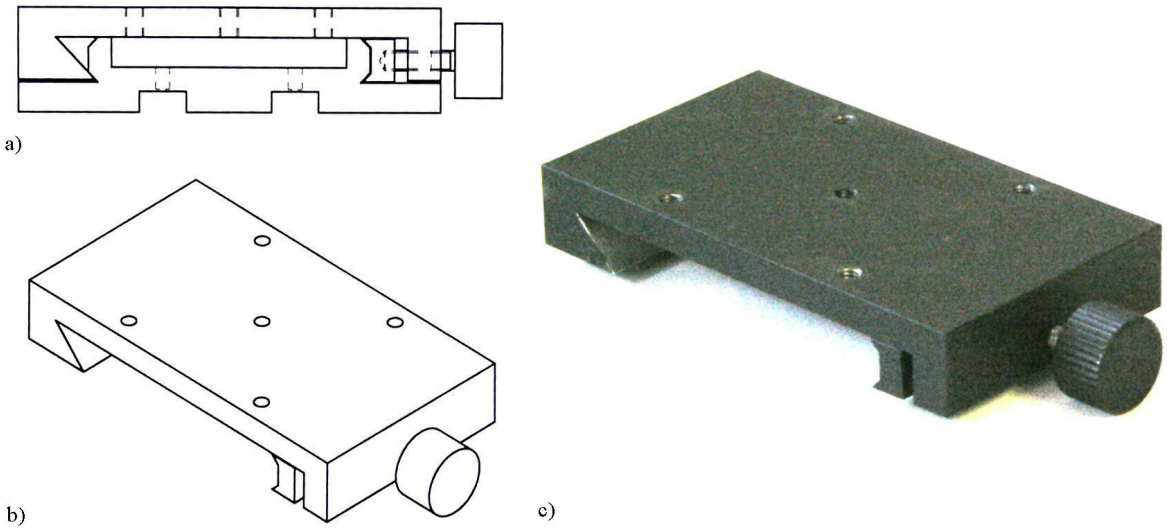


Figure 4.5 Slide mount a) Fit on rail, b) Drawing, c) Photograph

4.2.3 Precision Mounts

The precision mount is intended to provide precision movement of a support and component in either the *x* or *z* axes. Again, the mount has to be thin, provide the same mounting points as the slide mount and be adjustable with a thumbscrew. In this design, the assembly consists of five parts, the base, the upper plate, the shaft, the thumbwheel and the shaft lock.

Again, the operating principle is not a new one. The base is mounted on the slide mount, while the upper plate provides the moving surface. The shaft is located in the base by a shaft lock, a small disc connected to the shaft by a grub screw. The shaft is threaded so that it forms a worm gear for the upper plate to move up and down on. The shaft is turned by the thumbwheel, again connected to the shaft by a grub screw. The shaft is made from copper, since it is easier to machine and more durable than aluminium, while maintaining the corrosion resistance.

Once assembled, there was a certain amount of play between the base and the upper plate. This was taken up using a thin PVC shim down one side of the inside of the base. A second PVC strip down the other side further reduced the play but also made the thumbwheel stiff to turn. For this reason it was omitted. Once again, all non-contacting surfaces were sprayed matt black. Four precision mounts were manufactured. Figure 4.6 shows an assembly drawing and a photograph of the precision mount.

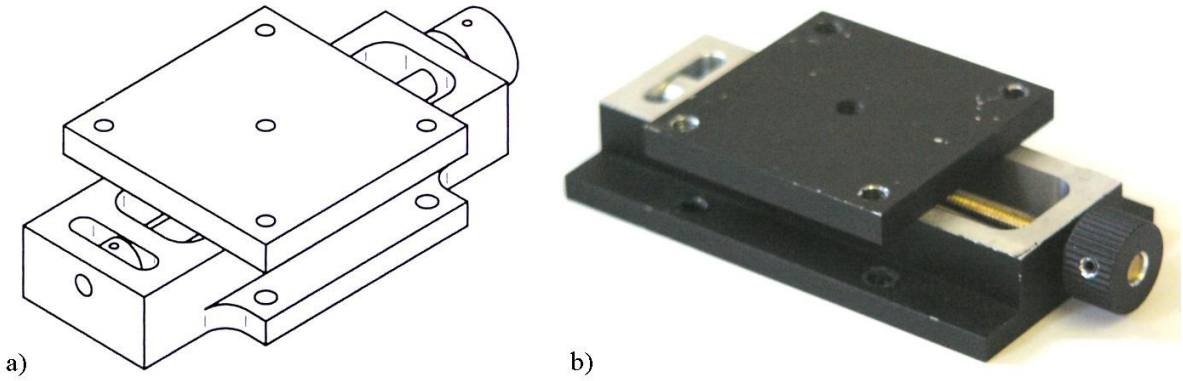


Figure 4.6 Precision mount a) Assembly drawing, b) Photograph

4.2.4 Tilt Mount

The cutoff grid requires precision alignment in the *yz* plane. This requires a tilting mount. In this case, there can be very little or no play between the base and the upper plate. Once again, the mount has to be flat, as the cutoff grid has two precision mounts, a slide mount and the tilt mount between it and the optical rail.

The tilt mount consists of 7 components, the base, the tilting plate, the shaft, two teeth, a pin and a thumbscrew. The tilting plate is mounted near the top on the base using the pin. This allows the tilting plate to rotate about 12° either side of vertical by pushing the bottom of the tilting plate backwards and forwards. The shaft is threaded into the base and turned with the thumbscrew. This allows it to be moved forwards and backwards within the base. The two teeth are joined to the bottom of the tilting plate, leaving a 5 mm gap between the two. The shaft is 7 mm in diameter, except below the tilting plate, where it is machined down to 5 mm so that it engages the teeth. Because the teeth rotate about the pin, the angle they make with the shaft changes, so they have a sharp vertical edge which engages the shaft. Likewise, the open angle of the 5 mm cutout in the shaft has to be greater than the sharp angle of the teeth, otherwise it would jam beyond a certain angle of tilt. By turning the thumbscrew, the tilting plate is rotated about the pin.

This design results in a simple to manufacture tilt mount, but has a few disadvantages. Firstly it is quite delicate. A large force on the cutoff grid, such as being dropped, might damage the teeth. For this reason, two spare teeth were made. In fact, a better solution is to make the teeth have a thick narrow end (say 5 mm), rather than a point. Then the shaft has a thick cutout (also 5 mm). This makes the teeth much stronger, without changing how the system works. Also, the play on the tilting plate is very dependent on the alignment of the shaft and the teeth. To solve this, a spring was inserted between the base and the tilting plate. While not eliminating play, it does help to prevent hyteresis within the mount.

Once again, all non-contacting surfaces were sprayed matt black. Once again, all components are aluminium except the shaft which was made from copper and the pin which was stainless steel. A section drawing of the tilt mount is shown in Figure 4.7a while an assembly drawing and a photograph are shown in Figure 4.7b and 4.7c respectively.

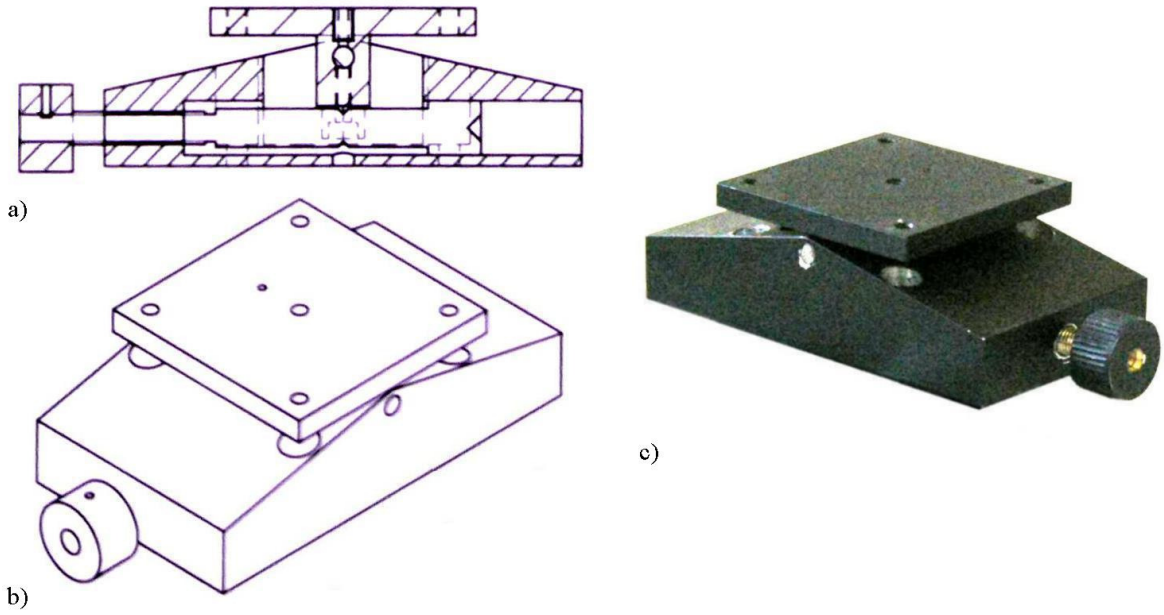


Figure 4.7 Tilting mount a) Section view, b) Drawing, c) Photograph

4.2.5 Light Source

This is probably the most complex single component made for the project. It consisted of a light bulb and its socket, a cooling fan, a support structure, a method of adjusting the height of the bulb, a shroud, a power supply and a control box. Previous experience had indicated that a 60 W incandescent bulb was insufficient to provide illumination. It was also desirable to have a variable brightness light source. For the bulk of the project, a Fresnel lens would be used, ensuring plenty of light however the second part of the project would require a brighter source for use with a retroreflective screen.

A 650 W incandescent bulb, its mirror and its socket, was scavenged from an obsolete overhead projector, along with the cooling fan. A cage was made to hold the bulb socket and the mirror in the right place. The cage also blocks the bulk of the light not going in the right direction. The mirror was screwed down against springs at three points to allow later fine adjustment to its position. The cage from the projector was too bulky to be used directly. The cage was mounted on a telescoping pillar very similar to the one used for the lens support. This in turn is screwed into a base plate. A large sheet aluminium piece was bent into a channel and used to hold the fan directly above the cage,

together with a ring around the fan blades. This makes the fan a bit safer as well as providing a mounting point for the shroud.

The shroud itself has to perform two functions. The first is preventing light from escaping the source in all directions. The second is to channel air for the fan over the bulb. Matt black cardboard was used for the shroud. It does have a tendency to absorb a large amount of heat from the bulb though so a piece of sheet aluminium is required to prevent the closest parts of the shroud from overheating during sustained use at full brightness. Once again the components are sprayed matt black to absorb unwanted light, with the exception of the interior of the cage. The large amount of heat generated simply burns off the paint this close to the bulb.

The power supply consists of a 220 volt AC, 1000 watt variable power supply and a 12 volt DC, 2 amp variable supply. The 12 volt side was originally going to be used to power an LED ring light for use with the retroreflective part of the research, though in the event was not used. From a standard computer power supply socket, a fuse provides some protection. A switch determines which power supply is to be used, with a neutral position for off. The 220 volt supply uses a standard 1 kW dimmer circuit. As the circuit is not suited to inductive loads, the fan bypasses the dimmer, drawing power as soon as the 220 volt side is powered. This allows the fan to be used for cooling even when the bulb is off. The dimmer is a diac triggered triac circuit, as shown in Figure 4.11c. A 100 mH inductor prevents power spikes being sent throughout the system. Both power supply circuits are screwed down onto an earthed aluminium chassis and housed in a plastic box. The box has been sprayed black. A four core cable is used to carry power to the light source. The four cores are earth, live for the fan, variable live for the bulb and neutral. Both the light source support and the cage have been earthed, to eliminate any threat of electric shock.

Originally, the Fresnel lens was going to focus on the filament of the bulb itself. This worked very badly however, as the large image of the filament formed was too large and strangely coloured owing to the chromatic aberration of the lens. For this reason, a small piece of thin frosted glass was placed just in front of the bulb. Three small aluminium baffles were made and could be changed to provide a very bright circular aperture of 2, 5 or 8 mm diameter. The Fresnel lens now focuses on this aperture with much better results. Figure 4.8 shows an assembly drawing without the shroud, a photograph with the shroud on, the circuit diagram and a photograph of the constructed circuit.

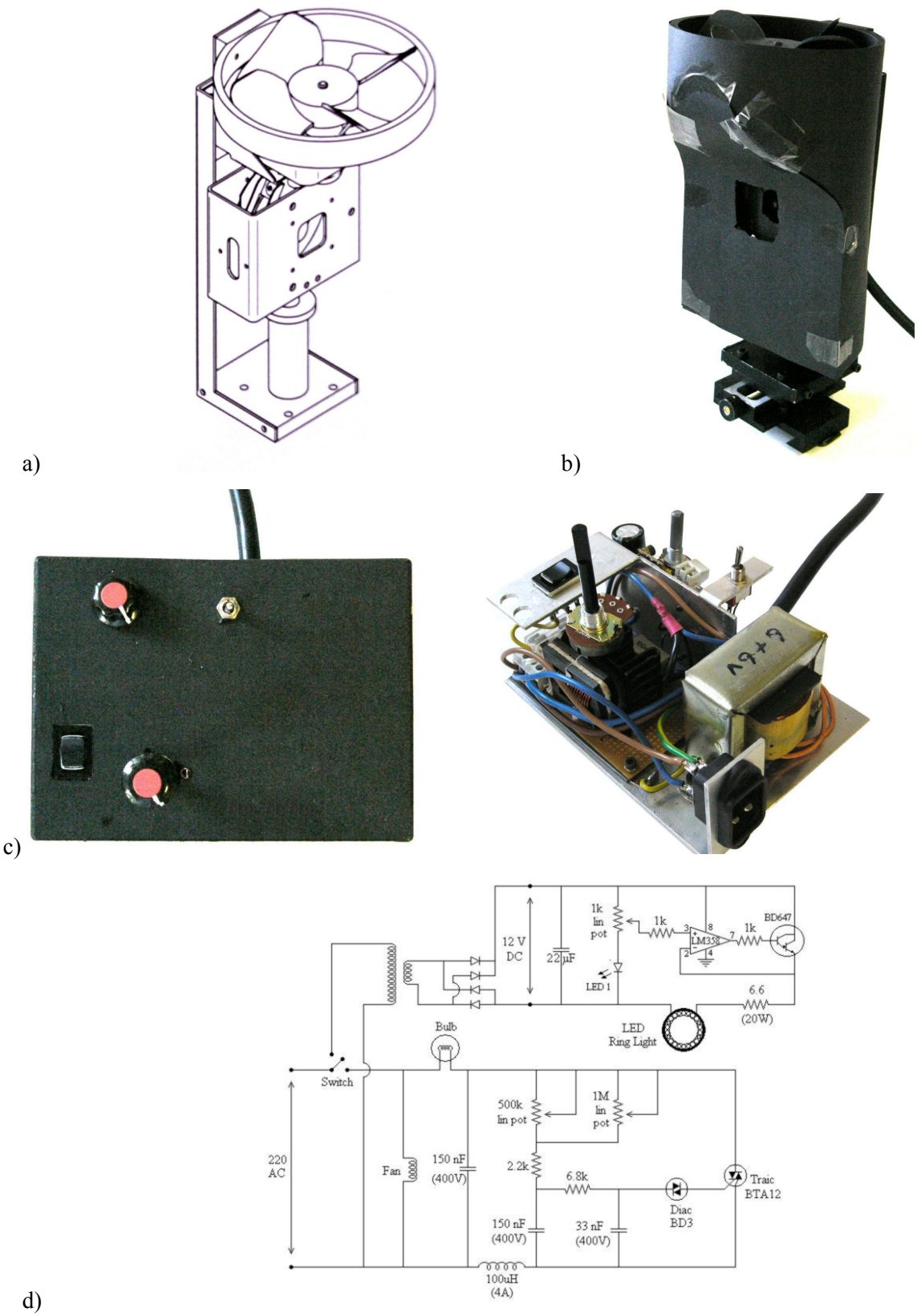


Figure 4.8 Light Source a) Drawing, b) Photograph with shroud, c) Power supply, d) Circuit diagram

4.2.6 Fresnel Lens Support

The Fresnel lens determines the height of the optical axis of the system, due to its large diameter. The Fresnel lens support was thus designed to be as low as possible. The support also has to hold the Fresnel lens in place without stressing or damaging it. The support consists of four parts, the base, the inner ring and two outer rings. The inner ring is a quarter sector, with it's inside diameter the same as the diameter of the lens, while the outer rings are half circles with the inner diameter slightly smaller than that of the lens. The inner ring is mounted between the two outer rings and all three are gripped by the base. The inner ring supports the weight of the lens and separates the two outer rings enough that the lens can fit between them. The outer rings prevent the lens from slipping off the inner ring. Because the outer rings are larger, long and flexible arms protrude beyond the inner ring. By bolting the two together, they can be made to grip the lens. By using wing nuts on the bolts, the lens can be gripped gently by finger tightening the wing nuts.

The inner and outer rings were water jet cut as this proved the cheapest and quickest method of manufacture. Once again, all surfaces were sprayed matt black. This time however, black felt was glued to all the inner surfaces which would contact the lens. The Fresnel lens support was mounted on a slide mount only, as it does not have to be adjusted, once assembled. Figure 4.9a and 4.9b show an assembly drawing and a photograph of the support.

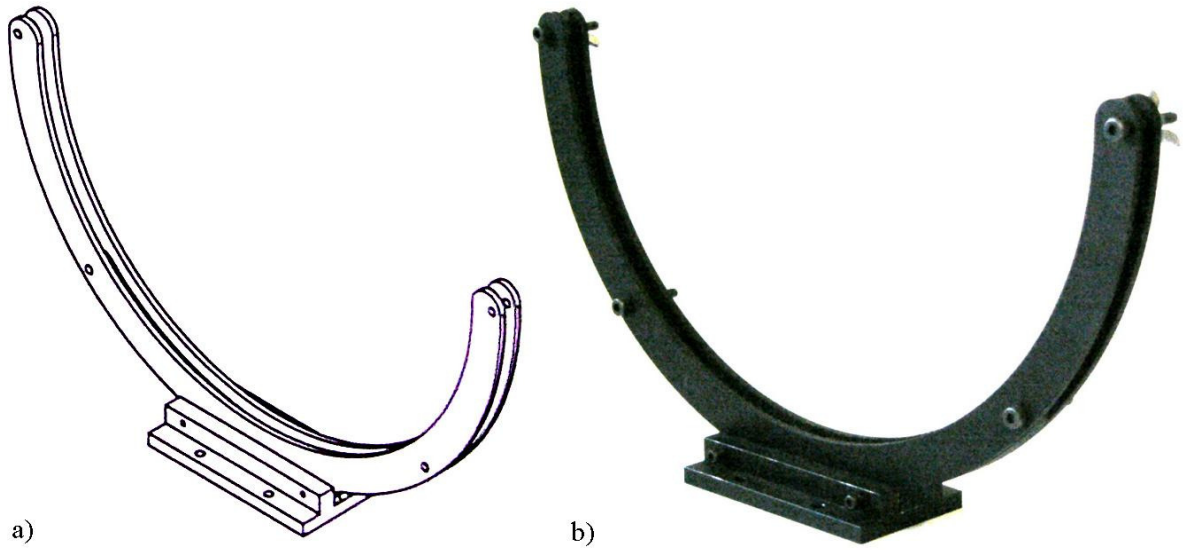


Figure 4.9 Fresnel lens support a) Drawing, b) Photograph

4.2.7 Source Grid Support

As experience was gained with the design of components, particularly with respect to manufacturing methods and costs, designs evolved. The source grid support is an example of this. Instead of a few complex machined components, it consists of 11 slightly modified flat plates held together with 16 capscrews and using 6 thumbscrews for adjustment.

The support essentially consists of a square frame, with a sliding clamp near the top and a stationary clamp near the base. The base of the frame and the clamp hold the source grid itself and the sliding clamp is pulled towards the top of the frame by two thumbscrews. This ensures that the source grid is held vertical and as flat as possible. The clamps themselves are tightened using thumbscrews. This allows the source grid to be changed and tensioned using only finger tightened thumbscrews.

The frame and clamps were sprayed matt black and black felt was glued to the inside of the clamps. In this case, the felt was intended to distribute the clamping load more evenly. The source grid support was mounted on a sliding mount as only rough positioning in the *x*-axis is required. Figure 4.10 shows an assembly drawing and a photograph of the support.

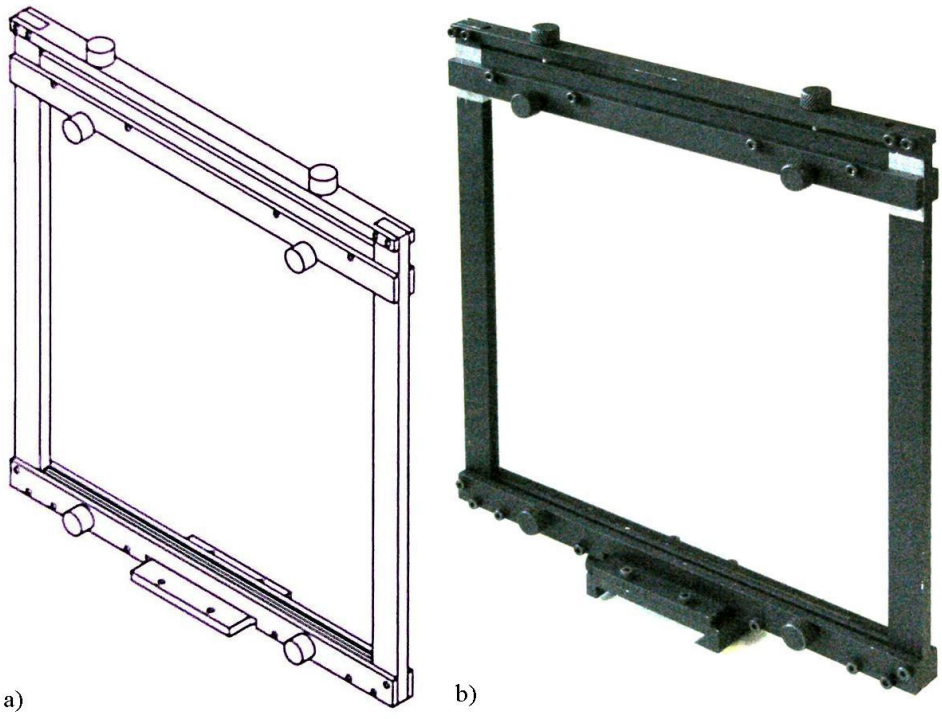


Figure 4.10 Source grid support a) Drawing, b) Photograph

4.2.8 Cutoff Grid Support

The cutoff grid support is essentially the same as the source grid support, though somewhat cruder, having been designed first and not being as large. As a result, it does not work quite as well. Again, it consists of a square frame and a sliding clamp. A clamp on the base grips the cutoff grid while a thumbscrew adjusts the height of the sliding clamp relative to the frame. Cut outs made in the frame reduce the weight of the support to less than half. This is to reduce the loads on the tilting mount, so that the spring in the tilting mount functions better.

The source grid support has two thumbscrews for tensioning, rather than one as in the cutoff grid support. With just one, the clamp tends to twist and jamb on the sides of the frame. Also, initially the clamps were a bit too flimsy to grip the cutoff grid evenly and so, they were replaced with stiffer ones. For both the source grid and the cutoff grid, the vertical and lateral positioning of the grids is not too important due to how they are made. For this reason, no adjustment in the height of supports is required. The cutoff grid does still require adjustment in *x*, *z* and *yz*, so two precision mounts, a tilt mount and a sliding mount are required.

Once again, the components were sprayed matt black before assembly and the figure below shows an assembly drawing and a photograph. The photograph has a cutoff grid in it, though the line spacing is too small to be seen in the photograph.

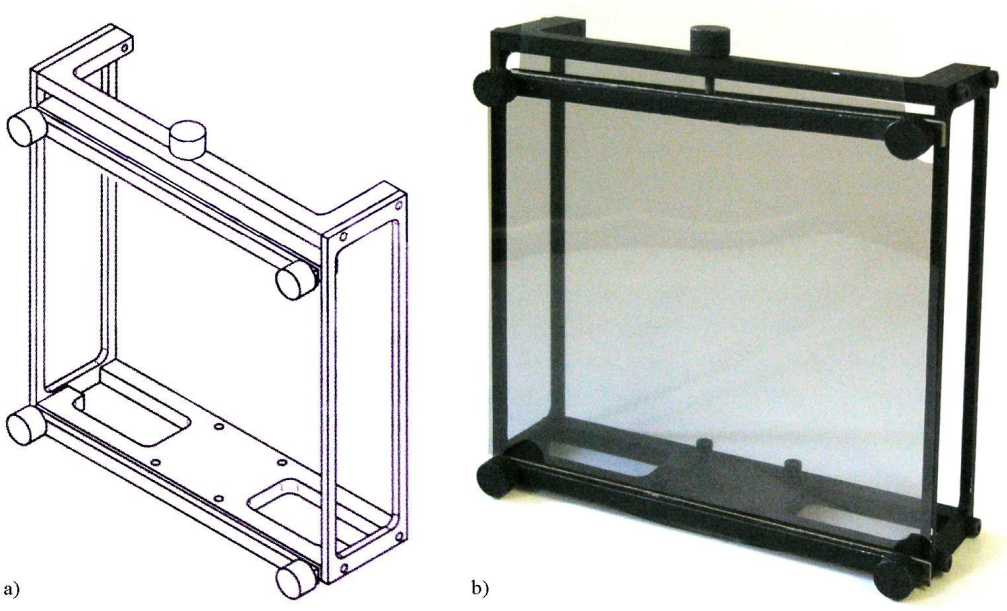


Figure 4.11 Cutoff grid support a) Drawing, b) Photograph

4.2.9 Lens Support

There are two lenses which need to be held on the optical axis. Because the lens might change, the height that the support holds the lens has to be adjustable. Also, any unforeseen objects may need to be held on the optical axis. Because the requirements are similar, a general support was designed which is capable of holding both circular and square objects of variable size.

The support consists of a telescoping pillar, a base and a top. The telescoping pillar consists of a hollow cylinder which screws directly onto one of the mounts. A threaded rod is inserted into this cylinder and held off the bottom by a thumbwheel. The thumbwheel is threaded and of larger diameter than the cylinder. Finally the threaded rod is prevented from rotating by a keyway cut into it and a screw protruding into the cylinder. Thus, when the thumbwheel is turned, the threaded rod is raised and lowered. It is held in place by gravity and has a threaded hole in the top for mounting the support base.

The support base has a square shaped cut out through the centerline. This provides a flat mounting surface for a square object and positive location for circular objects within a size range. The top is connected to the base by two long capscrews. The top has a shallow v-shaped cut out on the lower surface which fits on any circular object and positively locates a square one on the centerline. By tightening the two long capscrews, the object is held securely in the support. The non-contacting surfaces are sprayed matt black and black felt is used to line the top on the base and the bottom of the top piece to pad any object held. Figure 4.12 shows an assembly drawing and a photograph of the support.

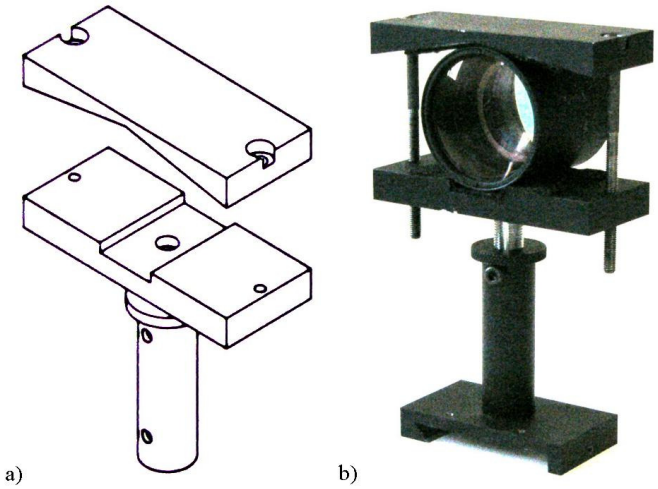


Figure 4.12 General support a) Drawing, b) photograph with lens

4.2.10 Screen Support

The screen support holds a screen on which the final image can be formed. Thus it is required to hold the screen vertically and fine adjustment along the optical axis. The support only consists of two parts, a base and a vertical surface. The vertical surface is made from sheet aluminium bent into a channel for greater stiffness. The base is then bolted into the channel at one end. The screen support is sprayed matt black.

The screen itself was initially just a sheet of paper stuck to the support. This was not ideal, as some of the light passed through the paper and it gave a yellowish tinge to the image. It was replaced with a cardboard usually used for framing pictures. This is a thick matt white board which makes an excellent screen. It does not, like most boards, have a top glossy surface, a core and a bottom surface. Instead it is homogenous through the thickness. This means the image is much brighter than paper or any other tested materials. Also, it does not appear to give any tinge to the image. When not in use, the screen is covered in a plastic sleeve to prevent dirt and damage to the surface. The screen support is shown in Figure 4.13.

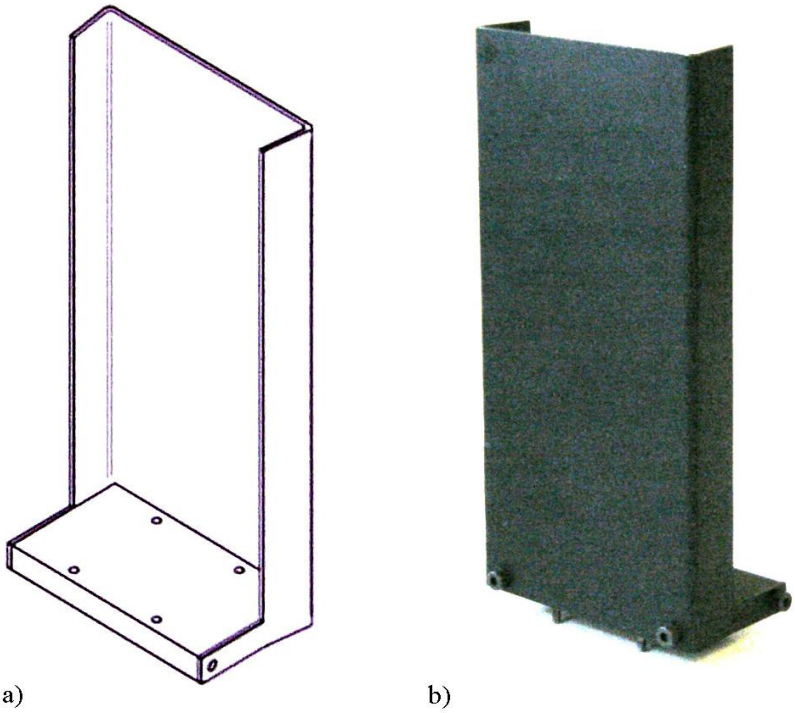


Figure 4.13 Screen support a) Drawing, b) Photograph

4.2.11 Baffles

Three baffles were used to prevent unwanted light from polluting the final image. The first, and most important, was used to shroud the light source and has already been described. There is a second baffle midway between the light source and the Fresnel lens. This is due to the fact that the light source shroud is too close to the bulb to be an effective baffle in the direction of the Fresnel lens. Finally a third baffle is located at the lens, preventing unwanted light from getting past it.

The retroreflective and projected systems required another large baffle because they both turn the light through 90°, exposing the image to the light source and Fresnel lens. This baffle was placed between the Fresnel lens and the beam splitter. A final baffle is placed beyond the beam splitter, to prevent light which has gone past from escaping.

The baffles are an effective barrier against unwanted light, though some light still escapes. This is primarily upwards through the cooling fan and downwards and backwards, through the cooling air intake. The room in which the apparatus is housed is a darkroom, with black ceiling, walls and floors. This greatly reduces the effect of this escaping light.

The baffles themselves are made from textured black cardboard, folded to increase stiffness as required and held in place with tape. Figure 4.13b shows the shroud around the light source, while Figure 4.14 shows one of the other baffles. Figure 4.22 shows the complete apparatus with baffles in place.

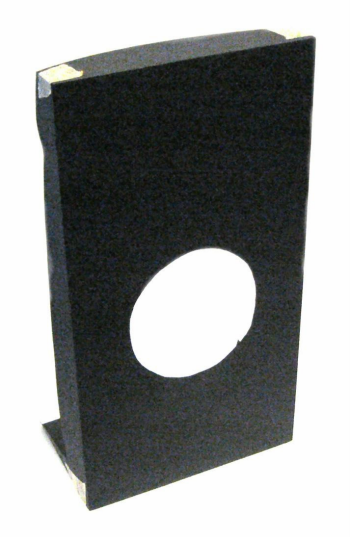


Figure 4.14 Baffle between the light source and the Fresnel lens

4.2.12 Fresnel Lens

One of the few specifically purchased parts, the Fresnel lens was regarded as too important to compromise on quality. An aspheric, 10.4 inch diameter (264 mm), lightweight plastic lens was purchased from Edmund Scientific. The Fresnel lens has a focal length of 9 inches (228.6 mm) and a refracting diameter of 10 inches (254 mm). The lens has 100 lines per inch and approximately 92 % transmission over the visible spectrum.

The Fresnel lens is designed to focus one plane at $4f$ (914 mm) from the grooved side of the lens onto it's conjugate plane at $4/3f$ (305 mm) from the smooth side. This somewhat prescribes the geometry but actually works out fairly closely to the designed geometry for a tabletop focusing schlieren system anyway. The lens is mounted with the grooves facing away from the light source for this reason.

The lens's aspheric quality is impressive and very important. The lens works far better in this regard than a cheaper overhead projector lens. Unfortunately, chromatisism is a fairly important problem, with the focal point spread over about one tenth of the image distance. This is perceived to be an unavoidable problem in a Fresnel lens, owing to the large diameter, low F-number and the thinness of Fresnel lenses.



Figure 4.15 Fresnel lens

4.2.13 Lens

The chosen lens has a substantial impact on the quality and geometry of the system. Of all the components, it is the most important. An aspheric, achromatic lens with an aperture of at least 30 mm is required. The lens resolving power has to be as high as possible to create a highly sensitive system. As the lens is projecting a 2D object onto a 2D image, distortion also has to be avoided. Finally, preliminary investigation has demonstrated that focal lengths of 200 to 300 mm are ideal for this application.

Many lenses were tested but finally, an obsolete slide projector lens was obtained from the University's media support department. It was a 200 mm focal length Leitz Wetzlar three element lens with an aperture of about 60 mm. The resolving power was crudely measured to be about 75 line pairs per mm, using a United States Air Force resolution test pattern. The lens also appears to be aspheric, achromatic and distortion free.

Unfortunately, only one could be obtained. For the projected retroreflective system, a similar lens, with 150 mm focal length was used. Also made by Leitz Wetzlar, it has an aperture of 55 mm. The lens resolution is less important for this lens and was not measured.



Figure 4.16 Projection lens, primary on the left, secondary on the right

4.2.14 Camera

Many of the theoretical and practical problems associated with the camera have already been discussed under design decisions (Section 4.1.1). The result of these requirements is that a Panasonic Lumix DMC FZ10 digital camera was used. The camera has a 4 mega pixel CCD and an F2.8, 6 - 72 mm Leica zoom lens. In addition, the camera has both macro and manual focus modes. The camera was mounted on a small tripod at the same height as the image and off axis to one side. Images were stored directly to computer and corrected for perspective.

Images were recorded as jpegs of 2304 by 1728 pixels. The image of the system formed on a rectangle about 930 pixels by 640 in the middle of the recorded picture. This means that the photographic resolution in the test section corresponds to about 7.5 pixels per mm in the vertical direction and 5 pixels per mm in the horizontal direction. The difference in vertical and horizontal resolutions is caused by the fact that the camera is located off axis, squashing the image horizontally. This error is corrected for (see data processing below) but the resolutions are still different.



Figure 4.17 Panasonic Lumix camera

4.2.15 Source and Cutoff Grids

For the experiments in this research report, both black and white (actually clear) grids and colour grids are required. In addition, a variety of patterns need to be made. Unlike most researchers, a decision was made fairly early on to use manufactured grids. Most authors have used photographic techniques to create first a source and then, by placing the camera at the cutoff grid position, creating a cutoff grid. This technique has a few advantages in that the cutoff grid is very accurate and compensates for any distortions inherent in the system. Unfortunately, it also produces cutoff grids with low contrast ratios and the cutoff grids can have fuzzy edges as it is very difficult to focus really sharply. This technique usually requires a cutoff smaller than the image size of the camera so that the entire source grid image fits on the film. Finally, there are several problems with developing the cutoff grids and mounting them in place properly.

Manufactured grids, by contrast have to be very high quality prints. While there are no contrast ratio or developing problems, the lens and other components also have to be good quality and accurately aligned to ensure that the source grid image and the cutoff grid match.

The best grids seem to be made from positives used in the printing industry. The positives are accurately printed to approximately 2400 dpi resolution, which translates to about 10.6 micron or 47 line pairs per mm. This is sufficient for a large cutoff grid, ensured by using a large image, but is a little limited for smaller grids. This may explain why this method has not been used extensively before. Positives can only be printed as black on transparent sheets. The sheets are completely clear, in that light which is parallel before passing through the sheet remains parallel afterwards.

Unfortunately, positives cannot be printed in colour which means that a standard colour printing method has to be used. This results in lower resolutions (about 400 dpi). In addition, the plastic used for colour printing is not completely clear, scattering any light passing through. For both these reasons, a printed coloured grid for a colour focusing schlieren system has to be the source grid. Generally in a colour system, there is a colour grid and a black and white grid, or two coloured grids. For this research, only a single coloured grid was used.

Usually the amount of light permitted to pass the black and white grid in a colour system is less than 25 %. This ensures that the resulting image has a large range and the colour comes through clearly. Unfortunately, at the cutoff grid, this means the system is more likely to be near the diffraction limit

of the system, due to thinner slits between the gridlines. Ideally the cutoff grid would be colour and the source grid black and white as this will result in greater tolerance of the diffraction limit.

One final benefit of manufactured grids is that the pattern repeats consistently. This means that the cutoff grid does not have to be matched exactly to the source grid image, as is the case with a photographic method of manufacture. For a typical grid, the cutoff only has to be adjusted in *x*, *z* and *yz*. A photographic grid would also have to be adjusted in *y* and a specific gridline would have to be matched up in *z*.

The specific dimensions and purpose of each grid used in experimentation will be discussed under the relevant experiment. A variety of the grids used in the research are shown below with the USAF resolution test pattern for testing lens resolving power. This was also useful for testing the resolving power of various printing processes, simply by looking at the resolution of the printed grid under a microscope.



Figure 4.18 A variety of source and cutoff grids

4.2.16 Test Object

In order to compare the variety of grids and systems, it is necessary to have a standard test object with which to test them. This test object needs to satisfy both quantitative and qualitative measuring requirements. There are six main requirements identified below:

- The test section must have regions of x, y and combination components for determining which directions the system is sensitive to.
- The test section must have finely detailed features so that the resolution of the system can be compared meaningfully.
- The test section must have a quantitative measurement of range and sensitivity.
- The extent of diffraction in the final image must be able to be determined.
- The test section has to be consistent with time. Fluctuating flow fields are very difficult to compare, thus turbulent or random features are not wanted.
- The test section must include a qualitative element so that the results here can be compared roughly with other works in flow visualisation.

The final test image is shown in Figure 4.19:

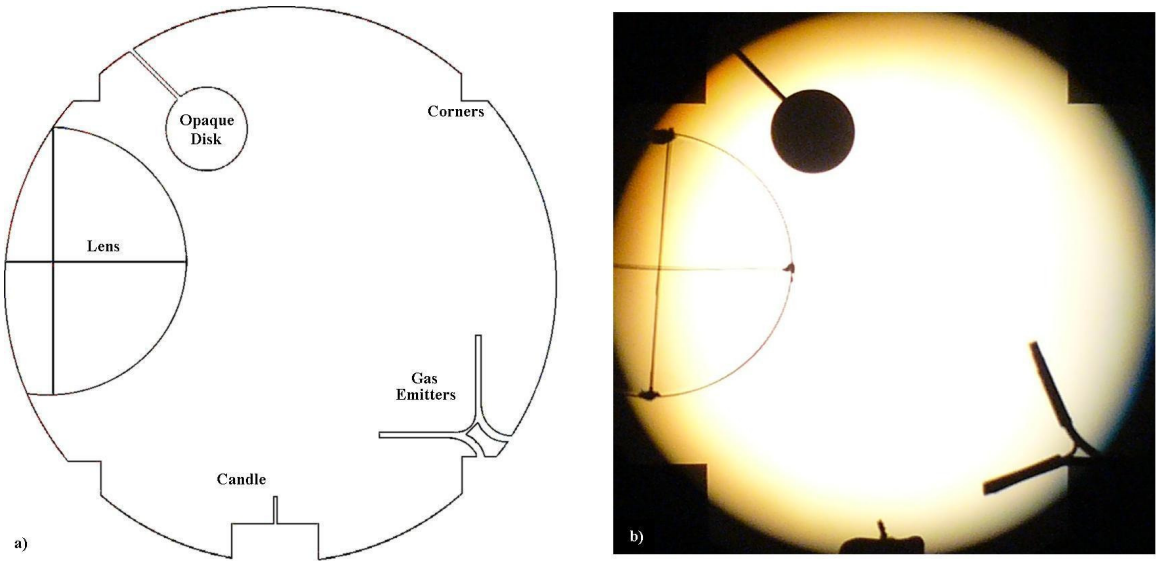


Figure 4.19 Standard Test Section a) Drawing, b) Photograph

The test section has four main elements. These are a lens, a candle plume, two gas emitters and an opaque disk.

The lens is a very long focal length (-40 meters) plastic lens and is fitted with a cross hair so that the position of the centre of the lens is accurately known. This is the single most important element in the test section. It provides an accurate measure of both range and sensitivity. Since the focal length is known, the deflection of any ray through the lens can be calculated in three dimensions. This means the lens gives a very accurate idea, not only of what tones in the image correspond to which deflections, it also demonstrates whether the system is sensitive to deflections in x, y or both. In addition, with 2D systems, it gives a very good idea of what is actually happening at the knife-edge. The center of the lens also provides an idea of the conditions of the system, whether darkfield, brightfield or in between since the center of the lens does not deflect light.

Many different methods were tested while trying to introduce small flow features into the test section. All the ones involving heat failed dismally. This is due to the fact that heat cannot introduce huge density gradients, as the heat moves through the air too quickly. Thus fine detail can only easily come from shockwaves or chemical mixing. The two gas emitters are cigarette lighters which have small hoses fitted to vary the angle at which gas is released. These provide fine flow features which can be used for testing the resolving power of the schlieren system. One ejects gas vertically and the other horizontally to confirm the x/y sensitivity of the system. The gas is released as a 0.5 mm diameter propane/butane mix with an average density about twice that of the surrounding air. This provides very high gradients without requiring great sensitivity to detect.

The candle plume is purely there to provide a qualitative feeling about the image. It is not consistent enough a flow field to be of much use other than to connect the images presented here to other works of research. Most authors have a rough idea of how strong a schlieren object a candle plume is, so it makes sense to use it as a standard. Unfortunately, the candle has to be placed slightly out of focus (about 30 mm) otherwise the flame lights the gas leaving the cigarette lighters. This not only destroys the finely detailed flow, it also burns the hoses! Moving the candle out of focus has far less effect than moving the gas emitters, since it is a much larger flow feature.

The last element is an opaque metal disk. This creates diffraction fringes when the cutoff percentage approaches 100 %. The fringes tend to set up only in the direction of sensitivity of the system. Four corners are included to make perspective correction of the digital images much easier. Finally, an important part of the test image is the background. By examining how even the background is, an estimate of how well aligned all the optical components are can be made. It is also very important for detecting banding, poor grid manufacture and so on.

4.2.17 Retroreflective Screen

The retroreflective screen used for the later parts of the research is a glass bead reflector fabric, designed for use in high visibility clothing. Total internal reflection within the beads results in a very bright reflection in a cone about the incident ray. The cone angle has been measured to be about 1.4°, after which the amount of light reflected drops significantly for each degree further from the incident ray. Since the beads are only partially embedded, the fabric reflects over a very wide range of entry angles and remains very effective up to incident angles of up to 70°. It also means that the properties of the fabric can be damaged by finger residues left behind after handling. Finger prints and dirt appear as darker regions on the source grid. As the operating principle depends on total internal reflection, the cone angle for blue and red light is slightly different.

For the retroreflective system, the fabric is simply mounted, with the source grid, in the source grid support. The tension is not really required for the fabric but does eliminate the shadows which would form if there were a gap between the source grid and the retroreflective fabric. For the projected system, the tension is not required and the source grid support is needed elsewhere. For this configuration the fabric was mounted against the wall. For both of these configurations, a circle of black cardboard provides a distinct circular edge to the screen. This improves the final image by ensuring the test section is the same size in all experiments. One drawback of this system for the retroreflective system is that the source grid reflects light back through the system. This manifests as a slightly brighter region in the centre of the images for the retroreflective system, though it has to be sought out to be seen.



Figure 4.20 Retroreflective fabric

4.3 System Geometry

With the core components selected and the layout known, the system geometry can be decided upon and specified. As stated in the analysis section (Section 3.2), the system of equations can be solved with seven variables. Since the size of the source grid (S) is limited by the Fresnel lens and the lens has been chosen, the lens focal length (f), resolving power (k) and aperture (A) are fixed. The three variables left are the test section position (l/L), the grid magnification (m') and the source grid line spacing (e).

The test section position is, in keeping with tradition, left at 50 % for calculation purposes. In practice, there is not much point in changing it and the effects of moving it have been described in Section 3.1.7. The source grid line spacing is a grid variable and, as such, will be varied in the experimental part of the research, along with the other grid properties. This leaves only the grid magnification to be decided, to specify the system.

Grid magnification ratios from about 0.2 to 0.67 result in an overall system length of less than 1,5 meters (from the source grid to the image plane), thus the magnification ratio should lie between these two values. Additionally, the Fresnel lens has been designed to focus conjugate planes at $4f$ and $4/3f$. This condition occurs in a system with a magnification ratio of 0.28. It has already been stated that the planned image height should be approximately 125 mm. This results in a magnification ratio of 0.33. By making the magnification ratio between grids precisely one third, it is much simpler to create the grids and keep track of which cutoff grid goes with which source grid. For example, 28 % of a 0.9 mm grid spacing is 0.252 mm while one third is simply 0.3 mm. Thus the grid magnification ratio was chosen as 0.33.

Once the assumption that the grid should be 50% black and 50% clear was dropped, it became necessary to include one more variable, called B, to define the quantity of light passing through the source grid. This has many effects on the cutoff grid sizing and performance characteristics of the system without affecting the geometry of the apparatus. Thus the spreadsheet was extended for the second part of the research.

Enough parameters have been chosen to specify the system. Using a simple one millimetre, 50% black and 50% clear source grid as an example, Table 4.1 shows the resulting system.

Table 4.1 System Geometry and Characteristics

Inputs

Source Grid Size	S	254	mm	Object Position	l/L	0.50	
Focal Length	f	200	mm	Grid Magnification	M	0.33	
Aperture	A	60	mm	Source Grid Line Spacing	$1/n'$	1	mm
Resolution	k	75	lp/mm	Source Grid light transmission	B	50	%

Outputs

System Geometry

Object Distance	l	400	mm
Image Distance	l'	400	mm
Source Grid Distance	L	800	mm
Cutoff Grid Distance	L'	267	mm
Cutoff Grid Size		85	mm
Object Magnification	m	1	
Cutoff Grid Space	F	133	mm
Object Size		127	mm
Image Size	I	127	mm

Grid Dimensions

Source Grid Line Density	n'	1	lp/mm
Source Grid Bright Width	e	0.5	mm
Source Grid Dark Width	$n'-e$	0.5	mm
Source Grid Image Bright Width	e'	0.167	mm
Source Grid Image Dark Width	$n-e'$	0.167	mm
Cutoff Grid Bright Width	b	0.167	mm
Cutoff Grid Dark Width	$n-b$	0.167	mm
Cutoff Line Density	n	3.00	lp/mm

Performance Characteristics

Sensitivity (0% Cutoff)	e_{min}	25.8	arcsec
Minimum Cutoff Grid Line Width	a_{min}	0.0267	mm
Maximum Sensitivity	e_{min}	4.1	arcsec
Optimum Cutoff Percentage	C_{opt}	84.00	%
Image Resolution	w	1.320	mm
Weinstein Criterion	f	30.0	
Range - Up (If opt cutoff)		4.1	arcsec
Range - Down (If opt cutoff)		21.7	arcsec
Depth of Field	DU	26.67	mm

The system geometry allows most of the components to be placed reasonably accurately. All final adjustment was done by hand to ensure primarily that the source grid image and the cutoff grid matched up properly. The basic geometry remains unchanged for changes in the grid patterns, thus the source and cutoff grids can be replaced to change the system characteristics. This is done by replacing the grids, without moving the supports for the grids. This allows many system characteristics to be investigated quickly and easily. It is important to note that the final geometry selected is the result of much iteration both theoretically and experimentally.

4.4 Data Processing

The data was captured on a digital camera and downloaded to computer in .jpg format. This requires far less processing than a conventional camera system. As far as possible, the original photograph was preserved, brightness, contrast and so on are not adjusted. This was to preserve any defects the given schlieren system under test may have exhibited. There is one exception to this rule. As the camera is offset from the optical axis, the pictures are corrected for perspective distortion. This is a three step process.

First, a shareware edition of Photo-brush, developed by Mediachance, is used to correct the perspective. This is a feature of the program, in which a grid is dragged over the picture until it fits rectangular co-ordinates on the picture. For this reason, small blackened corners are present in the image plane. The second step is to crop the image so that the displayed image contains just the circle of the image. The final step is to correct the aspect ratio of the image, so that it is a circle and not an ellipse. To maintain consistency between images, such as getting the candle plume vertical, several images were captured for each setting and the best chosen for processing and inclusion in the results.

Some images exhibited regions of colour, presumed to be caused by the poor chromatic properties of the Fresnel lens. For this reason, whenever it is not important to display colour, the images were converted to greyscale. This will be discussed further in the colour experimentation sections of the report. As the printed images are small, the resolution was reduced to 800 x 800 pixels to reduce the size. Appendix B contains all images before processing, after perspective correction and after all processing.

This was the process used for all the experimentation. Several other images have been included to illustrate better what is happening either with colours, blurring, contrast and so on. In these cases, several methods of enhancing the images have been used. These include increasing saturation, adjusting contrast, changing levels, etc. Anything found to improve the visibility of what was being illustrated in the image was used and is mentioned in the relevant text.

4.5 System Imperfections and Sources of Error

The system above has been revised and improved many times. This is a never ending process of reducing the significance of the most important problem as it arises. In the interests of progress, the apparatus has to be fixed to allow some actual testing to be done. This means there are still many problems which can be improved upon and many minor sources of error. These are discussed below:

4.5.1 Mechanical Grid Alignment

Aligning the source grid image to the cutoff grid is the greatest problem at this stage. For example, with a source grid spacing of 0.6 mm and the chosen geometry, every point on the cutoff grid has to be held within 10 micron of the correct position to keep the error on cutoff percentage down to 10 %. Thus every 1 micron error in positioning results in a 1 percent error in the cutoff percentage.

With the current apparatus, accuracies of a few micron are entirely reasonable however getting a consistent error over the whole grid is not. This manifests as unevenness of background illumination when using fine grids and will be examined further in the experimental section of this report.

Ultimately the cause of the error is the fact that the grids are not held perfectly. They are gripped at two sides and stretched taut to limit movement and distortion. This causes a certain amount of deformation, particularly near the thumbscrews. For the most part the deformation is fairly minor, however it is enough to cause certain regions to be worse aligned than others when using fine grids.

The solution is either a case of using a more sophisticated stretching device, capable of stretching the positive in two dimensions at a fixed tension, or printing or joining the positive to a rigid substrate. The obvious thought is to press the grid between two sheets of glass, or to print the positive directly onto glass. The problem is that neither of these actually works very well. Printing the positive onto glass reduces the resolution of the positive to about one quarter of what it was. Placing the grid between two sheets of glass seems to result in a certain amount of distortion of the grid, as the gap between the sheets of glass is difficult to get constant. Perhaps a vacuum could be used to hold the glass sheets together. Various manufacturers were consulted about making a grid out of stainless steel, copper or plastic sheets, using milling, water jets, lasers and chemical etching, all with the same result; it cannot be done at the required tolerance with a guarantee, at least not for a reasonable fee.

A further problem is the limit of print quality. The positives and colour prints are made with print resolutions of about 2400 dpi and 400 dpi respectively. This automatically limits the accuracy of the alignment of the positive grids to about 10 micron. Note that this only really affects the cutoff grid as it is smaller. This is also one of the main reasons a large image was selected, as a larger image results in a larger cutoff grid.

Another problem is the fact that the cutoff grid support can sway very slightly forwards and backwards, resulting in a slightly different distance from the top and bottom of the grid from the projection lens. This not only results in problems of matching the grid magnification but can cause problems with focus and evenness of illumination.

On a final note, the use of glass or any other reflective material to hold the source grid causes great problems using the retroreflective arrangement. The light can, and generally does, reflect from the light source to the final image, washing it out.

Most researchers have used the technique, described by Burton (1949), of placing a camera at the cutoff grid position and developing the negative for use as a cutoff grid. This technique has already been discussed above, however one further argument remains. For this work, more than 25 source grids were experimented with. As each source grid cannot be moved between taking the picture and installing the cutoff grid and the cutoff grid has been known to deteriorate within a week. As a result, this option was not investigated with much enthusiasm. In the end, a manufactured grid proved a far faster and more convenient method, despite its drawbacks.

4.5.2 Optical Grid Alignment

Apart from the purely mechanical issue of holding the grids in the correct place, there is the more complicated issue of making sure that the image of one grid exactly matches the second grid. Ultimately all errors of this sort result from imperfections in the lens, however as long as physical alignment remains the more difficult problem to overcome, the lens quality is not too critical. Improving the lens quality is mainly a matter of improving the resolving power of the lens while making sure no significant aberrations occur. At this stage, the lens is not a limit of system performance.

4.5.3 Chromatisism of Fresnel lens

As stated earlier, the Fresnel lens suffers from chromatic effects quite strongly. This means that the focused image of the light source is in different positions for different wavelengths of light. Thus, the blue light from the light source is focused about 100 mm closer to the lens than the red light. This appears as a bluish spot surrounded by a reddish haze at one focal length and as a reddish spot surrounded by blue haze a bit further from the Fresnel lens.

The effect can be reduced by using a larger light source. This means that virtually all the colours pass from the entire Fresnel lens to the center of the projecting lens. As long as the light source has a diameter of about 8 mm or so, the image should be evenly coloured. The problem reoccurs once either of the grids is brought into play. This causes regions of colour in the final image when the cutoff percentage is high, particularly near the edges of the test section. Even with a 10 mm diameter light source and the projection lens stopped down to 10 mm, the colours are apparent.

Quite how this happens is a little unclear. The image exhibits all the colours in the spectrum, though primarily blue and yellow are visible. The colour fringes are aligned with the grids, in other words, the rainbow spreads from left to right for a grid with vertical lines. When the Fresnel lens is replaced with a retroreflective screen, the fringes are reduced, as they are when either grid is removed. Somehow, the interaction of the Fresnel lens and the two grids causes the colours. Diffraction at the edges of the grids has been suggested but the colours appear as apparent using fine grids as they are when using coarse grids. Figure 4.21 shows the colour fringe contained within each gridline on the image plane. The image on the right has had levels reduced to enhance the colour.

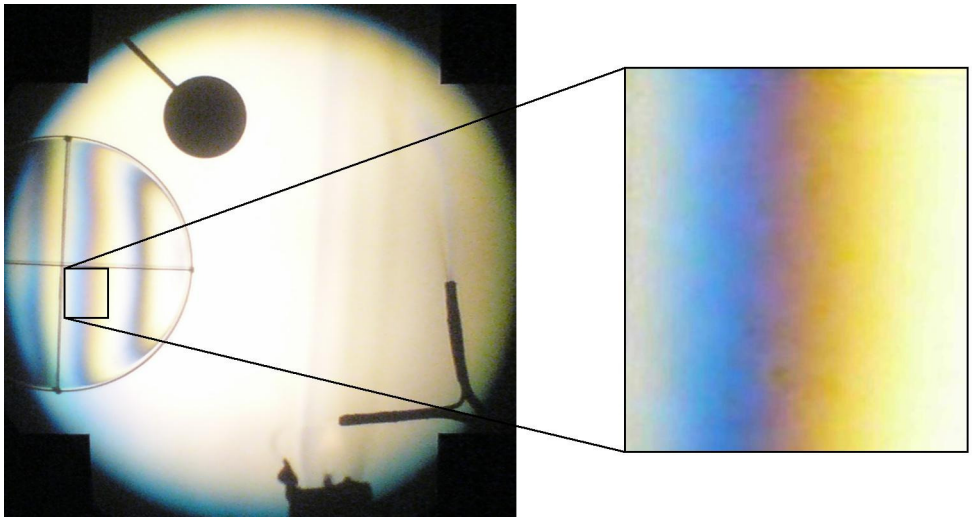


Figure 4.21 Enhanced portion of a typical image showing chromatism

4.5.4 Stray Light

Stray light is cut off by baffles as close to the light source as possible but some light always escapes. The effect of this is to allow a small amount of light over the entire image and wash it out. The current system of baffles is very effective at reducing this, but there is room for improvement. Stray light is more of a problem using the retro-reflective screen, as the screen tends to scatter light somewhat.

Another source of stray light is dirt, fingerprints on any of the illuminated optical surfaces. Apart from the scattering effect of such dirt, it also throws shadows downstream of the object. This is particularly a problem of the source and cutoff grids, which get handled a lot, and of the retroreflective screen which catches and holds dirt and fingerprints doggedly.

4.5.5 Camera Processes

When a digital camera records information, it uses a compression algorithm to produce files with the .jpg extension. This process makes the pictures one tenth the size but also looses some information. For the most part this is not important however pictures are captured at the highest possible resolution to be safe. The camera's picture processor also modifies the process depending on the selected ISO number and other factors. This results in pictures which have certain colour balance, tonal range, quantities of noise, white balance and so on. For the most part these have fairly minor effects and work well automatically. It is simply useful to be aware that such things are happening.

4.5.6 Data processing

Once the pictures have been uploaded to computer, they have to be converted to a standard form. This includes correcting for perspective, correcting aspect ratio and cropping the edges. During this process, the software uses various interpolation schemes to reduce the loss of information. With the noise inherent in a low light system, there will invariably be some errors. Once again, these are minor effects and using the highest resolution will mitigate the effect.

4.5.7 Quantifying cutoff

One of the largest problems with any schlieren system is knowing the amount of cutoff used in the test section. With conventional schlieren systems, only a single knife edge has to be positioned accurately and an idea of the cutoff can be obtained relatively easily from total light passing the cutoff or the portion of the image visible on the knife-edge. With a focusing schlieren system, the final image is an average of the cutoff of each of the gridlines over the image. As there is a fair amount of distortion in the grids, it is reasonable to assume that the cutoff, and hence the sensitivity and related properties, vary over the test section.

For all practical purposes, estimating the cutoff used to any great degree is largely guesswork, unless the mechanical alignment of the grids can be made significantly better. For this reason, the 'optimum' cutoff shall be defined, in the experimental part of the report, as the percentage cutoff that generates the greatest contrast in the image, rather than the more correct definition of the narrowest slit that the lens can accurately reproduce. In the event, the two definitions do seem to correlate rather well but again, that is largely guesswork.

To illustrate the complete apparatus, the completed system for the first configuration is shown in Figure 4.22. Only the candle has been placed in the test section in this instance.

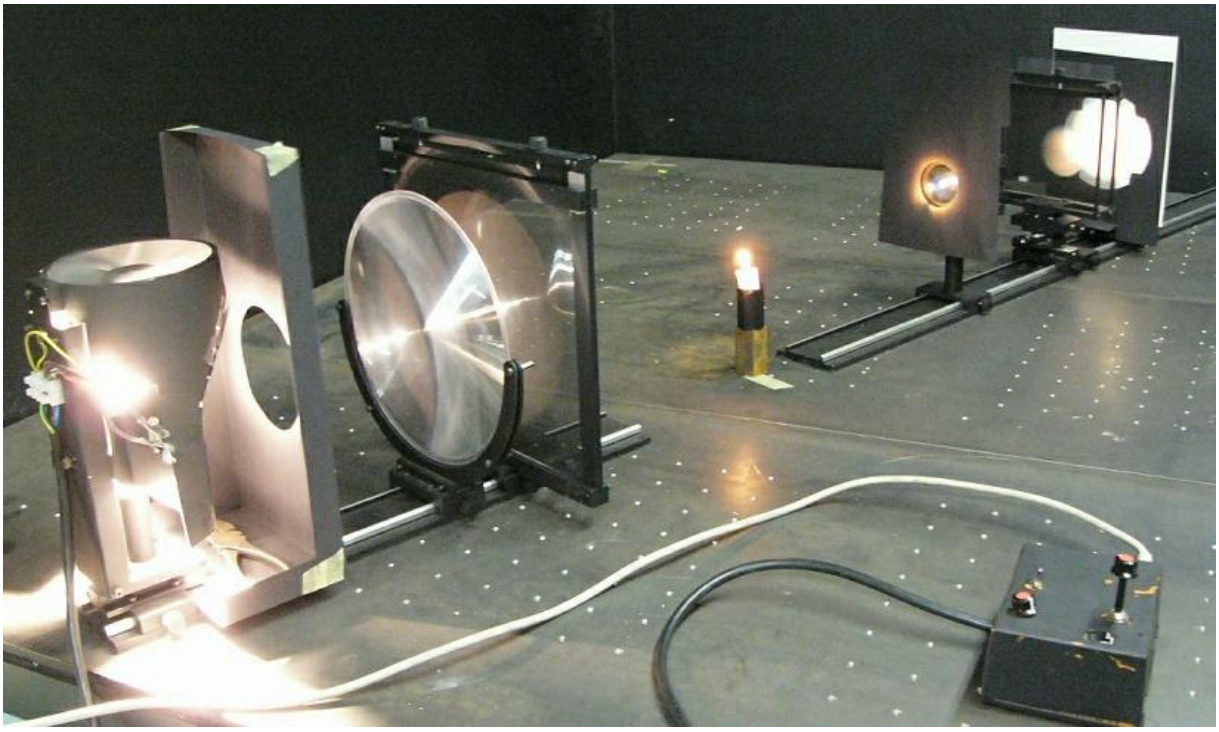


Figure 4.22 Complete apparatus for first configuration

5 EXPERIMENTATION

The purpose of this section is to describe in detail the experiments undertaken in completing the objectives of the project without getting too involved. It is intended to be an overview of what has to be done. Like the objectives, the experimentation was divided into two main parts. The first part was devoted to the exploration of a typical focusing schlieren system while the second investigates a number of different configurations and compares them to this typical system and to each other.

5.1 Exploration of Focusing Schlieren Systems

The references of this report contain a great deal of information on the history, techniques and predicted performance of focusing schlieren systems. In fact, the design and performance estimation of the apparatus used in this research is based entirely on the work of others. However this does not mean that nothing new can be learnt from experimenting with a fairly standard system. There were several objectives to this experimentation, described below.

The main purpose of the experimentation was to determine the optimum design for the source and cutoff grids, in terms of system performance. Primarily, this experimentation revolved around varying the source grid spacing ($1/n'$), which has a great impact on the system performance, and the amount of light passing through the source grid, which can delay the onset of the diffraction limit.

This will allow the current theory of focusing schlieren systems to be verified. This is particularly important because some of the techniques used to build the system are new. In particular, the use of a large image is unusual, as is the method of grid manufacture. While the theory will not specifically be compared to practice, it will be evaluated at least on a qualitative level.

The limits of the system will also be tested. This includes deliberately designing systems which meet or exceed certain limits to demonstrate what happens when they are exceeded. The wide range of testing will also provide a useful basis for comparison when it comes to testing the novel arrangements. It has also been suggested in the literature that varying the amount of light cut off by the source grid can make for a better system, as the clear bands in the cutoff grid can be made wider, thus delaying the onset of diffraction at the cutoff grid. This will be investigated.

5.1.1 Variation of Source Grid Line Spacing

The first set of experiments simply tested black and clear vertical grids with identical grid line widths. In other words, vertical black lines of width *e* were separated by clear spaces of the same width *e*. The major variable was, of course, the line width and how it affects range and sensitivity. Also using these grids, the theoretical system limits of banding and diffraction were investigated. The optimum line width was found by varying between these extremes and comparing the results. The optimum grid width is that which grants the best system performance, particularly sensitivity, while not exceeding any theoretical or practical system limits. Examples of practical system limits are ease of alignment, lens distortion, quantity of light and so on. The only difference between practical and theoretical limits is that theoretical limits have some sort of mathematical model to predict when they are likely to be exceeded.

Eleven different source and cutoff grid pairs were made and several pictures taken of the image under brightfield, darkfield and optimum cutoff conditions. In this experiment, optimum cutoff was very hard to measure quantitatively and thus will be defined as that amount of cutoff which grants greatest contrast between the schlieren object and the background without exceeding the range on the system.

In choosing the values of grid spacing to experiment with, both banding and resolution limits had to be exceeded, while having enough data points in between to be able to pick an optimum grid spacing with reasonable accuracy. The grid dimensions and important system performance information are given in Table 5.1.

Table 5.1 Varied line spacing grid specifications and expected performance

Grid	Spacing mm	Width mm	ϕ	w mm	Range arcsec	C_{Opt} %
a	0.15	0.075	200	8.800	3.9	-
b	0.3	0.15	100	4.400	7.7	46.67
c	0.6	0.3	50	2.200	15.5	73.33
d	0.9	0.45	33.33	1.467	23.2	82.22
e	1.2	0.6	25	1.100	30.9	86.67
f	1.5	0.75	20	0.880	38.7	89.33
g	1.8	0.9	16.67	0.733	46.4	91.11
h	3.75	1.875	8	0.352	96.7	95.73
i	7.5	3.75	4	0.176	193	97.87
j	15	7.5	2	0.088	387	98.93
k	30	15	1	0.044	774	99.47

The eleven grids have been chosen at values of e which best allow the following four areas to be looked at in detail.

- Use grids a, b and c to evaluate diffraction and its effects.
- Use grids a, b, c, e, g and h to evaluate the importance of resolving power (w).
- Use grids h - k to evaluate image banding (ϕ).
- Use grids a - g to determine the optimum grid spacing.

The results of these experiments provide a good idea of the system limits and how exceeding the limits manifests in the final image. It also provides an ideal source grid line spacing which will be required for designing all the subsequent systems and experiments.

5.1.2 Variation of Source Grid Light Transmission Ratio

The second variable to be investigated is the amount of light passing through the source grid. Normally, the total amount of light cut off by the source and cutoff grids is fixed at 100%, in other words, if the source grid blocks 50% of the light, then the cutoff grid blocks 50% of the light. If the source grid blocks only 25% of the light, then the cutoff grid has to block 75%, meaning that it has thick black bands and thin clear bands. This means that for a given line spacing (n), the width of the clear bands in the cutoff grid (b) can be varied. As seen in section 3.1.5, this can be used to delay the onset of the diffraction limit.

As a result of the first set of experiments, the optimum source grid spacing was chosen as 1 mm. Thus all the grids investigated in this section will have this spacing. Seven source and cutoff grid pairs were made, varying the amount of light passing the source grid from 5% to 95%. Once again, all the grids are aligned vertically. The most change occurs near the limits (0% and 100%), so the grids were chosen according to the Table 5.2, overleaf:

Table 5.2 Varied light transmission grid specifications and expected performance

Grid	Spacing	Transmission	Source Grid		ϕ	w	Range		C_{Opt}
			Black	Clear			limit	overlap	
	mm	%				mm	arcsec	arcsec	%
1	1	5	0.95	0.05	30	0.695	-1.5	44.9	-60.00
2	1	10	0.90	0.10	30	0.733	1.0	42.3	20.00
3	1	25	0.75	0.25	30	0.880	8.8	34.5	68.00
4	1	50	0.50	0.50	30	1.32	21.7	21.7	84.00
5	1	75	0.25	0.75	30	2.64	8.8	34.5	89.33
6	1	90	0.10	0.90	30	6.60	1.0	42.3	91.11
7	1	95	0.05	0.95	30	13.20	-1.5	44.9	91.58

Some explanation of the table is necessary, particularly the range and the properties of grid #1. The minimum resolvable width of a line, due to the projection lens quality, is slightly greater than the 0.05 mm wide clear stripes of the source grid # l. This means that to achieve optimum cutoff, a negative cutoff is required, an obvious impossibility. It also means that the range in one direction is negative, in other words the light has to be deflected a certain amount before the system starts to register a change in brightness levels in the image. Practically this means that the system is likely to be poor, with some difficulty expected in interpreting the images. This difficulty with range may be reason enough to avoid using transmission percentages other than 50%.

The range has been split into two columns. The first, limit, is how much the light can bend before it ceases to cause a change in brightness in the image. The second, overlap, is the amount the light has to bend before one cutoff grid line starts to interact with the adjacent source grid line.

One final note concerns grid #7. This grid has a resolution, *w*, worse than that of the worst grid in the first experiment. This is due to the extremely narrow lines being projected by the lens. Once again, a poor image will be the result. As can be seen from the table above, varying the transmission ratio of the source grid does not lead to a great improvement in the resolution for a fixed grid width on one side of 50% but does lead to a large worsening of the resolution on the other side.

To conclude, the seven grids above will allow the effect of varying source grid light transmission to be discussed. Once again, images of brightfield, darkfield and optimum cutoff were recorded and are presented. Finally, an optimum width will be prescribed and compared to the standard approach of using 50%.

5.2 Development of alternative Focusing Schlieren Systems

There are many alternative arrangements for focusing schlieren systems and the objective was to investigate some of them using the same apparatus. The different system characteristics were achieved simply by using different grids or by using a front lit source grid, instead of a backlit one. It was not always possible to use the same components but the same geometry and optics were used for all the systems. This ensures that comparisons between different configurations were meaningful. The alternative systems to be investigated were:

- A 2D system.
- Colour systems.
- A retroreflective system.
- A projected retroreflective system.

Each is described below. The results of the previous two experiments provide a good point from which to design the other systems, as well as something to compare them to. The results of the first experiment (discussed in section 6) showed that a grid spacing of about 1 mm is optimum while the results of the second showed that about 75% of the light should be blocked by the source grid. Also, optimum cutoff generally seemed to be about 80% under these conditions. These results are specific to this system geometry and should not be used generally. Due to the issues of range using a 75% source grid, a 50% grid is used for the comparisons between different systems.

5.2.1 Demonstration of a 2D system

A 2D system is one in which density gradients in both horizontal and vertical directions are apparent in the image. Since focusing schlieren systems are also sensitive in the third dimension as well, it is technically a 3D system however the focusing characteristics of these systems are not of interest for this report.

Surprisingly, very little appears to have been done before in the published literature. Burton's original system (1949) used a random pattern of holes as a source grid and a negative for the cutoff grid. Then Taghavi and Raman (1996) used a cross hatch pattern (vertical and horizontal grids superimposed) to achieve a similar effect in their study of supersonic screeching jets. Fu *et al*. (2000)

used a metal plate with holes drilled in a triangular pattern. At no stage have the characteristics of the 2D system been investigated or compared to a normal grid system.

The scope of the project does not permit a detailed study of all aspects of a 2D arrangement however a basic comparison of a 2D system and a normal grid system has been done. For this purpose, a source grid of circular holes, spaced in a rectangular pattern was compared to a grid with similar grid spacing. The grid has 0.8 mm diameter holes spaced with centers 1 mm apart in a rectangular pattern, giving a 50% light transmission ratio. A textured random pattern of black or clear squares, about 1 mm square was also briefly attempted without achieving the desired results; in fact no image resulted at all.

The analysis described in Chapter 3 is not valid for 2D systems, though the general principles will still apply and will apply for any angled plane within the system. For this reason, the 2D system will be compared to several results from the first two experiments. The cutoff is also somewhat different as it can now be varied in two different ways. One method is to move the cutoff grid either horizontally, vertically or at some angle to the source grid image. Another method is to construct a second cutoff grid in which the opaque dots corresponding to the holes are slightly smaller than the source grid image holes but at the same spacing. To a certain extent, both were tried. These different methods are illustrated in Figure 5.1:

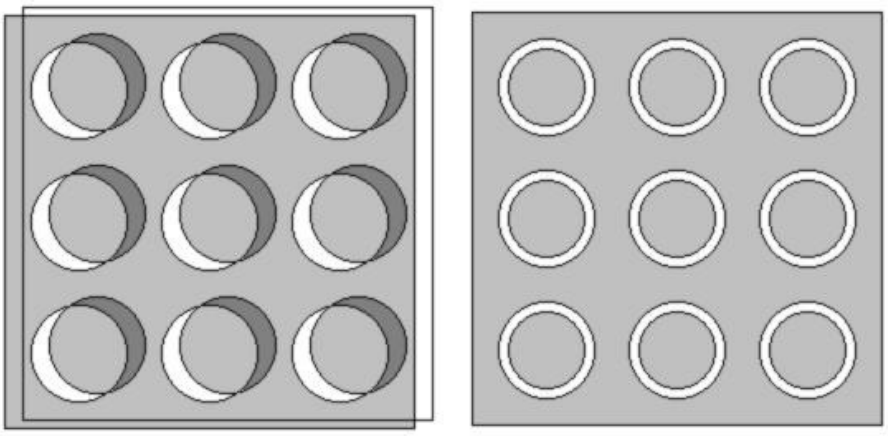
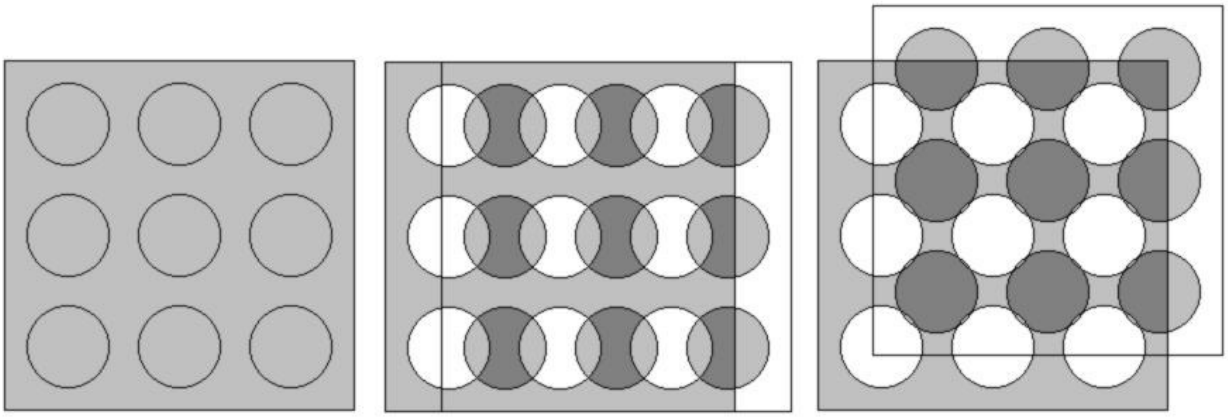


Figure 5.1 Different methods of varying cutoff in a 2D system

Three cutoff grids were made and compared for each of three conditions. The grids were made with dots which correspond to 100%, 80% and 50% of the diameter of the holes in the source grid image. Each grid was then either aligned so that the dot exactly overlapped the hole, was between two adjacent holes or aligned so that it was between four holes. These were called the centered, middled

or off-center condition respectively and are roughly analogous to darkfield, partial cutoff and brightfield respectively. These three conditions are illustrated in Figure 5.2:



a) b) c)

Figure 5.2 a) Centered, b) middled and c) off center conditions for 100% cutoff grid

Finally, photographs were taken and compared, resulting in 9 pictures in total. These were compared to a vertical and horizontal 50%, 1 mm source grid. This yields another 6 images. While aligning the grids, it became apparent that a lapse in foresight meant that there was no method of adjusting the cutoff grid up and down. This problem was overcome by adjusting the projection lens up and down instead. This has the effect of moving the source grid image up and down instead.

As can be seen, there are several advantages to using grids over a 2D system. These are that the construction and alignment is greatly simplified, the percentage cutoff can be varied easily and constantly over the whole area and the meaning of the images is clear. The only disadvantage is that the system can only detect density gradients in one direction. This is not as great a disadvantage as it sounds. Generally speaking, unless the density gradient is a feint feature, it will be visible provided it has even only a small component in the direction of sensitivity of the system. A reasonably strong gradient within 10° of the direction of non-sensitivity will still be clearly visible.

5.2.2 Development of colour systems

Colour can be used in flow visualisation to provide more information about the flow field. Without this fundamental purpose, colour just makes for pretty pictures. Colour has not been used much in focusing schlieren systems. In fact the only reference in this report is Rotem *et al*. (1969) who used colour in a multiple source schlieren system, not a focusing schlieren system. One of the reasons for this is that coloured grids do not greatly extend the system capabilities. A colour system shows as much information as a greyscale system in 1D and only slightly more in 2D.

Unfortunately, during testing, it soon became apparent that the chromatic aberration resulting from the Fresnel lens and two grids resulted in a wide range of colours. In addition, the grids themselves appear to cause some colour effects to be seen. This effect completely invalidates any method of using the colour quantitatively to provide more information about the flow field.

Several methods were tried to reduce the colour in the image. This included using colour filters at the light source and at the projecting lens. This resulted in monochromatic images with substantially reduced sensitivity. The loss of sensitivity seemed to depend on the specific colour and probably originates from the fact that the focusing point of the Fresnel lens moves for variations in colour. Another unsuccessful attempt at a cure was to increase the size of the light source and reduce the aperture of the projection lens. This should stretch the focused portion of the Fresnel lens to the same dimension as the chromatic aberration of the lens. Unfortunately it failed to have much impact at all on the amount of colour in the image.

The Fresnel lens was regarded as one of the primary causes of the problem and could not easily be replaced by an aspheric, ϕ254mm, f# 0.9 lens which was achromatic as well. Because of this, the objective involving colour had to be abandoned, though, not completely. While the planned colour systems would not be made or tested, some initial work had been done and is worth reporting.

Originally, three different colour systems were going to be made and tested. The first was a colour grid, consisting of a pattern of equally wide black, cyan, clear and magenta, repeating at a source grid spacing of 1 mm. The source grid would be a black and clear grid, with 25% light transmission. Unfortunately, the introduction of colour means that the previous method of grid manufacture, commercial positives, could not be used. Instead, more conventional printing methods had to be

employed. These have already been described in section 4.2.15. To test whether the print quality of a colour cut off grid would be adequate, a colour cutoff grid was made and tested.

The test resulted in a very poor image, due mainly to the fact that the plastic used for the colour cutoff grid scattered light somewhat. While the colour was clearly visible, the image was extremely blurry and somewhat darker than usual. As a result of this, no meaningful pictures could be taken, so there are no results to be displayed. All future systems would have to be made with a colour source grid and a black and white cutoff grid, despite the fact that this would increase the amount of diffraction within the system, due to the narrow gaps in the cutoff grid.

The two other systems planned were 2D systems, one of which would vary colour with the magnitude of deflection and the other of which would vary with the direction. These would essentially consist of a source grid of opaque dots surrounded by either coloured rings or sectors (for magnitude and direction respectively) and a cutoff grid of clear holes. One of the perceived problems was that the dots would represent a very small overall percentage of the grid particularly in the magnitude case (around 2.7%).

For the 2D colour systems, the range of possible colours seen in the image is infinite, depending on the quantities of the three colours overlapping at a given point. Interpreting such an image, especially quantitatively, becomes something of a challenge. This, combined with the difficulty of getting the system to work in the first place, when it is not clear what the source of the colour is, and time constraints means that the objective will have to be left for future work.

5.2.3 Demonstration of a Retroreflective System

The main benefit of this system is that it can be used to create very large test sections at relatively low cost. This is due to the fact that the size of the test section no longer depends on the size of any of the optical components in the system. Past experience has demonstrated that retroreflective systems have several unique problems, such as needing more light and difficulty with using a beam splitter compared to backlit focusing schlieren systems. For this reason it is necessary to compare the retroreflective system with a focusing schlieren system, as directly as possible, to outline the major benefits and penalties of using such a system.

To create a retroreflective system, the system has to be rearranged as shown in Figure 4.2 on page 45. As far as possible, the same components and geometry are used. As mentioned, this amounts to using a sheet of glass as a beam splitter and mounting the source grid and the retroreflective screen in the source grid support.

This causes two main effects. Firstly, because a beam splitter has been used, the total available light is at best quartered. In fact it is somewhat less than that because a glass sheet does not act like a 50% transmission, 50% reflection mirror at 45°. Secondly, the retroreflective screen has its own characteristics which affect light. These include affecting the colour, requiring additional adjustment to get the upstream and downstream components co-axial and a tendency to cast shadows wherever there are fingerprints or dirt.

Once the system was set up, using a 1 mm, 50% source grid, photographs were taken and were compared to the more conventional backlit focusing schlieren systems above. These results are presented in the next chapter.

5.2.4 Demonstration of a Projected Retroreflective System

This arrangement is like that illustrated in Figure 4.3 on page 46. The primary advantage of such an arrangement is that it contains every element of the system, except the retroreflective screen on one side of the test section. Essentially this means that all the elements could be assembled in a box while the screen remains separate. This has enormous potential for a quick to set up schlieren system and there is no good reason why it could not be portable as well. In its ultimate form, it would be a box the size of a shoebox which can be placed on a tripod, a fixed distance from a retroreflective screen. By moving one or both lenses in the box, the focusing plane can be adjusted and any density gradients between the box and the screen could be captured on film. By adjusting the position of the source and cutoff grids, the distance between the screen and the box can be varied.

Thus this is a system which can be set up very quickly and moved as required to suit a wide range of possible applications. However, before this ultimate form can be realised, the basic operating principle has to be demonstrated and compared first.

The arrangement requires that a source grid is projected onto the retroreflective screen, using a small grid and a secondary projection lens. This shadow on the screen then forms the effective source grid for the focusing schlieren system as for the retroreflective system. There is a perceived problem that any density gradient in the test section will distort the image of the grid on the screen. The light will then be reflected back along the path it came and be bent back to a perfect grid, to match the cutoff grid. This would result in no image, no matter what gradients were in the test section. In the event, this does not happen, as photographs in the results section clearly show. The reason for this is not known, though it is probable that it is because the retroreflective screen does not reflect light exactly back the way it came but in a cone of one or two degrees. Thus very little light falling on the image plane comes from the part of the screen that corresponds to a particular point on the image.

While a ‘schlieren camera’ would be the ultimate goal of a projected system, the goal of this report is simply to demonstrate that the principle works and to compare it to more normal means. To this end, the usual brightfield, darkfield and optimum pictures will be taken using a 1 mm, 50% effective source grid and comparing the results to the same grid for the backlit configuration. This requires a smaller grid, which is projected through a secondary projection lens. Once again, this arrangement results in an increase in the complexity and difficulty of set up. This will be discussed further when the results are presented in the next chapter.

5.3 Other Issues

During testing, several problems arose, most of which have been discussed above. These include colour in the images caused by chromatism in the Fresnel lens and grids, damage to the grids from overuse and abuse, poor printing of the grids and shadows caused by fingerprints and dirt on the retroreflective screen. In addition, the system geometry is critical to achieving a good system and has not yet been discussed. This aspect needs to be mentioned before the results are presented.

Given that the geometry calculations are based on the thin lens approximation, a better method for positioning components is needed. Initially, the system is set up according to the dimensions given by the thin lens equation. The core of the focusing system is ensuring that the source grid image is both the same size as the cutoff and in sharp focus, at the same time. Provided this condition is met, the placement of most of the other components is not absolutely critical.

To achieve this end, a small sliver about 2 mm wide and 60 mm long is cut from the cutoff grid, such that the lines are perpendicular to the sliver. This is then taped flat against a sheet of paper which in turn is fastened in the cutoff grid support. The cutoff grid is adjusted until the source grid image is sharply focused on the sheet of paper. By having the sliver there, the source grid spacing and the cutoff grid spacing can be directly compared. If the source grid spacing is smaller than the cutoff grid spacing, the lens is moved slightly closer to the source grid to make the image bigger. This is then refocused by adjusting the cutoff grid position. After a few tries, the source grid image will be sharply focused and at a similar grid spacing to the cutoff grid. Now the sheet of paper can be replaced by the actual cutoff grid.

Without this procedure, it is possible to get schlieren images simply by moving the cutoff grid until the spacing is similar to that of the source grid image however if it is not properly in focus, achieving brightfield or darkfield images is virtually impossible. This procedure needs to be performed for the retroreflective system as well and twice for the projected retroreflective system. Also, it has to be redone every time the system is moved or dismantled. Finally, a large grid is less hard on the eyes to determine exactly when it is in best focus, though half an hour of staring at bright stripes is invariably a little stressful!

6 PRESENTATION AND DISCUSSION OF RESULTS

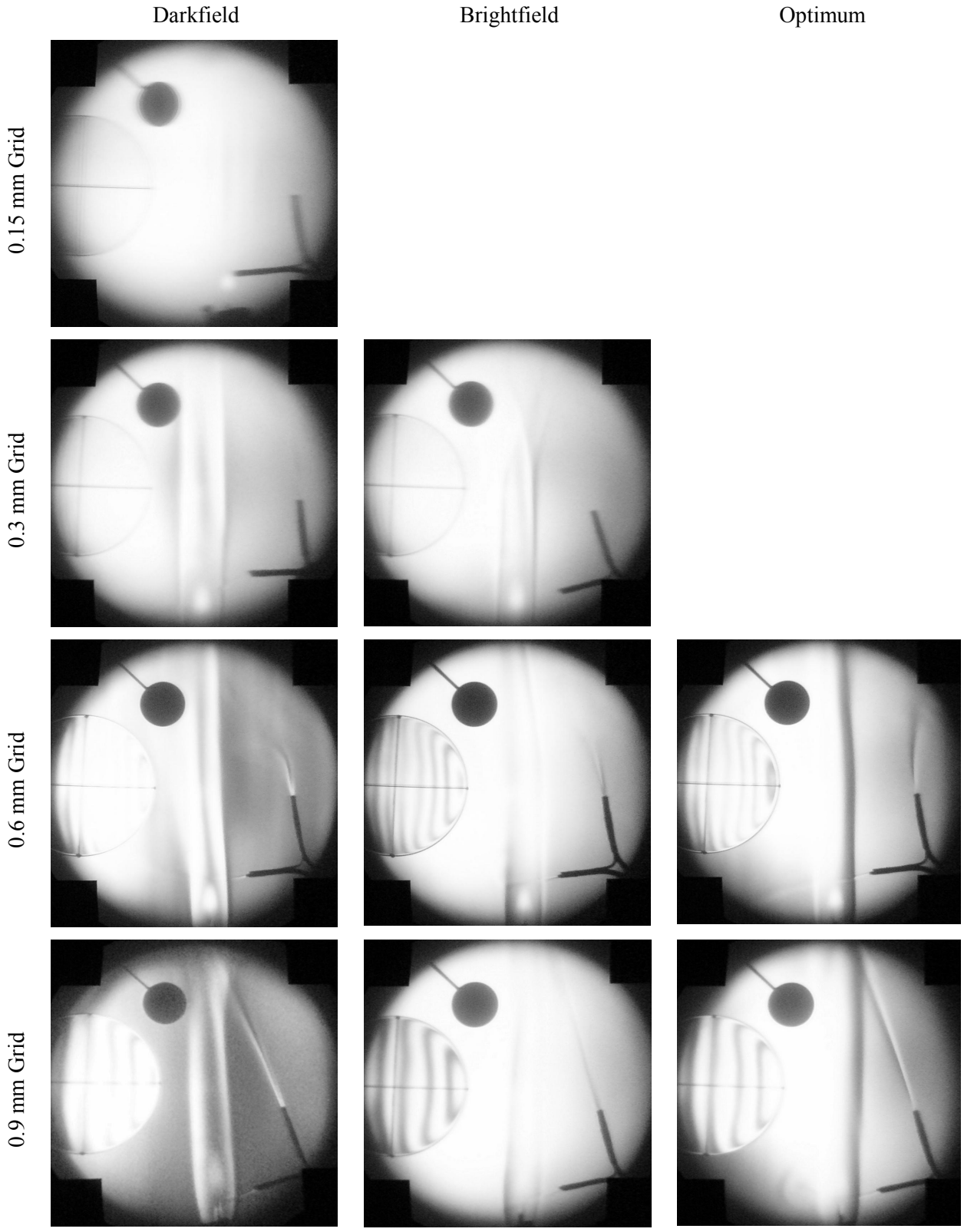
The preceding section has described five specific experiments which are to be undertaken to complete the objectives. The results of these experiments will now be presented and discussed.

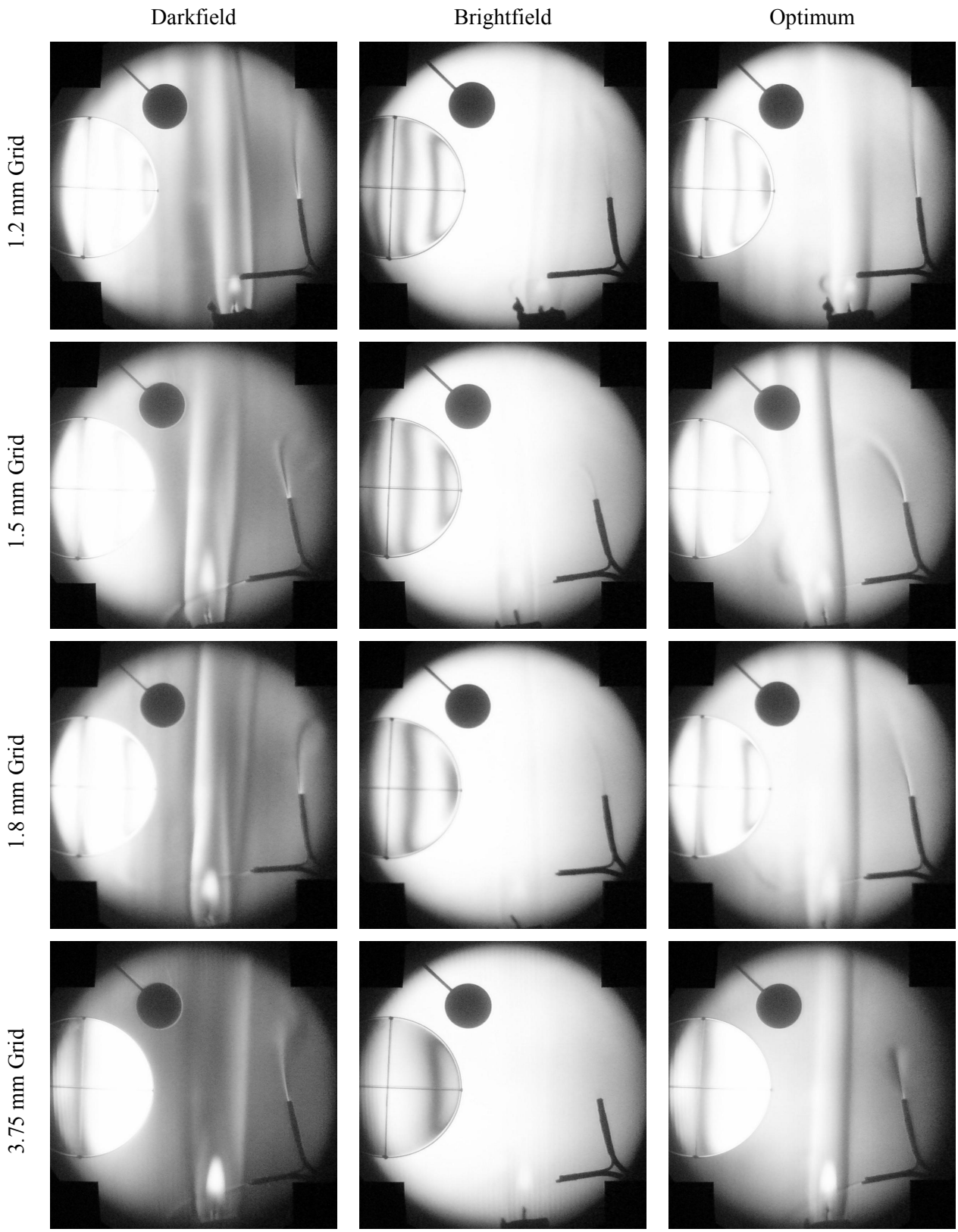
6.1 Variation of Source Grid Line Spacing

6.1.1 Results

The results of the first experiment are presented over the next three pages. There are 33 images consisting of darkfield, brightfield and optimum cutoff setting for each of the 11 test grids. Very fine grids result in very similar images for darkfield, brightfield and optimum images while very coarse grids result in very similar darkfield and optimum images. For these cases, duplicate images are left as blank spaces. For each picture below, there follows a summary of the features of the image and an explanation as far as possible of why those features are apparent.

The darkfield condition was obtained by adjusting the cutoff grid until the background of the image was as dark as possible. Brightfield was similarly obtained by adjusting cutoff until the background was as bright as possible. Finally optimum cutoff has been defined as the amount of cutoff which gives the greatest contrast in the image, without exceeding the range of the system.


Darkfield
Brightfield
Optimum
0.15 mm Grid
0.3 mm Grid
0.6 mm Grid
0.9 mm Grid


Darkfield
Brightfield
Optimum
1.2 mm Grid
1.5 mm Grid
1.8 mm Grid
3.75 mm Grid

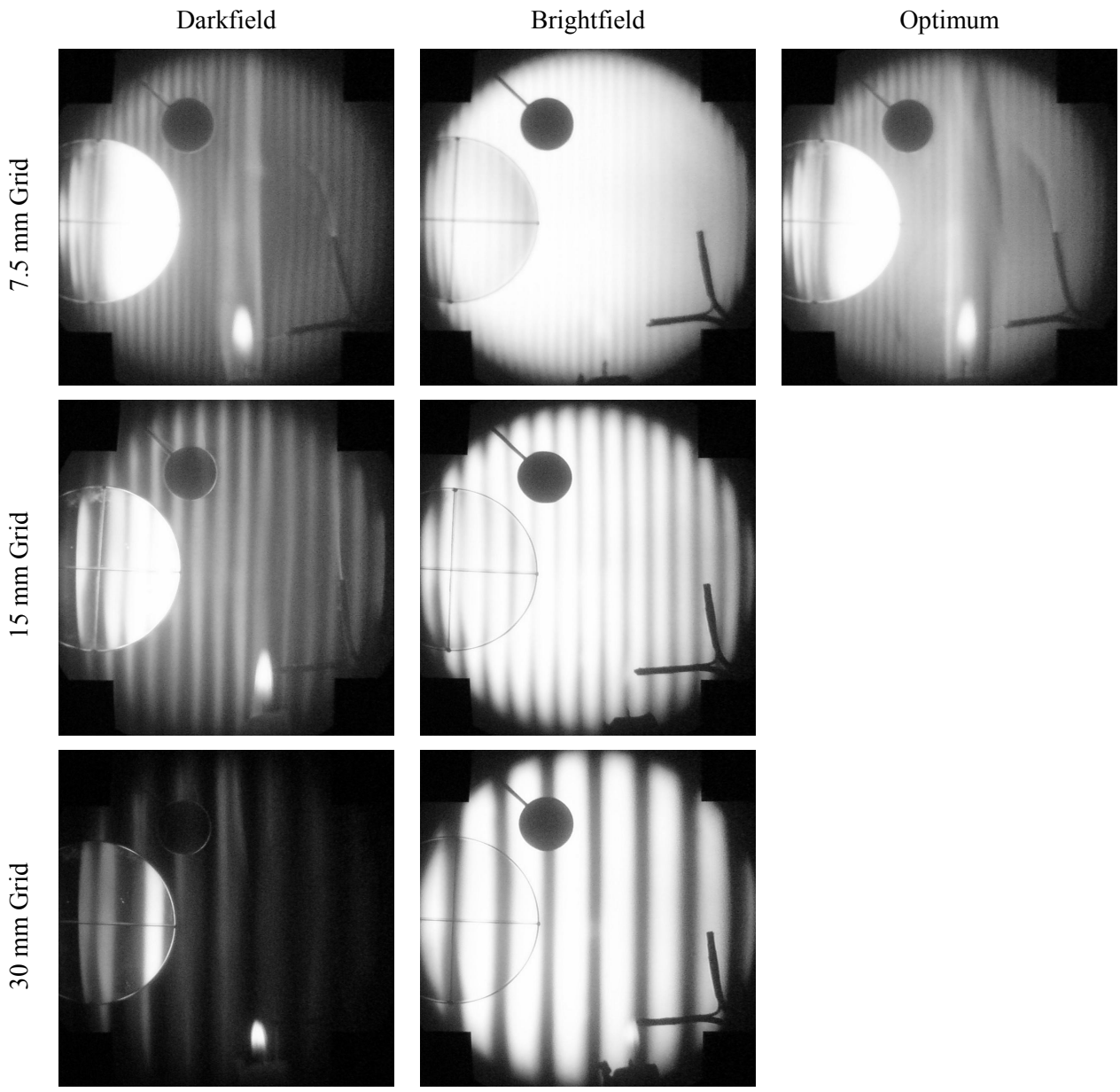


Figure 6.1 Results of variations in source grid width

6.1.2 Discussion of Images

0.15 mm Grid

In the first row of results, there is only one picture. This is because the images of brightfield and optimum look identical to the darkfield case. In fact, varying cutoff has no apparent affect on the image at all. The background is a uniform grey, slightly darker at the edges, the lens, candle and gas emitters have no visible effect whatsoever. Only the disk gives any information. The disk looks fuzzy and pale, compared to most of the other images. In particular, it looks blurred in a horizontal direction. Looking closely (see figure 6.2) shows that the image of the disk seems to be made up of several superimposed and not quite overlapping images. In fact, all the vertical lines in the image are blurred horizontally.

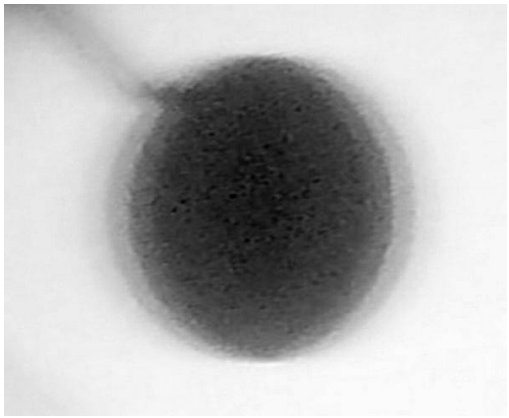


Figure 6.2 0.15 mm grid enhanced image of disk

In terms of system performance, sensitivity is non-existent. Even the lens has no detectable gradients. The resolution of the image is impossible to quantify, since there are no visible flow features, however the solid objects are blurred in the horizontal direction, suggesting very poor resolution. Functionally, the image and the system are useless as a schlieren system. It is very good at illustrating what happens when too fine a grid is used, however.

The main cause of the poor image is the fact that the narrow grid spacing of the source grid is beyond the resolving power of the lens, in other words, the lens is incapable of focusing the source grid onto the cutoff grid. Instead, an unresolved averaged grey is focused on the cutoff grid. This grey is uniform enough that virtually no information on the density field is identifiable. Each slit in the cutoff grid acts like a diffraction slit because it is only 50 micron wide. This explains the horizontal blurring of all the solid objects.

By looking at the properties of the system, in Table 5.1, it can be seen that the resolution is 8.8 mm. This is approximately the amount by which the disk is blurred in the horizontal direction. The disk is 21.0 mm in diameter. It can also be seen that the range of the system is 3.9 arcseconds. This is less than the minimum sensitivity the lens is capable of, namely 4.1 arcseconds. Thus an optimum cutoff cannot be specified. It is assumed that any time the range is less than the sensitivity, there will be no visible flow features since the strongest object the system can view cannot be resolved sufficiently well by the lens to make it visible.

0.30 mm Grid

The next grid spacing is double that of the previous system and has a range that exceeds the minimum sensitivity. There are two pictures this time, one for darkfield and one for brightfield. The darkfield image has a slightly darker region in the center while the brightfield case has a darker edge and a slightly brighter center. It is impossible to get the background evenly lit. The lens is just not capable of doing so. The solid objects are still somewhat blurred in a horizontal direction, though not nearly as obviously as the previous grid system. While the candle plume is clearly visible in both darkfield and brightfield images, the gas emitters are not apparent in either.

It is very difficult to say which of brightfield or darkfield displays greater sensitivity. This is the reason there is no optimum image. It can be seen that the darkfield case has the least contrast over the image compared to any of the subsequent darkfield images, while the brightfield case has the greatest contrast of any of the subsequent brightfield images. Overall, the images are very similar and the cutoff position does not have much impact on the final image.

From Table 5.1, it can be seen that the range is about double the minimum sensitivity and the optimum cutoff is about 50 %. This explains why the images are so similar. Interestingly, while 0% cutoff and 100% cutoff give similar results, so does 50% cutoff. This could be due to one of two things. Either the system is exhibiting standard characteristics, i.e. 50% cutoff really does look like any other cutoff value for cases where the range is double the minimum sensitivity. Or, the grids are not aligned accurately enough to be able to say accurately what the cutoff actually is. Since the cutoff grid lines are 50 micron wide, a misalignment of, say, 20 micron would be enough to cause significant uncertainty in cutoff. This would have the effect of making all cutoff percentages give similar images. It is not really possible to say which is the case, with this apparatus.

The gas emitters are not visible because the system has a resolution of 4.4 mm. This is much greater than the 1 mm or so diameter of the gas jet but much smaller than the 25 mm diameter of the candle plume. The lens appears to be a uniform grey, despite the fact that the candle plume is obviously capable of providing visible gradients. As the lens provides greater angles of deflection of the light in the test section, it should also provide stronger and more visible gradients. Perhaps the reason it does not is attributable to the fact that the lens is near the edge of the test section, where sensitivity seems reduced.

It appears that the system is more sensitive at the center of the test section than at the edges. This stands to reason, as lenses traditionally have better resolving power at the center than at the edges. This may also contribute to the lack of gas jets, since they are primarily located at the edge of the test section. This effect will become progressively less significant as the grid spacing and thus the range of the system increases. There is also slightly more light in the center of the test section than at the edges due to the Fresnel lens though it is doubtful this has much impact on sensitivity.

0.60 mm Grid

This system is better than the previous two in many ways. This is the first system in which there has been a significant difference in darkfield and brightfield images, justifying an optimum image. It is the first in which the solids are sharply defined and it is the first in which the gas jets are visible. It is also the first in which the lines of constant deflection in the lens are clearly visible (particularly the brightfield and optimum images). Finally, it is the first system in which the heat rising from a hand is visible. Unfortunately, the tiny variations in brightness due to this are trivial compared to the variations in background brightness, so the effect is not photographable. It is only the slight shimmering with time that makes it detectable.

The contrast is much higher, making it much harder to achieve a constant background illumination. This is particularly true of the darkfield case, where the left hand side is much brighter than the right hand side. Once again, the center of the image still exhibits greater sensitivity than the edges, indicating that the system is near the limits of resolution. This is shown most strongly in the darkfield case, where the dark area on the right hand side is darkest against the candle plume, in the center of the image.

The lens in all three images displays vertical lines, corresponding to the lines in the source grid. Each line is displaced by a progressively greater angle, moving from the center of the lens. These are lines of constant deflection. Despite the fact that the lens deflects light radially, only the horizontal deflections are visible, since the grid lines are vertical. This is further verified by the fact that the vertical gas jet, with strong horizontal gradients, is far more visible than the horizontal jet. The horizontal gas jet is not actually horizontal otherwise it would not be visible at all. It has been found that even small deflections of the gas jet from the horizontal (say 5° or so) are large enough to make the jet visible.

For this system, the range is 15.5 arcsec, meaning that each line within the lens is deflected by 31 arcsec more than the previous line. It can be seen that there are about 4.5 lines between the center of the lens and the edge. This corresponds to a deflection of about 140 arcsec. The actual deflection based on focal length and lens diameter is about 144 arcsec. Thus quantitative measurements can be made accurate to a few percent. There is one restriction however. While the gas jets appear visible, the resolution is poor enough that the lines of constant deflection are blurred out. Thus for flow objects smaller than the resolution of the test section, quantitative measurements cannot be reliably taken.

There is a minor problem here with the image capturing. In all cases, the camera exposed the pictures automatically. This means that the darkfield image was brightened while the brightfield image was made darker. This has the effect of making images all look similar except for contrast. To get an accurate idea of how much the camera adjusted brightness, the inside of the lens for each of darkfield, brightfield and optimum images are constant brightness. As can be seen in the darkfield case, the interior of the lens is completely overexposed, while for the brightfield case it is correctly exposed. This should give an idea of how dark even the bright portions of the darkfield images are.

It can be seen that the darkfield and optimum images display much greater sensitivity than the brightfield case. This is because the sensitivity is approximately the same as the range at 0% cutoff. The optimum cutoff, 73%, is much nearer the darkfield condition. The gas jets are distinct, though not at all detailed, even though the resolution is only 2.2 mm in the test section.

0.90 mm Grid

The 0.90 mm grid once again displays greater contrast than the previous system. Despite this, it is a little easier to align, resulting in a more consistent background in the darkfield case. A trend is beginning to form in that the darkfield case for any grid is much harder to align than brightfield to get a consistent background illumination. This is because the brightfield case involves much more light, so a given variation in position of the cutoff grid changes the light level by a few percent. In the darkfield case, there is much less light so the same variation in the cutoff grid position is much more important.

This same effect also means that the darkfield case displays a much greater sensitivity that the brightfield case. A density feature has to be quite strong to drop the light level in the brightfield case, while only small deflections will cause a large change in light level in the darkfield case. Of course, this explanation is where the definition of sensitivity comes from.

Looking at the opaque disk in the darkfield case, a halo can be seen surrounding it. The halo is only really visible along the bottom right edge, however once inverted, it can be seen more clearly. The halo is fairly typical of schlieren systems which are at or near 100% cutoff and is caused by diffraction round the edge of the object. The halo should only be visible in a horizontal direction, though this is not particularly obvious from Figure 6.3. It was possible to see that this was the case while using the apparatus however.

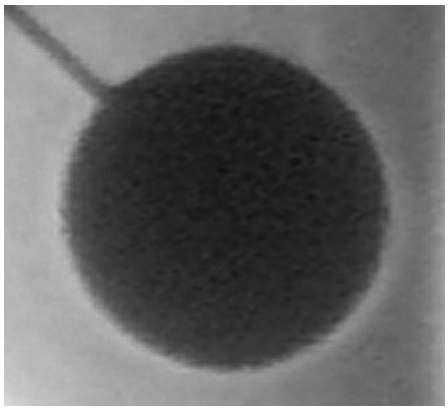
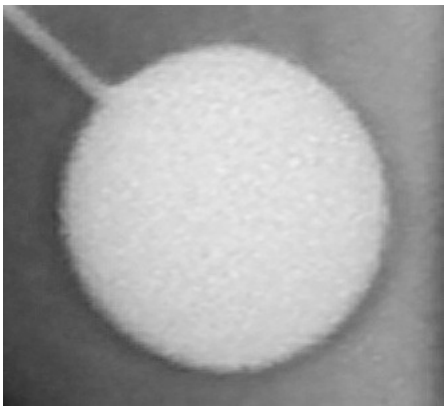
a)  b) 

Figure 6.3 0.90 mm grid a) enhanced disk halo, b)inverted

While the gas jets are much more distinct than for the previous grid, they are still just a smear. This indicates that the resolution of the system is still not that good. It is also starting to become apparent that the optimum cutoff does show a little more detail than the darkfield case. This is probably due to

the fact that the background is not the darkest object, so the jet is both darker and lighter than the background while for the darkfield case, the jet is just a bright smear. For these images, the jets were leaning over enough that the horizontal jet can be seen, albeit not very well. The tubes directing the gas had a tendency to sag when heated by close proximity to the candle.

1.2 mm Grid

The images from this grid look quite similar to the previous grid. Once again there is a halo around the disk, though it is not as visible as before. The lens is washed out in the darkfield case and clearly visible in the brightfield case. Once again the brightfield case has lost sensitivity, to the extent that the gas jet and candle plume are barely visible. While easier to align, the darkfield case actually has a less uniform background than the previous system, though this is probably due to one of the two grids being stretched too much, resulting in a slightly rippled surface. The optimum case does appear to have a more uniform background than the previous system.

The main point of interest is the gas jets. The resolution is now high enough to show a bit more information. In fact the optimum case looks particularly sharp. Looking at table 5.1, it is seen that the theoretical resolution is 1.1 mm. Interestingly, the sensitivity of the system is not as high as for the previous system. The jets are more detailed but also smaller.

1.5 mm Grid

The background of the darkfield case is more evenly illuminated than the previous system. The disk again has a halo and the gas jets are clear but even smaller than they were. The candle plume is beginning to look like a slightly weaker flow feature than before, due to a loss in sensitivity. (In other words there is less contrast across it.)

The brightfield case is almost completely useless. The candle plume is just visible around the base of the candle and the vertical gas jet is similarly only just visible. The sensitivity of the system in the brightfield case is 38.7 arcseconds. The lens is the only object which is strong enough to cause an obvious change in light level.

The optimum case is somewhat better than the darkfield case. The background is more even and the gas jets are larger, suggesting better sensitivity. There is also no halo around the disk and the lines

are visible inside the lens. The candle plume has as much contrast across its width but does not give as much information, since a large portion of it is just white. This is due to the fact that the range of the optimum case is not the same in both directions. In other words, the brightest and darkest a point can get are not different from the background illumination by equal amounts.

Overall the sensitivity looks worse and while the resolution should be better, this is not really apparent. The alignment was easier, though the darkfield case is still not evenly lit, suggesting that the main issue with alignment is no longer the grids themselves but rather the precision with which they can be lined up.

1.8 mm Grid

There is not too much to say about this grid. All the trends are continued. The darkfield background is more even though still not perfect, the halo is visible and the sensitivity is fractionally worse across all three images. Once again the resolution should be better although this is not really apparent due to the worse sensitivity.

There is some interest though. Firstly, the dark bands in the brightfield lens are now darker than previously. Whether this increase in contrast is due to the fact that the camera is compensating because the brightfield is brighter, making the bands look darker or due to the contrast genuinely being higher, is unknown. Whatever the case, this can be used in that strong schlieren objects should show up very clearly in the brightfield case. This means that a designer may deliberately make a system with worse than optimum grid spacing if they want clear pictures of strong schlieren objects.

The second point of interest is that the focus of the camera does not seem to be quite right. This is mainly visible by looking at the corners used for perspective correction. The corners have not passed through the optics of the system and are thus not subject to diffraction effects and the like. The blurring is not really significant enough to affect the results however.

Finally, this is the last system in which it is possible to see heat rising from a hand. Once again, it is not photographable and is only visible as a faint shimmering. For a few of the grids above, this effect was not as pronounced, mainly due to the importance of alignment. To achieve the upper limit of sensitivity, alignment has to be perfect.

3.75 mm grid

This grid dimension was chosen to give a Weinstein criterion of 8. This gives a starting point for looking for banding. It also gives a grid dimension about twice that of the previous grid, resulting in significantly different images.

The darkfield case is at last significantly dark and also very evenly lit. Unfortunately the sensitivity is not so good, so the candle plume and gas jet are not as visible as with previous grids. The halo is more visible in this image than any of the others due probably to the fact that the background is darker than any of the others. The brightfield image does not show any density gradients at all, except in the lens. By looking at the lens, it can be seen that deflections of about 100 arcsec are required to have an effect. Looking at Table 5.1, the range is given as 96.7 arcsec. The optimum case is still good enough to see both the candle plume and the gas jet clearly and is almost as good as any previous grid as a visualisation tool.

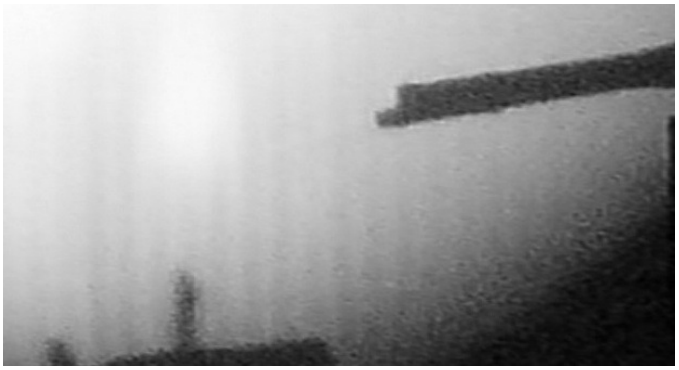


Figure 6.4 3.75 mm grid banding

Banding is just visible near the edges of the image, particularly near the top and bottom in the darkfield and brightfield cases. Figure 6.4 shows the banding near the candle base in the brightfield case more clearly. The banding is not really something that obscures or prevents meaningful results. It is also interesting that the banding is most obvious in the brightfield case, then the darkfield case and is least visible in the optimum case. The reason it is most visible near the edges is because that is where there are the lowest light levels, thus small variations in brightness are most clear.

7.5 mm Grid

With this grid, the most obvious thing is that banding is now a serious problem. It is still slightly less of a problem near the middle and in the optimum case, as before, but now it is very distinct over the entire image. The Weinstein criterion is 4 for this grid.

While the banding is a major problem, the main flow features are still visible. Both the candle plume and the gas jet can be seen, though they are much less clear than before. In fact the gas jet can only just be made out. Ironically, the resolution for this grid should be higher than for any previous system. The lens is now functionally less useful, since the first dark fringe occurs outside its radius. This means that the lower contrast features can be seen and the lens simply takes on the banding lines. Banding also means that the images cannot be used quantitatively.

In the darkfield case, the dark features, particularly the disk, now have a fine speckle pattern of noise over them. This is a result of using a camera in low light conditions. As the amount of light decreases, the signal to noise ratio increases, causing pixel-sized snow over the image. This also contributes to the loss of resolution.

As the range becomes very large, 193 arcsec in this grid, the darkfield and optimum images begin to look alike once again. This is a result of the fact that the optimum percentage cutoff is 97.9 %, not very different to the 100 % for darkfield cutoff.

The Weinstein criterion represents the number of slits in the cutoff grid which illuminate a particular point in the image. They do not necessarily overlap perfectly and the resulting image is a composite of all the partial images. As this number decreases, it is possible that the overlapping images are far enough apart that features are smeared and sensitivity lost.

Alignment may also play a role in that to achieve the optimum cutoff requires very precise adjustment, as the range is larger. Every time the grid spacing doubles, the range doubles, meaning that a given movement in the cutoff grid causes a greater variation in sensitivity. As this limit approaches the accuracy with which the grid can be positioned, the sensitivity is similarly affected.

15.0 mm Grid

Once again, there is so little difference between the darkfield and optimum cases that there is no point including the latter. As a flow visualisation tool, this grid is useless. The candle plume is completely invisible except for a slight blurring and the gas jet is only visible in the darkfield case by virtue of the fact that it happens to be near a light/dark boundary of one of the bands. In the brightfield case, nothing is visible.

Banding now dominates the image completely at a Weinstein criterion of 2. As nothing in the image is a strong enough feature, the actual effectiveness of the system cannot be judged. A deflection of about 400 arcsec would be required to show up on the image though. It is doubtful that much could be seen anyway, both due to interference from the banding and from the loss of sensitivity and resolution, causing blurring.

30.0 mm Grid

Everything that applied to the previous grid applies here, only more so. The Weinstein criterion is 1 for this grid. While banding is extreme, it is important to note that the loss of information in this and the previous grid is caused by the huge range of the systems. While the banding would make such information unusable, the information is not actually there in the first place.

The last four grids have not really been discussed comprehensively, limited just to what the image looks like. They will be discussed further in the next section.

6.1.3 Discussion of Series

The images are ordered by grid spacing, from smallest to largest. As would be expected, the images are very poor to begin with, get better as the system passes through an optimum and once again degenerate at the other extreme.

The series of darkfield images proved the most difficult to align, particularly at the smaller grid spacings. Special concern had to be paid to alignment for grid spacings less than 1.2 mm. Once above 1.8 mm though, alignment was comparatively simple. All the systems were initially aligned in

the darkfield condition, since misalignment showed up most clearly. The brightfield and optimum images were then obtained simply by varying the cutoff, by moving the cutoff grid horizontally.

The darkfield series of images gradually improves in sensitivity until the 0.9 mm grid, where it is at its best. After this point, the sensitivity slowly reduces again. There is good enough sensitivity to see the candle plume from the 0.3 mm grid to the 7.5 mm grid. The gas jets are not visible in the 0.3 mm grid, due to very low resolution, not low sensitivity. The resolution of the darkfield images also gradually improves until it is at its best at the 1.2 mm grid. After this point, though the theory says the resolution improves, this is not apparent in the pictures. This is probably due to the fact that as the range increases, the sensitivity drops and the resolution suffers as a result.

The range of the images gradually increases as the grid spacing increases. Because of this, all the systems with a grid spacing of 0.9 mm or less exceed the range. In other words the range of the system is not sufficient to accommodate the strongest schlieren objects in the test section. This naturally includes the lens, which is designed to have a very large deflection. Banding is detectable for the first time with the 3.75 mm grid, though is only significant by the 7.5 mm grid.

One thing that is interesting to note is that the darkfield background gets darker as the grid spacing gets larger. This is due to three factors. The first is that diffraction through the narrower slits means that some light gets through the cutoff grid, despite the fact that the slits overlap 100%. The narrower the slits, the more light gets through by diffraction. The second reason is that the lens cannot accurately reproduce the source grid image on the cutoff grid, so some light gets through. Similarly misalignment of the grids means that some light gets through. With both of these, the more frequent the slits are, the more light gets through. The diffraction halo is visible in all grid spacings of 0.9 mm or greater. Prior to this, there is too much light getting through the cutoff grid and washing out the image.

It is worth noting that a large portion of this light passing through both grids is as a result of using manufactured as opposed to developed cutoff grids. While a manufactured grid has a far higher contrast ratio between clear and opaque regions, it means some light gets through wherever the source grid image is not perfectly focused on the cutoff grid. A developed grid will allow less light through the gaps and will match the cutoff grid perfectly but will also allow less light through the clear portions. Thus both the darkfield and the brightfield images will be darker. This may have the effect of increasing sensitivity in the darkfield condition, since there is less light or it may worsen the

sensitivity as the light has to bend through a greater angle to miss the cutoff grid. This effect can be replicated somewhat using manufactured grids by making the cutoff grid opaque bands slightly wider than the source grid image bright bands.

The brightfield series of images was far easier to align to get a constant background illumination. In fact the problem with this series is determining how much cutoff was used. For the most part, the image was made as bright as possible and the crosshair in the lens was used to judge the cutoff. Also, the brightness of the background did not vary with grid spacing as in the darkfield case.

With the brightfield images, the sensitivity is roughly equal to the range of the system. Because of this, the sensitivity is at its best at 0.9 mm but drops off very rapidly until at 1.8 mm, the flow features are no longer visible. Interestingly, the 0.9 mm system does not seem to exceed the range like the darkfield case. The resolution similarly drops off very sharply, meaning that it is at its best with the 0.9 mm grid. The resolution is never very good though. Once again banding is just visible with the 3.75 mm grid, though only becomes serious with the 7.5 mm grid.

Finally, the optimum series of images was almost as difficult to align as the darkfield images. Like the darkfield images, best sensitivity was achieved at the 0.9 mm grid and best resolution at 1.2 mm. Also like the darkfield images, the range of the 0.9 mm system was exceeded. Unlike the darkfield images, the optimum series of images is remarkably consistent in appearance. All the grids, from 0.6 to 3.75 mm, look the same except for minor differences, mainly in resolution. The background is a constant brightness and the sensitivity is very similar. Interestingly, banding appears less of an issue in the optimum case. The 3.75 mm grid does not show banding as obviously as darkfield and brightfield images and the 7.5 mm optimum image is far more useable than the darkfield image, despite the banding.

6.1.4 Discussion of Experiment

Originally, four factors were to be investigated concerning variations in grid spacing. These were diffraction, resolution, banding and determining an optimum spacing for this system geometry. Of these, diffraction and resolution are very closely related and will be discussed together.

The theory includes an equation for the resolution of the test section, limited as a result of diffraction at the cutoff grid. Once diffraction is no longer significant, the resolution should continually improve until banding occurs or the sensitivity is reduced enough that the flow information is lost. This theory works well near the diffraction limit of the system and seems to predict the system performance reliably. Unfortunately, in practice, the resolution appears to pass through an optimum and then slowly get worse again. This optimum occurs at a grid spacing of approximately 1.2 mm for this system geometry. The worsening of resolution is barely noticeable at first but can certainly be seen by the 7.5 mm grid. This suggests that something is missing from the theory, particularly once diffraction at the cutoff grid is no longer as important.

There are a number of possibilities. The first is that the resolution is sufficient to see the finest detail available in the test section. This would explain why there seems to be an upper limit to the resolution. The worse resolution of the 7.5 mm grid could simply be a result of the lower level of light available for photography. This reduces the capability of the camera to reproduce what appears on the screen. Banding, combined with fewer grid lines means that the 7.5 mm darkfield and optimum images are darker than any of the previous systems. This can be checked by including a reasonably strong schlieren object of very small dimension. Unfortunately, the brightfield image does not have the required sensitivity to display the gas jets, the smallest dimension flow feature in the test section.

A second possibility is that the resolution depends on the grid spacing through an undiscovered mechanism. For example, as the range gets larger, there is greater difficulty in achieving optimum cutoff, sensitivity is reduced and alignment requirements become more difficult to meet. It is possible that this has some effect on resolution.

A third possibility is that the resolution is limited by some other element in the system. This could be due to distortion in the lens, poor image capturing by the camera, grain in the screen, or a number of other causes. This can be checked by including an opaque solid object of fine detail. If the image of

its shadow is sharply defined, then the lens, diffraction at the cutoff grid, the screen and the camera can all be eliminated as the cause. While there are no such elements in the image, looking at the finer solid objects in the last two rows, it can be seen that the darkfield images display much worse resolution than the brightfield images. This suggests that a low light level is at least partially responsible for the lower resolution.

In conclusion, diffraction at the cutoff grid is clearly a cause of reduced resolution in the test section and the theory appears to model this specific cause well. There are also other causes however, particularly the light level. How much the optical components, alignment, system geometry and other factors affect the resolution remains to be seen. A useful concept for testing resolution in future is that both solid objects and brightfield conditions can be used to give useful information on the resolution. Another is that low light level causes loss of resolution in both vertical and horizontal directions (as do most geometry and optical factors). The loss of resolution due to diffraction only reduces resolution in the direction of sensitivity of the system (as do most grid dependent factors).

Banding appears to have a significant effect in reducing the quality of the image. In truth this is only partially correct. There are really two issues here. The first is banding and how it puts broad black lines all over the image. The other is the loss of information in that image in the first place. Both are important in achieving a useful image. While banding occurs when information is lost, it is not directly a cause of the loss. The factors that lead to banding also lead to a poor image.

In general, loss of information seems to depend on the range of the system. It is thus predicted that if a system is constructed in which the range is low when banding occurs, it is possible to have an image in which the flow information is visible, despite the black bands. Such a system would look something like the 7.5 mm optimum image.

Interestingly, the center of the image appears to suffer less from banding than the edges. This is visible in both the 3.75 mm and 7.5 mm images. Once again it appears that the light level has an effect on the system. More light in the center of the image means that the bands are washed out by the image. This has the effect of reducing the contrast of the bands. This supports the above theory, since the center of the image has more flow information and apparently suffers less from banding.

Two previous works (Settles, 2001 and Goulding, 2002) have constructed systems which work well enough for their purposes despite banding. Figure 6.5a shows a candle plume with a system with a

Weinstein criterion (ϕ) of 1.25, while Figure 6.5b shows a photograph by Settles (2001) with a ϕ of 2.8.

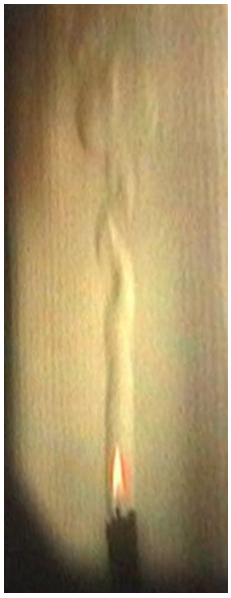
a)  b) 

Figure 6.5 a) candle plume at ϕ = 1.25 and b) heat extractor at ϕ = 2.8

As can be seen, both systems are much clearer than the results presented in section 6.1.1 for similar values of ϕ. The ranges of the two systems are 176 and 18 arcseconds respectively. By keeping the range small, the contrast of the banding is relatively less significant compared to the contrast of the object in the test section.

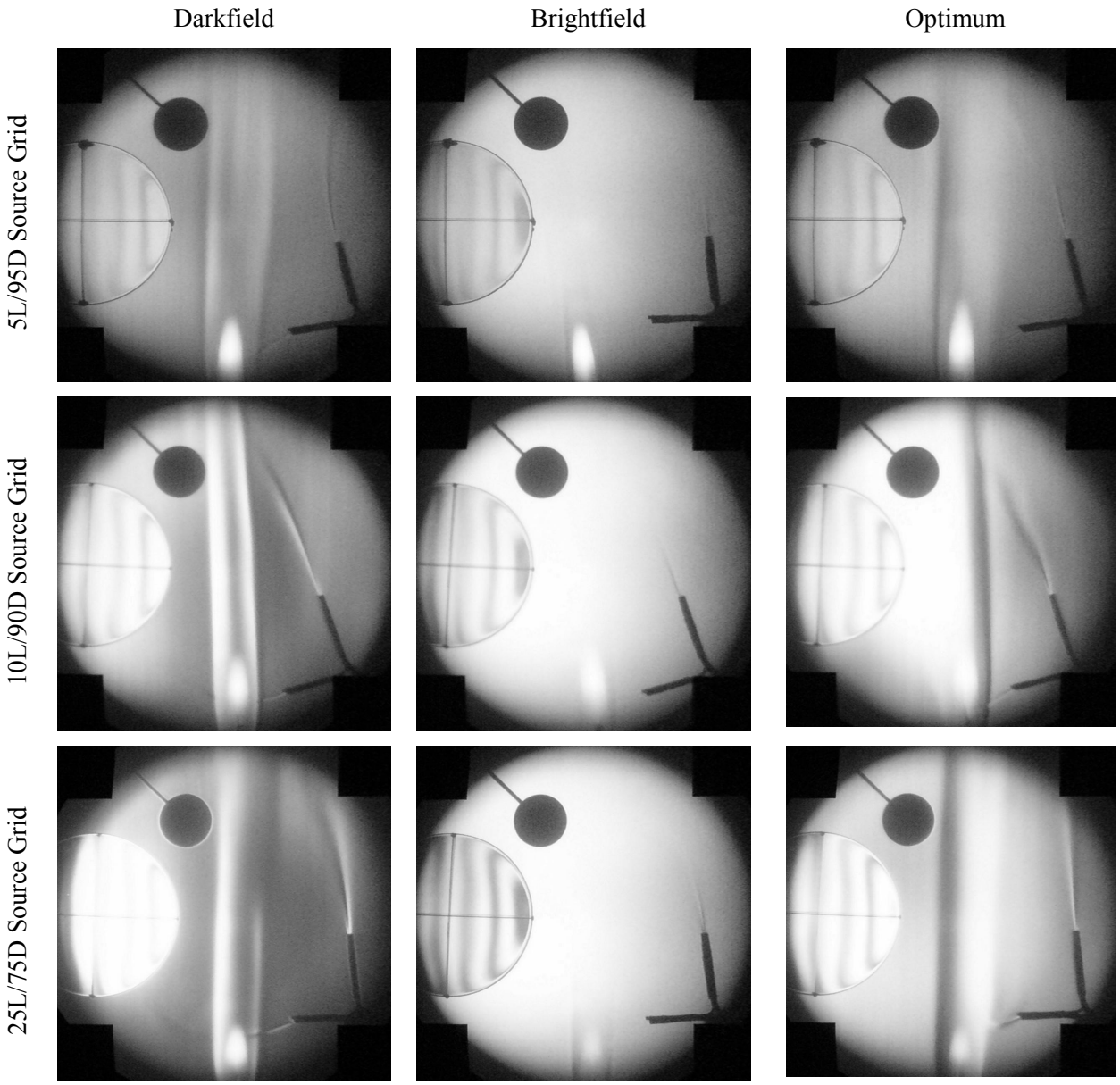
In conclusion, banding is a problem to be avoided. The guidelines given by Weinstein (1993) are guidelines only. Weinstein's criterion seems to be an accurate predictor of banding but not necessarily of information loss, as seen in large scale systems. Systems with a smaller range seem to be more resistant to banding and can still yield perfectly usable results. The effect of cutoff on the amount of light in the image and the effect of range on the image contrast has to be taken into account.

Finally, the optimum spacing has to be discussed. The best sensitivity for all three conditions appears to be achieved with the 0.9 mm grid. The best resolution occurs at 1.2 mm. The flow features in the darkfield and optimum images of the 0.9 mm grid exceed the range of the system, though this may be useful for discussion. The brightfield image is more useful for discussion with narrower grid widths. For these reasons, the optimum grid spacing is chosen between the 0.9 mm and 1.2 mm grids. A spacing of 1 mm is chosen for simplicity.

6.2 Variation of Source Grid Light Transmission Ratio

The results of the second experiment are presented in the 21 images below. Once again, there are three columns representing darkfield, brightfield and optimum cutoff. This time there are seven rows for the seven different grid transmission ratios. The reader is referred back to Table 5.2 to see the properties of each pair and to Section 5.1.2 on page 79.

6.2.1 Results



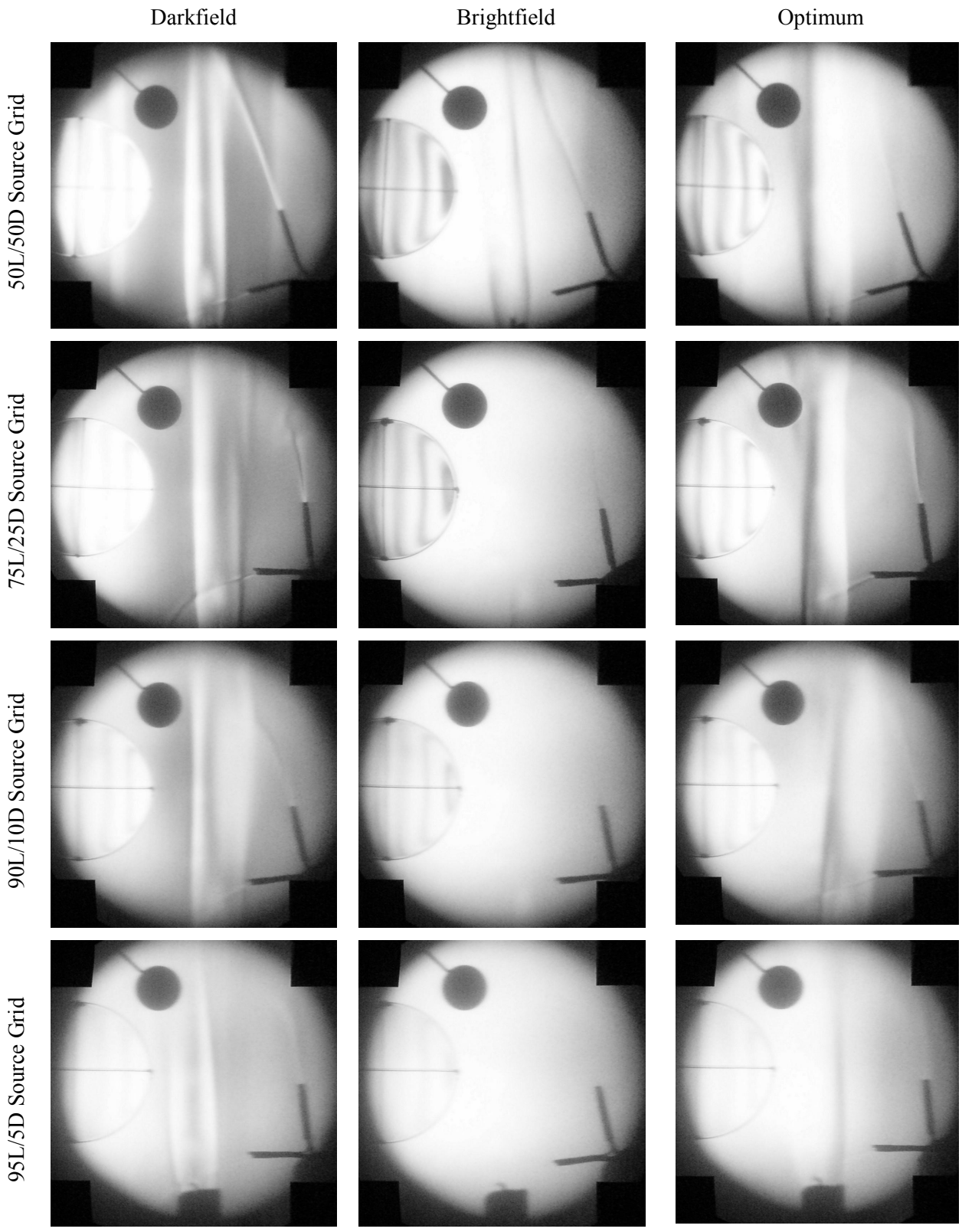


Figure 6.6 Results of variations in source grid light transmission ratio

6.2.2 Discussion

The first grid pair allows 5 % of the light through the source grid and cuts off 95 % simply by having 0.95 mm black lines separated by 0.05 mm clear gaps. It is convenient to define such a grid as a 5/95 grid, being the ratio of clear to dark bands in the source grid. The cutoff grid is a negative of this, though a third of the size. This means that the clear gaps in the cutoff grid are large and should have less trouble with resolution loss due to diffraction. Obviously a black source grid and clear cutoff grid will form no image, so somewhere between 0 % and 50 % will be an optimum quantity of light passing through the source grid. It will also be interesting to investigate what happens beyond 50 %.

5/95 Source Grid (5 % Light, 95 % Dark)

The first grid results in a low contrast image on a very uniform background. The contrast is so low in the darkfield case that the bands within the lens are clearly visible rather than overexposed like in all the other systems. Like the very narrow grids in the previous experiment, the system displays greater contrast and thus sensitivity in the center of the test section, suggesting that optical alignment is an important factor.

Both the candle plume and the gas jets are clear in the darkfield and the optimum case, though only the gas jets are visible in the brightfield image. The base of the candle plume is just visible, where the gradients are highest. This is relatively unusual, since in all the previous experiments both flow features have vanished together. It suggests that the system has poor sensitivity but good resolution.

This grid exhibits several properties which suggest it is at one extreme of the experiment. Not only are each of the three images low contrast but the differences in the background tone between the three is smaller than any other system. Also the opaque disk in this system is darker than for any of the following systems and the total quantity of light is less than any of the subsequent systems, in other words, the images are darker. Finally, there are very faint vertical lines in the darker regions of the darkfield and optimum images. They are not noticeable in the printed images, only the images contained in Appendix B. These lines also appear in some of the other images and appear to be caused by a periodic mismatch of the source grid image and the cutoff grid. This is probably caused by the resolution limitations of the printer used to create the grids.

10/90 Source Grid (10 % Light, 90 % Dark)

This system is somewhat more typical in appearance. The darkfield image displays greater contrast, though the center is still more sensitive than the edges. The lens is also overexposed, suggesting that there is greater contrast between brightfield and darkfield images. The sensitivity is significantly better and the resolution is marginally better, though this can only be seen by the solid objects, rather than the flow features. Interestingly, the disk is much brighter than the previous system, probably due to the greater quantity of light in the image.

The brightfield image has even worse sensitivity than the previous system though the resolution is largely unchanged. The entire image is brighter than the previous system, including the background and the disk. The optimum image is also brighter than the previous system and once again the sensitivity is much better.

25/75 Source Grid (25 % Light, 75 % Dark)

The darkfield image has a darker and more even background than any other darkfield image in this series, resulting in increased exposure and a visible halo around the disk. The halo is also visible near the vertical gas jet. The contrast is higher and the sensitivity better. In addition, the resolution appears better than any of the other systems in this series. The brightfield image is not the best though it is better than the previous two systems. The resolution is the best of any brightfield image, and sensitivity is only worse than the next grid. The optimum case repeats the pattern of the darkfield image, with best sensitivity and resolution.

50/50 Source Grid (50 % Light, 50 % Dark)

Unfortunately, the results for the 50 % grid are a little blurry, making comparison difficult, particularly with respect to resolution. The lack of focus is not as strong as one first suspects however. The four points in the corners of each image, used for perspective correction, give an accurate idea of the focus of any of the images, as these are in the plane of the image and are high contrast enough to be strongly visible. In addition, they have not passed through the optics of the system. As can be seen from the difference in focus of the corners compared to the solid objects, such as the gas emitters, the fuzziness of the image is at least partly optical in nature.

The brightfield sensitivity is better than any other system in the series though it is not as good as the previous system in the darkfield and optimum conditions. The background of the darkfield image is somewhat lighter than the previous system. It also shows quite strongly visible vertical lines caused by a periodic mismatch of the source grid image and the cutoff grid. Except for the vertical lines and the poor focus, this grid's results bear a strong resemblance to the 0.9 mm grid from the experiment above, as would be expected.

75/25 Source Grid (75 % Light, 25 % Dark)

The first of the grids with narrower clear bands in the cutoff grid is worse than a normal grid. Both the sensitivity and the resolution are acceptable but they are worse. The brightfield image is completely clear of flow information and both the darkfield and optimum images are lower contrast than the previous system. Despite the fact that the camera is sharply focused, the various elements in the test section are distinctly blurry. It is also apparent that this is more of a problem in the horizontal direction, indicating that diffraction at the cutoff grid is starting to become an important issue.

90/10 Source Grid (90 % Light, 10 % Dark)

With this system, diffraction is a serious problem, dropping the resolution to the point that the gas jets are no longer more than just a vague shadow. Also, it is now clear that the vertical gas emitter is much less sharply focused than the horizontal emitter. The sensitivity has also decreased as the theoretical sensitivity approaches the range of the system. Once again, the center of the test section is more sensitive than the edges, indicating that the lens cannot accurately superimpose the source grid image on to the cutoff grid. Finally, the contrast between the background and the flow objects and between the darkfield and brightfield backgrounds is low.

95/5 Source Grid (95 % Light, 5 % Dark)

The final system in this experiment has very low contrast, to the extent that the lines which should be visible inside the lens are not visible at all in the brightfield case and only one of them is visible in the darkfield and optimum images. The candle plume can just be made out against the background. The resolution is so poor that the gas jets cannot be seen. Diffraction is once again the dominant effect, smearing the image horizontally. Outside the edges of the test section, the screen is much brighter

than any previous system, indicating that there is significant scattering of light at the cutoff grid. Somewhat less critically, the candle, which had steadily been getting shorter, was raised about 2 cm.

During grid manufacture, the cutoff grid for this system proved to be the very troublesome. The clear spaces were only 0.0167 mm wide and the printer simply filled one in every now and then, making the grid useless. To rectify the problem, the width was increased slightly to ensure the printer left a gap. This was essentially a case of making sure the grid resolution matched up to the printer resolution. This did change the system from a 95/5 system into about a 94/6 system. The effect of this on the results is negligible however. This grid was included to establish a trend, which is still clearly visible in the results.

Summary

It is interesting to compare the first and last row of these results. Both suffer poor sensitivity, low contrast images. However the last row suffers from poor resolution as well, while the first row has very good resolution. The solid objects are sharply focused and the gas jets are clearly visible despite the low sensitivity, while in the last row the solid objects are very fuzzy and awash with scattered light. It is clear that changing the ratio of clear and dark line widths has a serious impact on the resolving power of a focusing schlieren system.

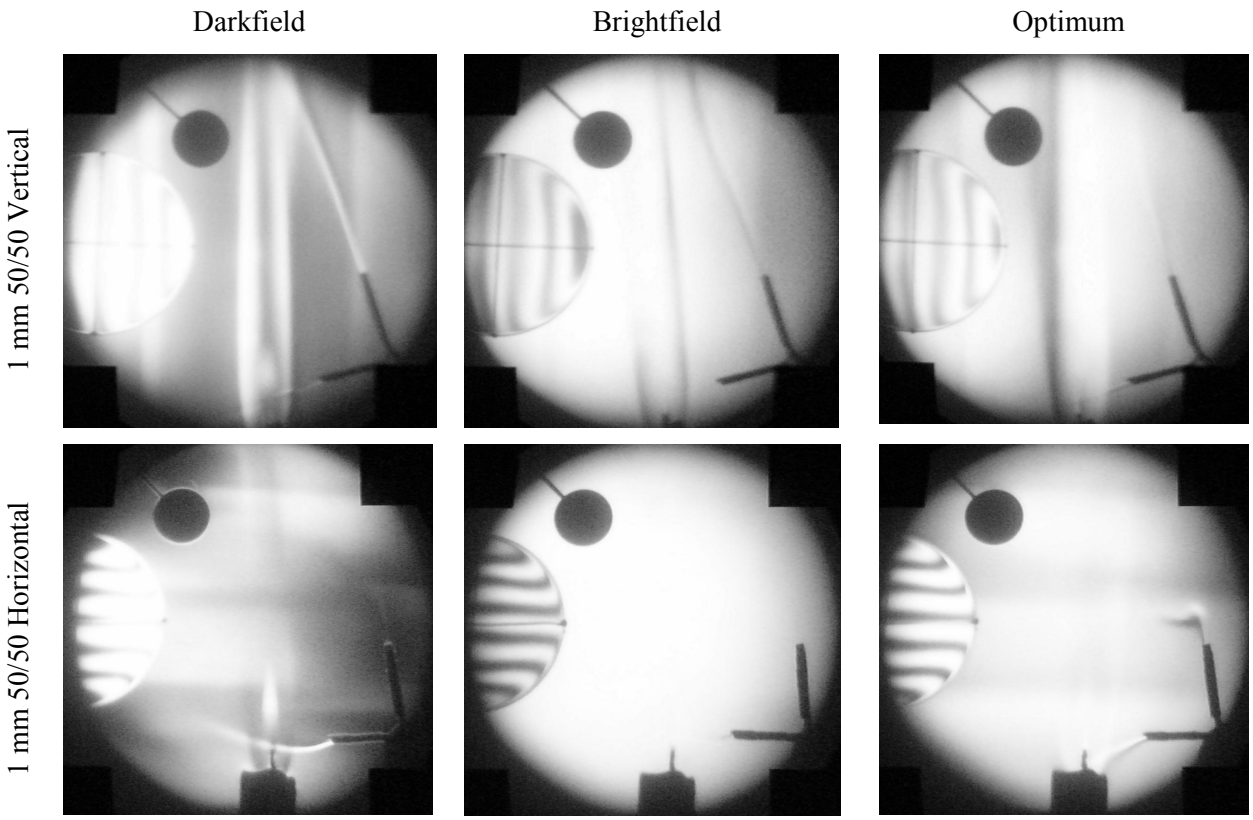
While it is easy to make a system much worse by going to extremes with the clear/dark ratio, smaller changes can make the system better, though only slightly better than a simple 50/50 grid. Grids which make the cutoff grid clear bands narrower only seems to lead to a worse system, in other words, there is no advantage to doing so. Making them wider can lead to a slightly better system. The optimum ratio lies somewhere between the 50/50 grid and the 10/90 grid, probably quite close to the 25/75 grid. Certainly for this system geometry, the 25/75 grid is the best tested.

While the gains are not large, it is probably worth considering using this technique in operational systems which will not be modified often. It is a particularly useful technique in systems where diffraction is taking place. The disadvantage to using this technique is that any system other than a 50/50 system will have sensitivity gaps in the range. In other words, there will be a range of ray deflections which all result in a similar lightening or darkening of the image. Alternatively, the range must be reduced to the point at which this starts to happen. While this has very little impact on the appearance of the image, this technique should be avoided if quantitative results are required.

6.3 Demonstration of a 2D System

The results of a 2D system are demonstrated and compared to the 50/50 grid with 1 mm spacing from above. In addition to the usual vertical grid, a set of pictures has been produced using the same grid horizontally. As described earlier, there are two methods of varying cutoff with a 2D system. Both have been tried by producing one source and three cutoff grids. The three cutoff grids vary by having opaque dots of 100 %, 80 % and 50 % of the diameter of the clear holes in the source grid image. For each cutoff grid, images have been captured in centered, middled and off-centered positions, as described in section 5.2.1. Roughly speaking, 100 % centered is analogous to darkfield and 100 % off centered is similar to brightfield for a 1D system. The results are presented in the images below.

6.3.1 Results



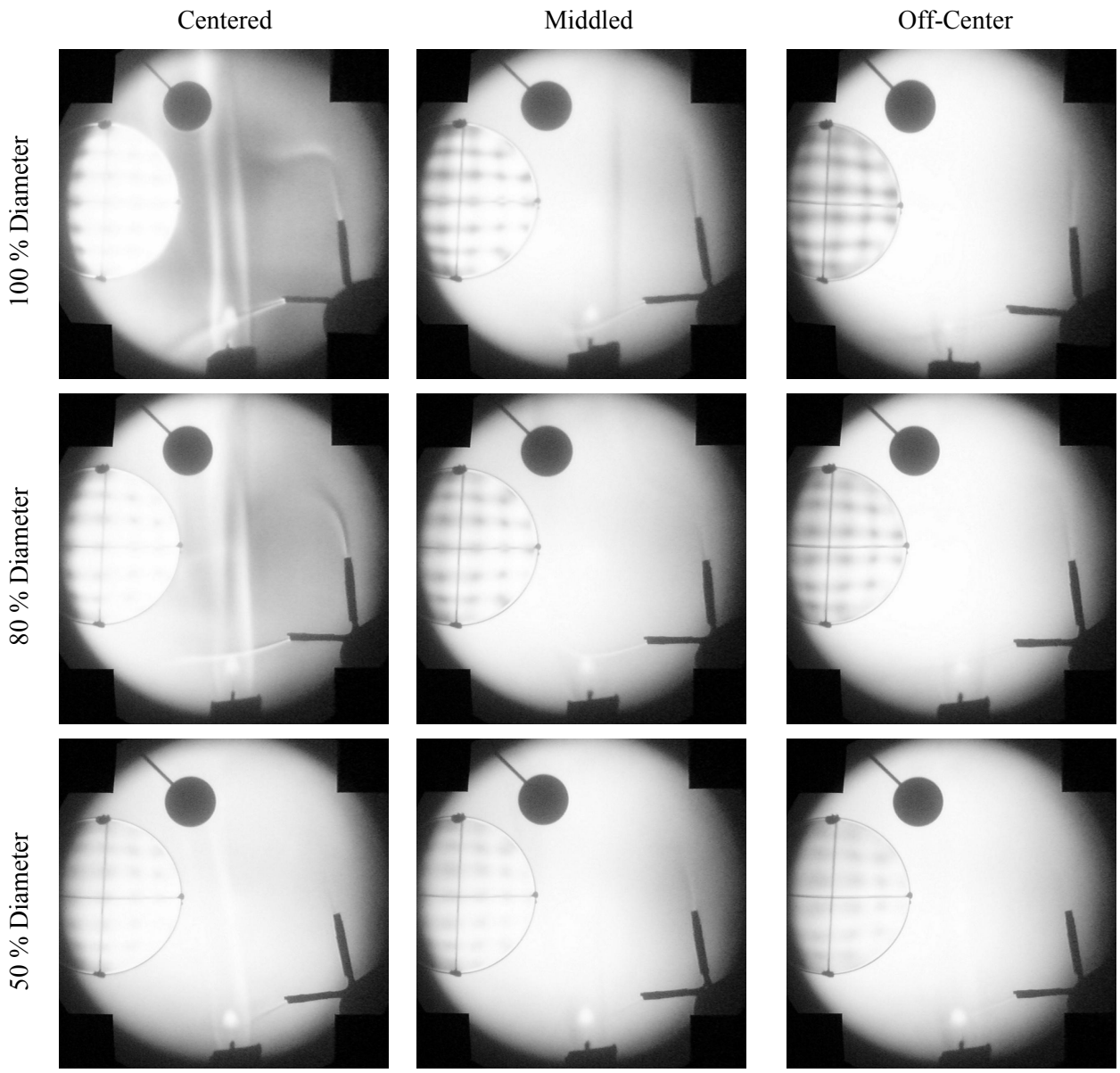


Figure 6.7 Results and comparison of a 2D system

6.3.2 Discussion

The 50/50 grid was chosen over the 25/75 grid for comparison. While the 25/75 grid is a better system, the 2D grids all have a 50 % light transmission ratio. In addition, the 25/75 grid was felt to be a modified system itself, while the 50/50 grid is the standard to which all other systems should be compared.

The first row of images shows the results from the previous experiment and has already been discussed on page 111. The second row shows the same grid turned 90° with respect to the test section to give a system sensitive to vertical gradients. As can be seen, the horizontal gas jet is significantly more visible than the vertical one. The candle plume is not very visible at all, except near the base, where gradients are not quite horizontal.

In the darkfield image, it is the horizontal gas jet which has a halo, not the vertical one. Also, the background is quite uneven in the horizontal direction. This is partially due to the poor cutoff grid (the same as used in the previous experiment) and partially due to the fact that no provision was made to shift the cutoff grid vertically. This effect was achieved by adjusting the lens up and down but the results were not ideal as there was a certain amount of play.

The brightfield image is almost completely blank, except for the strong lines within the lens and a just detectable plume from the horizontal gas jet. It is surprisingly clear of any gradients when compared to the vertical system.

Finally, the optimum image has a far more even background than the darkfield case, though the candle plume is probably less visible. It is interesting to note the vertical gas jet in which the gas starts to flow horizontally and thus becomes strongly visible.

100 % 2D Grid

For the first time, the gas jet from the vertical emitter can be seen to flow around a corner, from vertically up to a slight downward angle. This is due to the fact that the gas is denser than air and tends to sink. In principle this is the first time that the horizontal gas jet should be visible at all, however a bent nozzle and sagging emitters have ensured that the gas jet was very seldom actually horizontal for the previous experiments. The 2D system shows more than a usual 1D system, displaying both vertical and horizontal gradients however the sensitivity of the system is not as good as a 1D system. Resolution on the other hand seems to be on a par with a 1D system. In principle, the resolution will vary according to which part of the cutoff grid the light passes though and will also vary in the vertical and horizontal directions however a general average resolution seems to apply; no particular part of the image appears to have a vastly different resolution to another.

The background of the 100 % centered image is fairly consistently dark, except near the edges, as can be seen from the overexposure of the lens. It is also significantly darker than any of the other 2D images and, as a result, has greater sensitivity. However it does also display lower contrast than the 1D system. The brightness round the edges suggests that alignment is slightly out or that the lens is having trouble projecting the source grid onto the cutoff grid. As the vertical adjustment of the cutoff grid is a bit crude, neither can be discounted.

The 100 % middled system is interesting in that it displays greater sensitivity to horizontal gradients. This is due to the fact that the cutoff grid has been shifted horizontally. As can be seen from the inside of the lens, this means that a light ray only has to be deflected a small amount before it becomes cutoff in the horizontal direction but has to be deflected about twice as far in the vertical direction to achieve maximum darkness. As already mentioned, the 1D analysis is not valid for 2D systems and this is an illustration. The range and sensitivity in the vertical and horizontal directions is very different and one affects the other. The lens provides a very clear demonstration of how the image varies according to ray deflection. For example, a ray deflected slightly up allows more light through, while a ray deflected slightly across allows less light through.

The off center image is similar to a brightfield condition as rays deflected in any direction can only get darker, though not necessarily by the same amount. Unlike the middled case, sensitivity is the same in the vertical and horizontal directions. Only the vertical gas jet is visible, however this is due to its proximity to the edge of the image, where the image is darker and thus of higher sensitivity. The horizontal gas jet does not pass as close to the edge and is washed out by excess light.

80 % 2D Grid

The 80 % grid is similar to the 100 % grid, only brighter. More light is allowed through the two grids resulting in images that look washed out and reducing sensitivity a little. Once again the darkfield image has a fairly even background which is lighter at the edges. This time though the lens is not quite as overexposed. There is little to say about the middled and off centered images, except that they too are too bright and lack sensitivity. Except for the lens, they can only just be told apart by the fact that the background of the middled image is darker than that of the off centered image. One interesting point is that the resolution, particularly of the solid objects appears to be better. This is due to the fact that the clear gaps in the cutoff grid are larger, thus diffraction is not as prevalent as in the 100 % grid.

50% 2D Grid

Like the 80 % grid, this set of images is only brighter, the excess light serving only to wash the images out and reduce sensitivity. This is not analogous to brightfield, as there is no magnitude of deflection which results in dark regions in the image. This setup only offers reduced sensitivity. Once again, the resolution is fractionally better however there are no flow features strongly discernable in any of the three images.

General Comments

Only the 100 % centered image shows any potential at all, all the remaining images are significantly worse in sensitivity. The two methods of varying cutoff have been described and tested but both fail to replicate the results of a 1D system. Varying the cutoff by varying the diameter of the dots seems less damaging than shifting the cutoff grid into new positions however it too does not yield a brightfield or optimum type image.

Another feature of the 2D system is that even the darkfield image appears to be a bit washed out. This implies that a fair amount of light is passing though both grids which in turn suggests that there is poor alignment. This may be overcome by using an over-ranged system, say dots 120 % the diameter of the holes. Hopefully this would limit the light level somewhat without compromising the range too much. This would add complications to the range and direction of deflection though as rays deflected exactly vertically or horizontally might never pass through the cutoff grid.

The fact that both the magnitude and direction of deflection of a ray bundle is important to the final brightness on the image plane means that a 2D system cannot be used for quantifiable results, at least not in the form presented here. If the range is known, it may be possible to design a system in which the sensitivity is adequate for a very limited range by using fewer holes in the source grid placed further apart. Ultimately though, a 1D system is far superior if measurable results are required.

One final comment is that throughout this experimentation process, the vertical gas jet has gradually been reducing in flow rate. This is not much cause for concern as the gradients are across the jet, not down its length, so although the length of the jet is decreasing, the width stays the same. This appears to be caused by the gas leaking where the pipe connects to the cigarette lighter rather than by running out of gas.

6.4 Demonstration of a Retroreflective System

The results for a retroreflective system are presented below. The system arrangement is the same as that shown in Figure 4.2 (page 45). Again, darkfield, brightfield and optimum images are presented. The results of previous experiments have been left out to avoid repetition.

6.4.1 Results

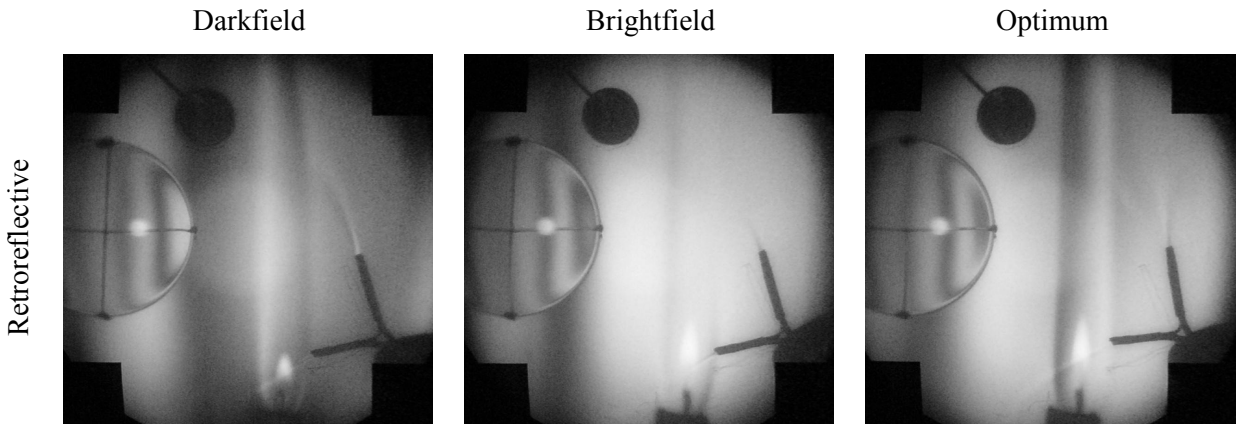


Figure 6.8 Results of a retroreflective system

6.4.2 Discussion

Compared to the earlier 1D or 2D images, the retroreflective system images are all quite dark. This is due to decreased light levels as a result of the beam splitter. With all the previous systems, less light could be seen as a good thing because it means less undeflected light washes out the image caused by deflected light. This is not the case here however as both deflected light and undeflected light are darker.

Another problem with the retroreflective system is that there are two reflections in the images, both caused by the fact that the source grid is lit from the front. The first is a small bright reflection from the lens, to one side of the crosshair. This is a reflection of the light source from the lens. The reason it is not in the middle of the lens is that the lens is off to one side of the centerline of the test section. It is also curved so that the center of the lens is closer than the edge which also explains why the

reflection is small. The reflection occurs at the point on the surface which is a normal to the light source, since both the light source and the image end of the system are co-axial. This reflection is visible in all three images and will always be present in a front lit system.

The second reflection is a large diffuse spot in the middle of the test section, about one quarter the diameter of the test section. This reflection is most visible in the darkfield image. It is caused by the reflection of the light source off the source grid. As the source grid has been printed on a clear sheet of plastic, the plastic is reflecting the light between the gridlines. This reflection can be avoided in retroreflective systems by printing the source grid onto the retroreflective material directly or by using a retroreflective paint rather than a material.

Compared to the earlier systems, the background of the image is very uneven. All three images tend to be darker near the edges and exhibit broad vertical stripes of darker background. This is primarily due to the difficulty of alignment. With the retroreflective system, the source grid is clamped with the retroreflective fabric in the source grid support. This results in a slightly less flat source grid. It is also possible that the beam splitter itself distorts the image of the source grid, though this is regarded as a minor concern. Finally, because the source grid is not mounted on the optical rail, it is important to ensure that it is exactly perpendicular to the optical axis otherwise part of the source grid image will not be focused on the cutoff grid.

With the previous systems, the vignetting of the image was clearly marked because the Fresnel lens limited the size of the light source. Thus the edge of the image was sharply defined. With the retroreflective system this was not the case, since both the source grid and the retroreflective fabric were larger than the area illuminated by the front light source. For this reason, a baffle was added at the source grid to keep the images looking similar to the previous work. Were this not the case, the image would gradually worsen with radius as the light level decreased, the alignment got worse and the lens resolution decreased.

While converting the system from a backlit to a front lit configuration, light pencil lines were drawn on the image to indicate where the various components in the image should appear to keep the test results the same as for the previous experiments. Unfortunately, it was assumed that they would not be visible. They can just be seen below the horizontal gas jet in the brightfield and optimum images. They did allow all the other elements in the test section to be aligned accurately though.

One problem the pencil lines did not solve adequately is the rotation of the test objects. The lens in particular is not perpendicular to the optical axis and this can be seen by the fact that the crosshair no longer indicates the center of the lens.

Most of these problems are relatively cosmetic and caused by the fact that the system was designed to be a good backlit system, rather than a front lit system. The resolution displayed in the image is similar to that of the previous experiments, though the sensitivity is a bit worse. The sensitivity of the brightfield image is better though, suggesting that the worse sensitivity is once again a matter of accurate alignment.

Most of the issues listed above can be overcome through proper design of the system. Reflections can be reduced or eliminated, alignment should be improved and light levels can be increased. Ultimately the main problems are caused by poor mechanical alignment of the source grid image and the cutoff grid. This can be improved with the use of a new source and cutoff grid pair and a source grid which is printed directly to the retroreflective fabric.

Ultimately, the results are still useful as all the flow features are clearly visible. The main difference is that the images are much darker. While the results are useable, quantifiable results should be avoided, at least until the mechanical alignment of the grids can be improved.

6.5 Demonstration of a Projected Grid System

Below are the results of the projected grid retroreflective system as illustrated in Figure 4.3 (page 46). Again, there are darkfield, brightfield and optimum images corresponding to dark as possible, bright as possible and maximum contrast.

6.5.1 Results

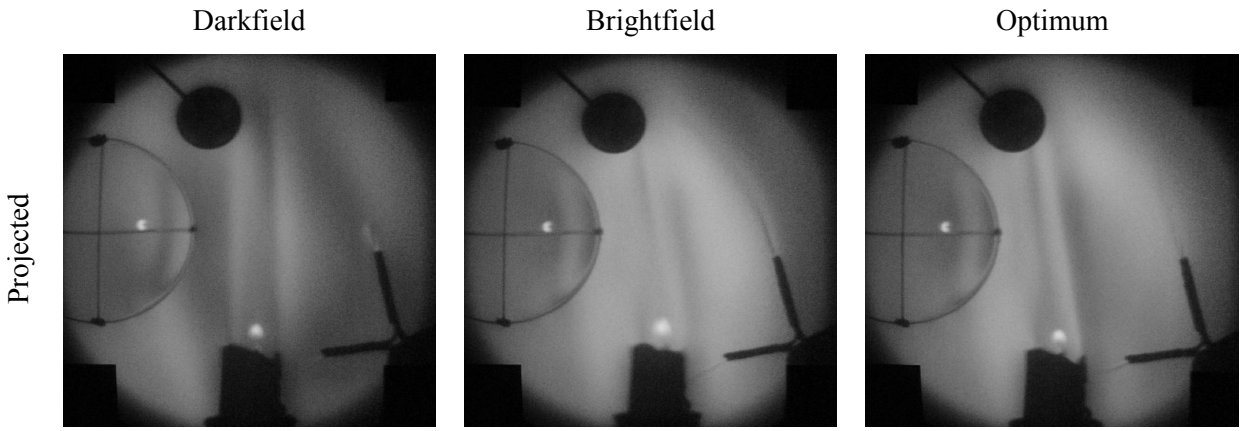


Figure 6.9 Results of a projected retroreflective system

6.5.2 Discussion

The images presented above bear far more resemblance to the retroreflective system than to any of the backlit systems. Once again the images are dark, owing to the use of a beam splitter and once again there is a very uneven background, owing to poor alignment. The brightfield sensitivity is fairly good compared to backlit systems, indicating that there is far less light washing out the image than there should be. In addition, the tones inside the lens are vague shadows spread over the lens, rather than a set of well defined stripes. Both of these highlight the poor alignment of the source grid image and the cutoff grid. Overall, the alignment is somewhat worse than that of the retroreflective system. This is mainly due to the increased complexity of the source grid setup. Now, not only is the source grid not completely flat, it is also a small grid which has been enlarged and projected through a lens system first. Any errors in printing are enlarged and any distortion in the secondary lens is very important. Also, any errors in placement, and thus focus, are amplified for the second grid.

Talking only about the physical differences, the candle has been lifted to allow it to be seen. Also, the vertical gas jet is very long in the brightfield image and fairly short in the darkfield image. Once again, it is the gradients across the jet that are important, not the length.

Unlike the retroreflective system, there is only one reflection this time, caused by the lens in the test section. The cause is exactly the same as for the retroreflective system and it cannot be removed in any front lit system, except in post-processing. Another difference from the retroreflective system is the presence of large blurry shadows behind each solid object in the test section. The most obvious place to see it is near the opaque disc, particularly in the brightfield and optimum images. This indicates that the larger the solid object, the darker the shadow. Also, the shadow seems to be more apparent on the edge side of the object. As can be seen, the shadow is stronger between the disc and the edge than between the disc and the center of the test section.

Interestingly, Settles (2001) observes a similar shadow with his large scale retroreflective schlieren system. His explanation is that the solid objects cast shadows onto the retroreflective screen causing regions of darkness. His system used an offset light source, rather than a co-axial one, perhaps explaining why the shadows were visible with a retroreflective system, while they were not visible here. They are again visible with the projected system because the beam splitter for the projected system is small (using a mirror) while that of the retroreflective system is large (using a sheet of glass). By having a smaller effective light source, the shadows formed by the solid objects are larger and more sharply defined, as would be the case with an offset light source such as Settles used.

Overall, the system is not terribly good though all the important flow features can still be seen. The resolution is reasonable, comparable with that of the retroreflective system though not as good as a backlit system. The sensitivity is slightly worse than the retroreflective system with the candle plume in particular lacking edge definition. Once again if quantifiable results are required, the system will need considerable improvement, mostly with respect to alignment of the two grids.

Having said all this, the main point of this experiment was to demonstrate that the system works. This is unquestionably the case, though the quality is poor. It will be possible to improve the system significantly with more work. The important thing at this stage is that the method of projecting the source grid can still create useful schlieren images.

7 CONCLUSIONS

The conclusions fall into several sections, those that deal with the project in general and those that conclude each of the six objectives. General conclusions are:

- A suitable apparatus for the design and testing of focusing schlieren systems has been developed. This will enable future research to be done in this field more easily.
- An attempt has been made to formalise the current terminology in a consistent and more definite way than the current literature has demonstrated.
- A comprehensive body of data concerning focusing schlieren systems has been compiled for the first time in a publication. This includes an exploration of the system and system limits as well as a comparison of most of the methods used for achieving the effect.
- While all of the components are important, the projection lens is the most critical item for improving the quality of the system.

7.1 Variations of Source Grid Line Spacing

The actual values of grid widths are not really important for the conclusions, since they depend on the system geometry and components. Thus the general principles and the mathematics are discussed.

- The limits of focusing schlieren systems have been investigated rather than just described. The mathematical models that exist have, for the most part, been confirmed as accurate predictors of system performance.
- The upper limit on grid spacing is limited by the effect of banding. The lower limit is limited by diffraction. Between these two limits, sensitivity and resolution are the primary issues. Depth of field is another possible variable, though deemed unimportant for large scale systems.
- The limits of diffraction and banding have been investigated. The diffraction limit is accurately modelled by the mathematical equations. The banding limit is slightly less well modelled as additional factors seem to affect the final result.
- Diffraction removes information from the flow field by smearing out every part of the image. This results in an unacceptable loss of resolution if it is bad enough.

- In addition to the current model, banding also appears to depend on the range of a given system. A system with a small range when banding occurs does not show the bands as strongly as one with a large range.
- Minor banding does not remove flow information from an image; rather it superimposes bands on it. Major banding does remove flow information as the bands become broad enough and dark enough to cover regions of the image. Often it is the same factors that cause banding and a loss of flow information at the same time. One does not cause the other.
- The finer the grid, the more important the alignment becomes, until the resolving limit of the lens is reached.
- Resolution appears to be limited primarily by diffraction at the cutoff grid but also by light level and sensitivity. Other elements in the system, such as image size and the camera, can also affect the final resolution. A resolution of 2 mm is low enough to see all the flow features present in the test section quite clearly. Only very weak shock waves or shocks in rarefied flow will require a lower resolution.
- Resolution and sensitivity are linked by the fact that good resolution cannot exist without sufficient sensitivity. As sensitivity decreases, the finer details of a system are lost and the mathematical resolution becomes unimportant.
- To achieve the theoretical limit of sensitivity, the alignment has to be perfect. Any tiny error in alignment reduces the sensitivity at that point.
- For strong schlieren objects, worse sensitivity is actually desired, since it gives better flow information by not exceeding the range. This can be achieved by using a brightfield rather than darkfield image.

7.2 Variation of Source Grid Light Transmission Ratio

- The technique of increasing the width of the clear gaps in the cutoff grid can be used to delay the onset of diffraction. The images produced have better resolution and sensitivity for a given line spacing.
- The gains are not large however, so the technique is probably only useful in systems that are more permanent fixtures or suffer diffraction or resolution problems.
- A source grid which has dark lines three times wider than the clear lines appears to be about the optimum ratio for improved performance.
- The major disadvantage of using this technique is that the range of the system is truncated.

7.3 Demonstration of a 2D System

- The principle can be shown to work and can be useful for visualising flow in two dimensions.
- The system using 100 % cutoff appears to yield the best results.
- A 2D system has worse sensitivity and resolution than an equivalent 1D system.
- The method of varying cutoff for the 2D system is not clear. Two methods were tried and both were unsatisfactory, simply flooding the image with more light, rather than varying cutoff.
- Quantifiable results for the 2D system are more or less impossible, since the magnitude and direction of a deflection both influence the brightness of the final image.
- Ultimately, the effectiveness of a 2D system depends on the grid used to achieve two dimensions of sensitivity. There are certainly many more methods of obtaining 2D images than using a grid of dots and holes, as tried in this report. One of them may produce far better and more useable images.
- Typical solutions to achieving two dimensions in a conventional schlieren system do not lend themselves to systems with multiple sources. This is due to the interference of one system with the system adjacent to it, resulting in an overlap of contradicting flow information.

7.4 Development of Colour Systems

- Owing to problems of chromatism in the system, grid production and time, colour systems were not investigated deeply.
- Colour systems have to be treated with a degree of suspicion because quantifiable results are very hard to produce and verify are working, even in one dimension.
- Given the difficulty with 2D systems, 2D colour systems will be an even more difficult problem to solve.
- Given that the only use of colour in a schlieren system is to provide more information about the flow field, preferably as 2D, quantifiable system, development in this area does not look promising.

7.5 Demonstration of a Retroreflective System

- The retroreflective system is compared directly to a backlit focusing schlieren system.
- There is a much lower light level due to the use of a beam splitter. This can be solved relatively simply by using more light and more baffles.
- Resolution is about as good as for an equivalent backlit system while sensitivity is a little worse.
- Accurate alignment between the grids is much more difficult to achieve with this apparatus. In fairness, the apparatus was optimised for a backlit system rather than front lit. This inaccuracy leads to a very uneven background, making quantifiable results impossible with the current apparatus.
- Retroreflective systems will yield reflections from any shiny surfaces in the test section. In this case, it also yields a reflection from the source grid itself, due to the method of grid manufacture. This problem can be overcome relatively simply by using a source grid printed directly onto the retroreflective screen.
- Most of the problems of a retroreflective system can be overcome through proper design of the apparatus. The requirements are slightly more stringent, particularly for the light source and the alignment however very similar system characteristics, such as sensitivity and resolution, should be achievable.
- The retroreflective method has far more potential as a large scale system than a backlit system.

7.6 Demonstration of a Projected Retroreflective System

- This novel system arrangement is used and tested for the first time. The operating principle is demonstrated to work and yield useable results.
- Like the retroreflective system, the results are much darker in appearance than a backlit system. Also like the retroreflective system, poor alignment, dark images and reflections are the main concerns. Again, these concerns can be addressed through proper system design.
- Sensitivity and resolution are somewhat worse than the retroreflective system. This is due to the even more stringent alignment requirements.
- This arrangement can be developed into a very portable, large scale system.

8 RECOMMENDATIONS

There are many recommendations which can be made both to improve the current system and to extend it somewhat further into new areas of research.

8.1 Recommendations for the current work

- The current tilt mount for the cutoff grid suffers a certain amount of hysteresis. This should be fixed. In addition, a method of shifting the cutoff grid up and down would be beneficial for 2D and horizontal grid systems.
- One problem with the grids is holding them rigidly flat. One possibility is to silkscreen the positives onto glass plates. This may reduce the resolution unacceptably, but if not, should make a much better system for alignment.
- The 50/50 1 mm grid spacing cutoff grid was manufactured quite badly and should be remade to improve the results. In particular, the horizontal grid images in the 2D section are poor quality.
- Another method of varying 2D cutoff is to use an exact copy of the source grid image for brightfield, an exact negative for darkfield and a concentric ring per hole as an optimum. The range is still different for ray deflections in different directions beyond a certain magnitude however small magnitude deflections should have a very similar range. This method should be tried and compared to those presented here.
- For the backlit systems, colour in the image is the greatest problem to be solved. For the front lit systems, the alignment of the grids is still the most important issue.
- The source of colour in the images is still not fully understood. While the Fresnel lens has generally been blamed, colour is still present in the front lit systems. In addition, the grids appear to worsen the effect. Neither grid is actually required to be there, they simply make the colour stronger. Also, the colours typically vary perpendicularly to the grid direction, again suggesting the Fresnel lens is not directly to blame. Finally, narrower grids do not have more colour in the images than coarse ones, as may be expected if the grids were the cause.
- Chromatic effects of the Fresnel lens can possibly be eliminated as a cause using a diffuser but this will result in significant loss of light. Making the light source larger does not appear to have much effect on the colour.

8.2 Recommendations for further work

- To make the system really useful as a flow visualisation tool, the chromatism needs to be fixed. If all else fails, using a monochromatic light source or monochromatic filter will fix it. In addition, using a pulsed light source would enable shock wave studies to be conducted, the main use of schlieren systems.
- Currently, the mathematics enables systems to be designed and performance predicted however there is a need to make completely different systems comparable through a few dimensionless variables. There are strong trends in system design which cannot be expressed adequately with the current mathematics. Ideally, any predictions using the new mathematics should be verified experimentally.
- The effect of banding is still not entirely predictable. For a given value of ϕ banding can be more or less visible. Mainly this variability appears to depend on how strong the banding is compared to how strong the image itself is. Often the factors that lead to banding, such as a coarse grid spacing, small distance between the cutoff grid and the image, etc, also lead to a low sensitivity, high range image. The two effects need to be divided and investigated.
- For this work, manufactured grids have been used throughout. Developed and adaptive cutoff grids should be compared for a given system. There is reason to believe that the differences could be quite large, given the difference in contrast ratios, edge definition and so on.
- It may be possible to create a system in which the cutoff does not need to be adjusted while still achieving a schlieren image. This has been shown to be somewhat possible, with the second row of the first experiment. The cutoff still has to be precisely located in the correct plane and at the correct angle of rotation though.
- Other methods of achieving 2D images can be investigated. This includes square or hexagonal holes, different hole sizes and hole patterns. Also, the development of mathematics relating to 2D systems can be investigated, though it is likely very complex.
- The retroreflective and projected retroreflective systems have the most potential for large scale use and should be developed further.

9 REFERENCES

Behun, E. (1956) Application of Multiple-Source Schlieren Systems, United Aircraft Corporation Report R-0885-13.

Boedecker, L.R. (1959) Analysis and Construction of a Sharp Focusing Schlieren System, MS Thesis, Dept of Aeronautics and Astronautics, MIT.

Bowker, A. (1970) NAE Multi-Source Schlieren Apparatus for 5 x 5 foot Transonic Wind Tunnel, *NRC Quarterly Bulletin* (Canada), no. 3, pp. 27 - 49.

Burton, R.A. (1949) A Modified Schlieren Aparatus for Large Areas of Field, *Journal of the Optical Society of America*, vol. 39, no. 11, pp. 907 - 908.

Burton, R.A. (1951) Notes on the Multiple Source Schlieren System, *Journal of the Optical Society of America*, vol. 41, no. 11, pp. 858 - 859.

Butler, C.P. (1974) Schileren System for Fire Spread Studies, *Journal of Fire and Flammability*, vol. 5, no. 1, pp. 4 - 15.

Buzzard, R.D. (1968) Description of Three Dimensional Schlieren System. High Speed Photography, Proceedings of the 8th International Congress on High Speed Photography, Wiley, NY.

Collicot, S.H. and Salyer, T.R. (1994) Noise Reduction of a Multiple-Source Schlieren System, *AIAA Journal*, vol. 32, no. 8, pp. 1683 - 1688.

Collicot, S.H. and Salyer, T.R. (1994) Quantification of Noise Reduction in Multiple-Source Schlieren Systems, AIAA Paper 94-0279.

Dixon-Lewis, G and Isles, G.L. (1962) Sharp Focusing Schlieren Systems for studies of Flat Flames, *Journal of Scientific Instruments*, vol. 39, pp. 148 - 151.

Doggett, G.P. and Chokani, N. (1993) Large Field Laser Holographic Focusing Schlieren System, *Journal of Spacecraft and Rockets*, vol. 30, no. 6, pp. 742 - 748.

Downie, J.D. (1995) Application of Bacteriorhodopsin Films in an Adaptive Focusing Schlieren System, *Applied Optics*, vol. 34, pp. 6021 - 6028.

Fish, R.W. and Parnham, K. (1951) Focusing Schlieren Systems, British Aeronautical Research Council, Report CP-54.

Goulding, J.S. (2002) Large Scale Schlieren Imaging, Final year project, University of the Witwatersrand.

Groves, T.K. (1960) A Photo-Optical System of Recording Shock Profiles for Chemical Explosions, Canadian Defence Research Board Report, DRB Project Number D89-16-01-05.

Hanenkamp, A., Mirzkirch, W. and Peters, F (2000) A Fourier Approach to the Sharp Focusing Schlieren System, Proceedings of the 9th International Symposium on Flow Visualization, Paper no.120.

Hartmann, J. (1940) Den Akustiske Luftstraalegenerator Fysisk Tidsskrift, no. 3-4, In Danish.

Holder, D.W. and North, R.J. (1963) *Schlieren Methods*, NPL notes on applied science, no. 31, Her Majesty's Stationary Office, London.

Hooke, R. (1665) *Micrographia*, J. Martyn & J. Allestry, London.

Jenkins, F.A. and White, H.E. (1950) *Fundamentals of Optics*, McGraw-Hill, NY, pp. 284 - 285.

Kantrowitz, A. and Trimpi, R.L. (1950) A Sharp Focusing Schlieren System, *Journal of Aeronautical Sciences*, Aeronautical Research Council.

Merzkirch, W. (1974) *Flow Visualization*, Academic Press, New York, pp. 98 - 99.

Mortensen, T.A. (1950) An Improved Schlieren Apparatus Employing Multiple Slit Gratings, *Review of Scientific Instruments*, vol. 21, no. 1, pp. 3-6.

Peale, R.E. and Summers, P.L. (1996) Zebra Schlieren Optics for Leak Detection, *Applied Optics*, vol. 35, no. 22, pp. 4518 - 4521.

Peale, R.E., Ruffin, A.B. and Donahue, J.E. (1997) White Light Schlieren Optics using Bacteriorhodopsin as an Adaptive Image Grid, *Applied Optics*, vol. 36, no. 19, pp. 4446.

Richard, H., Raffel, M., Rein, M., Kompe, J. and Meier, G.E.A. (2000) Demonstration of the Applicability of a Background Oriented Schlieren (BOS) Method, 10th International Symposium on Applications of Laser Technology to Flow Visualization.

Rotem, Z., Hauptmann, E.G. and Caassen, L. (1969) Semifocusing Colour Schlieren System for use in Fluid Mechanics and Heat Transfer, *Applied Optics*, vol. 8, no. 11, pp. 2326 - 2328.

Salyer, T.R. and Collicot, S.H. (1996) Multiple Source Schlieren System Noise Reduction Measurements, *AIAA Journal*, vol. 34, no. 11, pp. 2444 - 2446.

Schardin, H. (1942) Die Schlierenverfahren und ihre andwendungen, *Ergebnisse der exakten Naturwisseschaften* 10.

Settles, G.S., Hackett, E.B., Miller, J.D. and Weinstein, L.M. (1995) Full Scale Schlieren Flow Visualization, Flow Visualization VII, Begell House NY, pp. 2 - 13.

Settles, G.S. (1997) Visualizing Full Scale Ventilation Air Flows, *ASHRAE Journal*, vol. 39, no. 7, pp. 19 - 26.

Settles, G.S., Brandt, A.D. and Miller, J.D. (1998) Full Scale Schlieren Imaging of Shock Waves for Aviation Security Research, Proceedings of the 8th International Symposium on Flow Visualization, Sorrento, Italy, Paper no. 30.

Settles, G.S. (1999) Imaging Gas Leaks by using Schlieren Optics, *Pipeline and Gas Journal*, vol. 226, no. 9, pp. 28 - 30.

Settles, G.S. (2001) *Schlieren and Shadowgraph Techniques*, Springer-Verlag.

Settles, G.S., Grumstrup, T.P., Dodson, L.J., Miller, J.D., Gatto, J.A. (2004) Full-scale high-speed schlieren imaging of explosions and gunshots, Proceedings of the 26th International Conference on High-Speed Photography and Photonics, Alexandria, SPIE Paper 5580-174.

Smith, W.J. (1966) *Modern Optical Engineering*, McGraw-Hill, NY.

Toepler, A. (1864) Beobachtungen nach einer neuen optischen Methode, *Ein Beitrag zur Experimentalphysik*, M. Cohen & Son, Bonn.

Waddell, p. (1982) A Large Field Retroreflective Moire-Schlieren System, Proceedings of the Electro-optics/Laser International Conference, Brighton, UK, pp. 74 - 82.

Weinstein, L.M. (1991) An Improved Large Field Focusing Schlieren System, Proceedings of the AIAA 29th Aerospace Sciences Meeting, AIAA Paper 91-0567.

Weinstein, L.M. (1993) Large Field, High Brightness Focusing Schlieren System, *AIAA Journal*, vol. 31, no. 7, pp. 1250 - 1255.

Weinstein, L.M. (1994) An Optical Technique for Examining Aircraft Shock Wave Structures in Flight, NASA CP-3279.

Weinstein, L.M., Stacy, K., Vieira, G.J., Haering, E.A. and Bowers, A.H. (1997) Visualization and Image Processing of Aircraft Shock Wave Structures, First Pacific Symposium on Flow Visualization and Image Processing, Honolulu, pp. 6.

Winburn, S., Baker, A. and Leishman J.G. (1996) Angular Response Properties of Retroreflective Screen Materials used in Wide Field Shadowgraphy, *Journal: Experiments in Fluids*, vol. 20, no. 3, pp. 227 - 229.

10 BIBLIOGRAPHY

Burton, R.A. (1951) The Application of Schlieren Photography in flow field and heat transfer analysis, MSME Thesis, University of Texas.

Collicot, S.H. (1994) Evaluation of Options for Improved Large Grid Multiple Source Schlieren Systems, AIAA Paper 94-2301.

Cook, S.P. and Chokani, N. (1993) Quantitative Results from the Focusing Schlieren Technique, AIAA Paper 93-0630.

Fu, S., Wu, Y., Kothari, R. and Xing, H. (2000) Flow Visualization using the Negative-Positive Schlieren System and its Image Analysis, 9th International Symposium on Flow Visualization, Paper no. 324.

Garg, S. and Settles, G.S. (1994) Turbulence Measurements in a Supersonic Boundary Layer using Focusing Schlieren, *Bulletin of the American Physical Society*, vol. 39, no. 9, pp. 1890.

Gartenberg, E, Weinstein, L.M. and Lee, E.E. (1994) Aerodynamic Investigation with Focusing Schlieren in a Cryogenic Wind Tunnel, *AIAA Journal*, vol. 32, no. 6, pp. 1242 - 1249.

Heineck, J.T. (1996) Retroreflection Focusing Schlieren System, US Patent # 5515158.

Ponton, M.K., Seiner, J.M., Mitchell, L.K. and Manning, J.C. (1992) A Wind Tunnel Application of Large Field Focusing Schlieren, Proceedings of the 14th DGLR/AIAA Aeroacoustics Conference, vol. 1, pp. 169-176.

Schmid, F.P., Smith, V.A. and Swierczyna, R.T. (1997) Schlieren Flow Visualization in Commercial Kitchen Ventilation Research, Proceedings of the 1997 Annual Meeting, ASHRAE, vol. 103, no. 2.

Spraggins, D.A., Tabibi, B.M., Lee, J.H. and Weinstein, L.M. (1996) A Small-Field, high Sensitivity Focusing Schlieren System for Flowfield Visualization, American Physics Association, South Eastern Meeting.

Volluz, R.J. (1961) Flow Visualization, Navord Report 1488, US Navy Bureau of Ordinance, vol. 6, sec. 20, pp. 303-322.

Vasiliev, L.A. (1971) Schlieren Methods, Israel Program for Scientific Translations.

Walker, B.H. (1995) *Optical Engineering Fundamentals*, McGraw-Hill, NY.

Weinstein, L.M. (1998) Large Field Schlieren Visualization, From Wind Tunnels to Flight Proceedings VSJ-SPIE98, Visual Society of Japan, Paper AB124.

APPENDICES

APPENDIX A - Component drawings in Solid Edge format.

APPENDIX B - Images before, during and after processing.